ADDIS ABEBA UNIVERSITY

SCHOOL OF GRADUATE STUDIES

ADDIS ABEBA INSTITUTE OF TECHNOLOGY

DEPARTMENT OF CIVIL AND ENVIRONMENTAL ENGINEERING

Numerical Investigation of single Batter Pile Due to Inclined Loads

BY:

Worku Teklearegay Gebresilassie

A THESIS SUBMITTED TO ADDIS ABABA UNIVERSITY AS PARTIAL FULFILLMENT OF MASTER OF SCIENCE IN CIVIL ENGINEERING

June 2020

Addis Ababa, Ethiopia

NUMERICAL INVESTIGATION OF SINGLE BATTER PILE DUE TO INCLINED LOADS

BY:

Worku Teklearegay Gebresilassie

A thesis submitted to Addis Ababa University in partial fulfilment of the requirements for the degree of **masters of Science in civil engineering** (geotechnical engineering) in the faculty of civil and environmental engineering.

ADVISOR:

Dr. Ing. Henok Fikre

June 2020

Addis Ababa

Ethiopia

ADDIS ABABA UNIVERSITY

SCHOOL OF GRADUATE STUDIES

INSTITUTE OF TECHNOLOGY

NUMERICAL INVESTIGATION OF A SINGLE BATTER PILE TO INCLINED LOADS: in case of Addis Ababa soil

BY:

WORKU TEKLEAREGAY

Approved by Board of Examiners

Dr. Ing. Henok Fikre	_____	_____.
Advisor	***Signature***	***Date***
_____	_____	_____.
Internal examiner	***Signature***	***Date***
_____	_____	_____.
External examiner	***Signature***	***Date***
_____	_____	_____.
Chairperson	***Signature***	***Date***

DECLARATION

I, undersigned, declare that this thesis is my original work performed under the supervision of my research advisor Dr:-Ing. Henok Fikre and has not been presented as a thesis for a degree in any other university. All sources and materials used for this thesis duly acknowledged.

Name: Worku Teklearegay

Signature:_____

Place: Addis Ababa Institute of Technology

Date of submission: June 2020

Dedicated to my son

Abi worku

ACKNOWLEDGEMENT

Primarily, I would like to thank God Almighty for giving me the strength, knowledge, ability and opportunity to undertake this research study and complete it satisfactorily. Without his blessing, this achievement would not have been possible.

I have great pleasure in acknowledging my sincere gratitude to my advisor Dr. (Ing) Henok Fikre for the continuous support of my masters' study and research, his patience, inspiration, motivation, enthusiasm and immense knowledge. His guidance helped me in all the time of research and writing of the thesis.

I would also like to thank my office mate at Debre berhan university who were every dedicated to helping me with any problems which I face every problems.

My special thanks also go to my wife Genet Tesfaye for her endless support, positive energy unstoppable awakening and appreciable suggestions throughout the thesis work.

Last but not least I would like to extend my deepest thank for my family to their corporation by covering my private challenges throughout the years of the study.

ABSTRACT

Batter piles are used when the foundation structure is exposed to a considerable amount of lateral loads to support super structure safely. The behavior of batter piles had for many years been studied by performing laboratory tests. The difficulty of modeling the pile soil-interaction in the laboratory is assisted by numerical modeling/finite element/, which is increasingly gaining more acceptance and application. Besides, of laboratory and field tests, finite element method used increasingly to deal with this problem.

In this paper, the behavior of a batter and vertical pile subjected to lateral, axial and inclined loads are modeled with finite element software. The paper attempts to examine the effect of batter angle on its ultimate lateral and axial load carrying capacity. The overall response of vertical and batter pile subjected to lateral, vertical and inclined loads are investigated. Negative and positive batters inclined at angles ranging from 30^0 to -30^0 are simulated using the validated software PLAXIS 3D. The results showed that small inclination angle of piles give better resistance than vertical piles especially for lateral loads. From the analysis of a single pile, it is found that negative batter piles have more resistance than positive piles. For a specified pile property, batter piles inclined at -20^0 and subjected to lateral loads have more capacity to resist applied loads than vertical piles subjected to the same magnitude of lateral loads. The equivalent behavior of vertical pile is observed clearly from the analysis result. This shows batter piles inclined at 20^0 have more capacity and it is similar to vertical piles with that of 20^0 inclined load from the vertical. Batter piles subjected to vertical loads show continuous reduction in ultimate capacity for both negative and positive batter piles. Negative batter pile deformation reduced by 8.25 %, 2.11 % and 19.4 % for lateral, vertical and transverse components respectively for similar geometry, property of materials and equal magnitude of loads.

Key words: Batter pile, negative batter, positive batter, inclination angle

TABLE OF CONTENTS

LIST OF FIGURES

LIST OF TABLES

LIST OF ABBREVIATIONS

A_p	Area of the pile tip
B	Pile diameter
β	Inclination of batter pile
C	Cohesion of the soil supporting the pile tip
CBE	Commercial Bank of Ethiopia
CBEV	CBE pile vertical load only
CBEVH	CBE pile both inclined load 1, 2,… shows inclination angle increases
CBEH	CBE pile horizontal load only
Q_{ult}	Ultimate bearing load
q_p	Unit point resistance
q'	Effective vertical stress at the level of the pile tip
N_c, N_q	The bearing capacity factors
P	Perimeter of the pile length
f_s	Unit frictional resistance at any depth z
ΔL	Incremental pile length over which p and fs are taken to be constant
k_s	The earth pressure coefficient
S_t	Total pile top settlement for a single pile
S_s	Settlement due to axial deformation of the pile shaft
S_p	Settlement of a pile base or point caused by load transmitted at the base
S_p	Settlement of pile caused by load transmitted along the pile shaft
Q_{va}	Applied pile load
A_p	Area of cross section of pile
L	Pile length

E_p	Modulus of elasticity of pile material
k_h	Modulus of horizontal subgrade reaction:
k_b	lateral earth pressure coefficient
A_s	Area of the pile shaft
K_s	Average earth pressure coefficient of the shaft
α	Inclination of load on vertical pile
$Q_{\alpha u}$	Ultimate inclined load on vertical pile
$Q_{\beta u}$	Ultimate vertical load battered pile
σ_f	Failure normal stress
ϕ	Friction angle
ν	Poison ratio
ε	Strain
ρ	Density of soil and pile
g	gravity
h	depth below the ground surface
u	Pore water pressure
WB	Wogagen Bank
WBV	WB vertical load only
WBI	WB inclined loads 1, 2, 3…shows angle increases
WBL	WB lateral load only

CHAPTER ONE

1 INTRODUCTION

1.1 Background of the study

A geotechnical engineer faces different types of foundation designs corresponding to their applications for different types of soils and structural loads. For heavy structures and unfavorable soil bearing capacity, deep foundations are more relevant. When soft or loose soil extends to a considerable depth and the structure load is heavy as compared to bearing resistance of the soil, piles used to transmit vertical and lateral loads to the surrounding soil. Batter piles are more capable of resisting lateral loads because of ability to resist large lateral forces along its length and to convert overturning movement into compression and tension forces.

Analysis of pile structure is mostly done for vertical piles corresponding to their vertical loads. When structure is loaded laterally, i.e. the lateral load per pile exceeds the limiting value, batter piles are used in combination with vertical piles. Generally, a pile carries much larger axial loads than lateral loads. Standing from this, a designer expects to transfer a portion of the lateral load to axial load, thereby increasing the lateral capacity of a pile. Batter piles convert overturning moment into compression and tension forces. Therefore, it is better to analyze the batter (inclined) piles to meet the maximum resistance capacity of pile for both vertical and lateral loads. During the lifetime, structures are exposed to a significant amount of lateral loads in addition to vertical loads. Super structures exposed to wind, tension cable loads and other impact lateral loads, while substructures exposed to soil, water flow, ship impact and seismic lateral loads in addition to vertical loads of the structure. So batter piles have wide range of applications in engineering developments to handle such loads under control without hazard.

Deep foundations often used in weaker soil to transfer super structural loads to underlying ground, aiming to increase the bearing resistance of soils and decrease the settlement of structures. There is no general equations to predict the bearing capacity and settlement for single pile under different working conditions. Researches on this problem are still conducting by using field or laboratory tests. Recently, with the rapid development of computing technology, numerical analysis methods involving finite element method (FEM) are widely used to

understand the bearing capacity behavior of piles, especially for piles under combined lateral and vertical loading conditions.

Investigation on response of pile is an important issue in the analysis and design of many civil engineering structures. In past, many analytical and numerical methods for analysis of pile have employed with simplified assumptions such as, replacement of the soil medium by Winkler springs, treating the soil medium as an elastic continuum, and neglecting the interaction between various components. Most of previous studies have been concerned with vertical piles and relatively few investigations have involved on batter piles. For three dimensional finite element analyses, inclined piles pose difficult problems, specifically from the point view of mesh generation. For a structure having potential for high lateral loads, it is desirable to consider in the analysis the batter pile geometry and nonlinear behaviour of soil medium.

Large-scale finite element software PLAXIS 3D specializes in the calculation of various combinations of materials, complex loading processes and varying contact conditions. The advantage of finite element analysis lies in its ability to address complex soil layer and the interaction between soil and structure.

In this paper, an investigation is made to assess batter pile contribution on the bearing behaviour of pile foundation. Commercial Bank of Ethiopia (CBE) head quarter building and Wogagen Bank (WB) has been taken as a case study by partial replacement of existing pile with batter pile. The complex geometry and interaction of single batter pile foundation can be accounted for using Finite Element Method modelling. So, this method used for modelling and analyzing the batter pile foundation system. Prior to detail modelling a preliminary assessment of the foundation has been carried out using simplified method.

1.2 Classification of Batter Pile

Piles are classified as vertical/plumb/ and batter depending on the alignment of a pile with the vertical axis. Batter piles are inclined with some angle from the vertical axis and they further more classified as positive and negative batter piles depending on the loading direction and pile inclination. Piles are called "Pile battered reverse", if the lateral load acts opposite to the direction of pile inclination (negative batter angle), and "Pile battered forward", if the lateral load acts in the direction of the pile inclination (positive batter angle) (Zhang et al 2002).

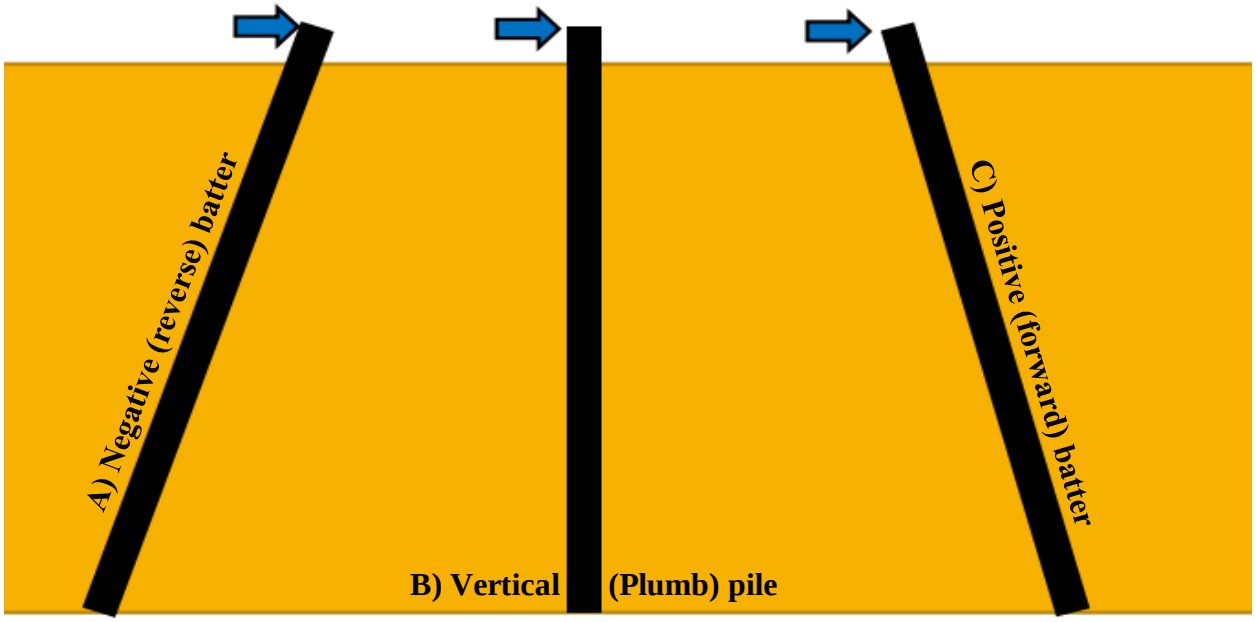

Figure 1-1: Classification of piles depending on the alignment

1.3 Statement of the Problem

In Ethiopia, only vertical pile is common rather than using a combination of batter pile as a partial replacement of vertical pile to resist lateral and vertical loads. Knowing the ultimate capacity of batter piles with different inclination angle requires its own analysis. The load carrying capacity of these batter piles with respect to those angles need more detail investigation. In Ethiopia, it is not common to use batter piles in addition to vertical piles to support the vertical and lateral loads in deep foundations. There are no more researches that has been done for inclined loads from the vertical axis and their effects on the pile behavior. As compared to the practical use of battered pile, there were no more researchers those studies on battered pile to overcome it safer, serviceable and economical.

The research is done to investigate the behavior of batter pile loaded with inclined loads using numerical modeling. In doing so, the study try to answer the following questions:

1. At what range, battered pile inclination angle gives more bearing capacity resistance for inclined resultant loads.
2. What look like the deformation behaviour of battered pile corresponding to load direction?
3. Why laboratory tests of battered pile simulated with finite element modeling?

To address such concerns of the pile behavior, the analysis of the pile with different inclination angle must employ. Thus, there is a growing need for analysis tools and simplified approaches with finite element modeling approach.

1.4 Scope of the study

Commercial bank of Ethiopia (CBE) and Wogagen Bank building sites were used for the study to assess the behaviour of pile foundation for Addis Ababa soils. Batter pile modeled to incline at an angle Ɵ from the vertical axis and load applied is only static response on the pile. Then a continuum-based analysis perform, which rigorously connects the properties of the three-dimensional continuum surrounding the pile to those of the soil springs. A three-dimensional model of pile and soil would use for the study. The effect of inclined loads from the vertical would study thoroughly and the magnitude of the bearing pressure investigated. The influence of the contact condition at the pile–soil interface also investigated. The pile is assumed as a free head and it can away in n any direction.

1.5 Objectives

General Objectives

To compare the behavior of batter pile in partial replacement to vertical piles in new head quarter building of Commercial Bank of Ethiopia around national theatre and Wegagen bank building site around stadium by using finite element technique.

Specific objectives

- To analyze the behaviour of battered pile for horizontal, lateral and inclined loads.
- To compare the effect of batter angle on ultimate load carrying capacity of batter and vertical pile.
- To investigate load versus deflection behaviour of batter pile on its ultimate capacity.

1.6 Methodology

Batter pile load carrying capacity has been analyzed using numerical analysis and through modeling finite element software PLAXIS 3D is used. It based on the assumption that vertical pile with central inclined load is equivalent to batter pile inclined and subjected to vertical load.

The analysis carried out using an elasto-plastic constitutive law based on the non-associated Mohr–Coulomb criterion. From the analyses, the effect of load inclination with regard to the pile's axis for both the lateral and axial response of the battered piles is studied. So the numerical modeling simulated with three-dimensional finite element modeling software.

Methodology on numerical modeling with finite element employs the following phases:

1. Modeling: give the proper properties and dimensions of the pile and soil using finite element software:
    - ✓ Model the soil and pile in their proper positions in the soil mass
    - ✓ Describe the behavior of the physical quantities on each element
    - ✓ Generate 2D and 3D meshes for the discretization of nodes
    - ✓ Solve the system of equations involving unknown quantities at the nodes (e.g., displacements).
    - ✓ Calculate desired quantities (e.g., strains and stresses) at selected elements

2. Data Generation: Determining the displacement, load and model behaviour.
3. Formulate from the test data, simple but realistic constitutive models that accurately reflect response under states and conditions of practical concern.
4. Apply the analysis procedures to real situations, point out the limitations. In this manner, analysis tools that are of practical value developed.

1.7 Thesis organization

Chapter one describes the overall introduction about the pile, statement of the problems and research objective are described. Chapter two presents the literatures that have been published in journals and books described. Experimental, numerical test and finite element equation derivations are included in this chapter.

Chapter three presents the information about site geology and assessment of preliminary bearing capacity determination of the two sites. In chapter four the pile soil system is modeled with finite element software PLAXIS 3D with a given soil parameters described in chapter three. Model size, mesh sensitivity analysis and validation of the software are properly described in this chapter.

In Chapter five the analysis and discussions of the model are described in detail. This portion investigates the answers of the research objectives. Standing from analysis and discussions described in chapter five results, conclusions and recommendations are made in chapter six. Finally, references are described at the end of this chapter.

CHAPTER TWO

2 LITERATURE REVIEW

2.1 Historical Development of Batter Pile

Until 1990 s, batter piles were used to carry lateral loads, especially when lateral loads were large, unsupported pile length and weak soils present at the ground surface. In 1990s following the poor performance of batter piles in series of earthquakes, some engineers began advising against the use of batter piles (Mahmoud G. *et al* 2014). However, once the reason for the poor performance of batter piles understood, engineers develop design strategies to address these problems. Using these strategies, batter piles have once again become an important weapon in the engineer's field for the designing foundations subjected to lateral loads.

Shamshar Prakash & Hari D. Sherma (1990), Source of lateral load on deep foundations include not only seismic loads but also winds, blasts, impacts, waves currents, lateral earth pressure and displacements. Throughout the 20^{th} century, batter piles employed routinely to carry lateral loads. Retaining walls founded up on soft soils, anchored bulkheads, pile supported decks, breasting dolphins and bridge piers regularly employed batter piles. In fact, batter piles were the preferred methods for deep foundations subjected to lateral loads until the second half of the 20^{th} century. Reasons for this include the extremely poor moment (bending) capacity of some of the more common deep foundations employed in the first half of the 20^{th} century. Through the 1960s, major bridges routinely employed a large number of relatively small driven piles to support the main piers, including several rows of batter piles to carry the lateral loads.

In the 1970s and 1980s, more and more bridges employed large diameter drilled piers for bridge foundation elements. The increased popularity of the large diameter drilled piers for the bridge foundations due to the larger part to the development of reliable procedures for their design and construction. However, batter pile remained a popular means of carrying the large lateral loads associated with pile-supported decks and for limiting the displacement of foundations subjected to lateral loads. Towards the end of the 20^{th} century, poor performance of batter piles in a series of earthquakes cast batter piles in a poor light. Damages recorded on bridges and other structures composed of batter piles. Because of these incidents, some engineers began advising

against the use of batter piles. As the cost of not employing batter piles for many seismic design problems became apparent, many engineers began to question the conclusion that batter piles were unsuitable for seismic loading. Forensic analysis of the observed failures suggested that the poor performance of batter piles in seismic events was due to the fact design analyses typically assumed the head of the pile was "pinned", i.e. free to rotate, and thus was not designed to sustain any moment loading.

However, due to the design details, the heads of the prestressed concrete piles could not rotate freely and subjected to large shear and moment loads, resulting in failure at the pile head. This suggested that the observed deficiency in the performance of batter piles remedied by a combination of strengthening the pile head so that it resist the applied moment and shear loads and provide sufficient ductility to the pile head or pile-structure connection allow it to rotate without a loss of capacity. With this understanding the source of the observed poor performance and how it could be mitigated, in the past few years batter piles have re-assumed their traditional role in withstanding large lateral loads applied to deep foundations.

The use of batter piles along with vertical piles in the pile-soil system increases the overall efficiency. In many fields, battered pile used especially when the resultant of forces inclined such as retaining walls, bridge abetments offshore structures, slope stability power transmission poles and high rise water tanks. The ability to install driven piles on an angle, or batter, gives them a distinct advantage with respect to their ability to carry lateral loads. Batter piles carry lateral loads primarily in axial compression and/or tension while vertical deep foundations carry lateral loads in shear and bending. Large shear and moment loads induced at the pile head have been a source of performance problems with batter piles in some cases. However, these problems can be mitigated by appropriate design and detailing of the pile-structure connection.

The most frequent situation for the design of pile structures against lateral and uplift forces occur when the piles are required to restrain forces to the sliding or overturning of the structures. Vertical piles have very low resistance and uneconomical to lateral loads. Substantial loadings are designed to be resisted by groups of inclined/batter piles. Thus, the batter piles reduce horizontal forces in to two components of a group piles, one producing axial compressive in one-side piles and tensile forces to opposing piles.

If battered pile installed in fill or compressible soil, which is settling under its own weight or under the surcharge pressure, considerable bending stress induced in the piles requiring a high moment of resistance to withstand the combined axial and bending stresses.

2.2 Estimating the load capacity of piles

In most situations, single pile behaviour is different from group piles with respect to load resistance and design characteristics. Therefore, procedures developed to determine the allowable load of a pile group derived from that of a single pile. The analysis covers a wide range of methods according to the pile and soil properties with respect to the pile inclinations (Shamsher prakash and Hari D. Sharma 1990). Pile load carrying capacity depends on various factors, including

- Pile characteristics such as pile length, cross section, and shape;
- Soil configuration and short- and long-term soil properties;

Two widely used methods to estimate the load carrying capacity of piles are α and β methods Reese & William (2011). The former method used to calculate the short-term load capacity of piles in cohesive soils, and the latter method used to calculate the short- and long-term load capacity of piles in both cohesive and cohesionless soils.

According to Johansson and Kate (2005) the ultimate bearing capacity can be estimated by extending the straight line through the elastic region of the load displacement curve, so that it intersects a straight line extending back from the plastic region of the curve.

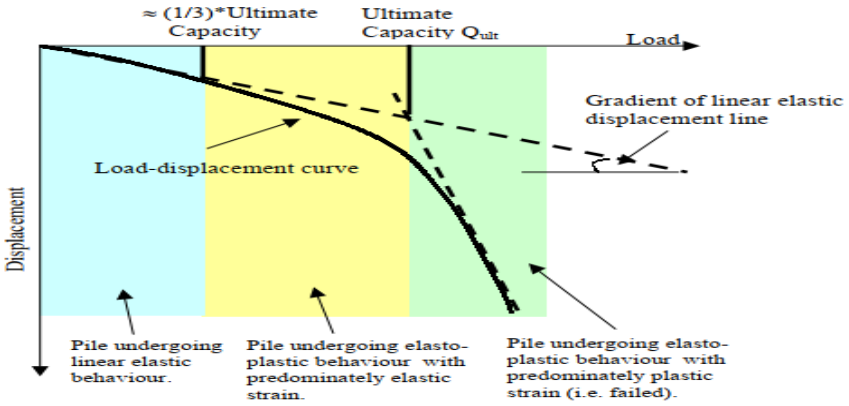

Figure 2-1: Ultimate capacity of a pile from load displacement curve

The corresponding load at the intersection is the ultimate capacity of the pile. It noted that straight line extending through elastic region of the curve is the linear elastic response and only represents the displacement response in elastic region of the curve. It assumed by researchers such as Craig (1992) that the elastic region extends from zero load to approximately 1/3 of the ultimate load.

2.2.1Vertical piles with axial compression load

Bearing capacity

Ultimate bearing load Q_{ult} for a single pile subjected to axial loading can be determined using statics or dynamics depending on the pile installation technique. The static approach is based on soil mechanics and requires the input of soil properties as described by Shamshar Prakash & Hari D. Sharma 1990. The dynamic approach is highly unreliable and factors of safety in the order of 5-6 is applied to the predicted loads. The static approach is commonly used and it requires the estimation of the ultimate shaft friction and end bearing loads, as shown in figure 2.2 below.

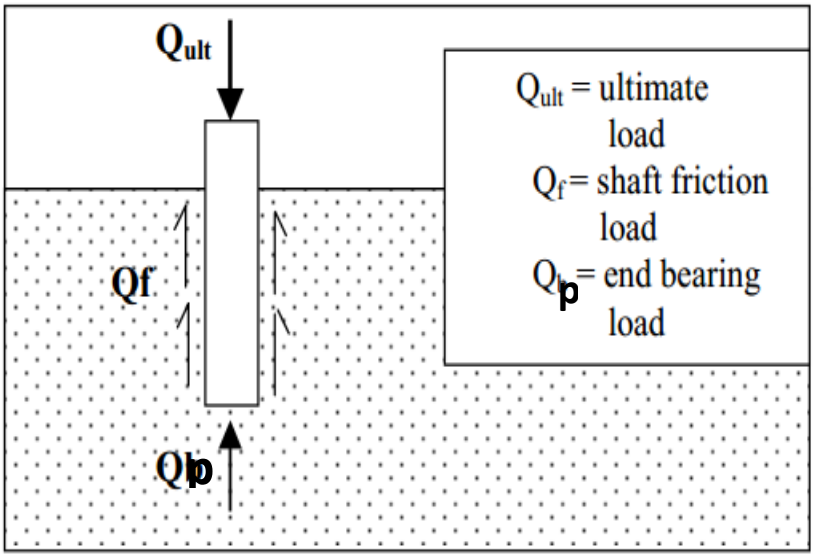

Figure 2-2: Forces acted on axially loaded vertical pile

The ultimate bearing capacity of the pile is the sum of end bearing capacity and frictional capacity along the pile length. $Q_U = Q_p + Q_f = A_p q_p$ (2.1)

Where, $Q_p = A_p(CNc + 0.5\gamma BN_\gamma + \gamma D_f N_q)$ and

$$Q_f = P \sum_{L=0}^{L=L} f_s \Delta L$$

Where, A_p = area of the pile tip

C = cohesion of the soil supporting the pile tip q_p = unit point resistance

q' = effective vertical stress at the level of the pile tip N_c, N_q = the bearing capacity factors

P = perimeter of the pile length f_s = unit frictional resistance at any depth z

ΔL = incremental pile length over which p and fs are taken to be constant

All of the methods used to approximate the ultimate capacity of (Q_{ult}), based on the assumption that the skin friction and end bearing resistance have been fully mobilized. The design engineer also divide the ultimate load by a factor of safety (F_s) usually equal to 3 to reduce the risk of failure. This enables the allowable design-working load (Q_{all}) to be determined for a working pile.

2.2.2Vertical piles with lateral load

Lateral loads and moments may act on piles in addition to the axial loads. The allowable lateral loads on piles is determined from;

1. Allowable lateral load obtained by dividing the ultimate failure load by factor of safety.
2. Allowable load is corresponding to an acceptable lateral deflection Shamshar Prakash1990.

Therefore, the smaller of the two above values is the one actually adopted as a design of lateral load. A pile subjected to lateral loading has to satisfy the same design as a pile under axial loading. The criteria are an adequate factor of safety against ultimate failure and acceptable deflection at working loads. Generally, each of the above criteria are analyzed separately and should satisfy their individual safety margins. Two categories of calculating lateral resistance of vertical pile.

Calculating ultimate lateral resistance

Brinch Hansens method

Brinch Hansens method (1961) based on the earth pressure theory and applicable for c - ϕ and layered soils. It consists determining the center of rotation by taking a moment of all forces by taking about the point of the load application and equal to zero. The ultimate resistance, then calculated by using the sum of all horizontal forces equal to zero.

Brom's method calculating the ultimate lateral loading

Broms (1964) describes the lateral resistance of laterally loaded piles. This method also based on earth pressure theory, but simplifying assumptions made for distribution of ultimate soil resistance along the pile length. This method is applicable for short and long piles, considers both purely cohesive and cohesionless soils and considers both free head and fixed head piles that analyzed separately.

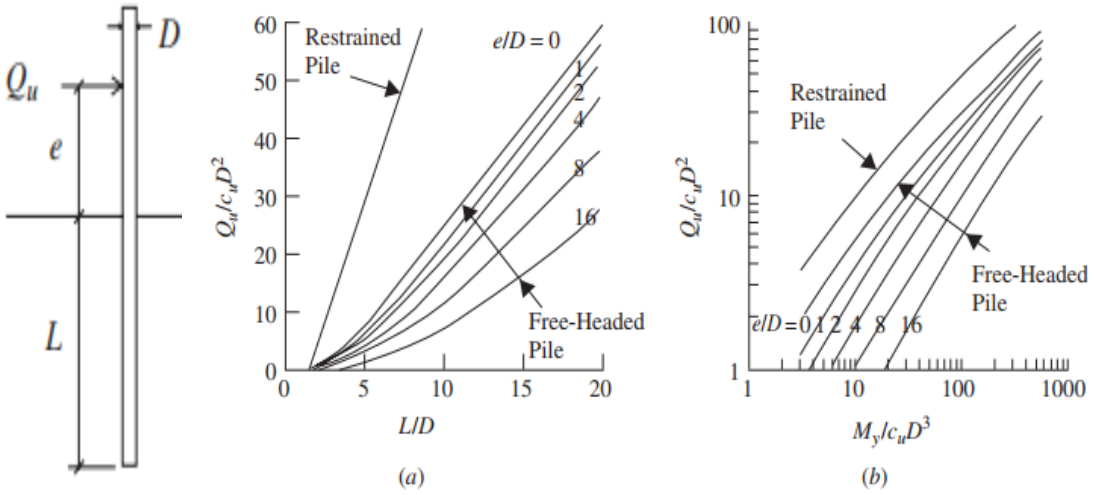

(a) Short pile (b) Long pile

Figure 2-3: Broms' method solution for piles embedded in cohesive soils

Broms' method presents the solution for short piles embedded in cohesive soils with a set of curves shown in figure 2.3a. The curves relate the pile's embedment length-to-diameter ratio, L/D, to the normalized ultimate lateral force, Q_u/c_uD^2, for various e/D ratios. In general, piles having a length-to-diameter ratio L/D greater than 20 are long piles. Figure 2.3b used for long

piles embedded in cohesive soils. The curves in this figure relate the normalized ultimate lateral force, Q_u/c_uD^2, to the normalized yield moment of the pile, M_{yield}/c_uD^3, for various e/D ratios. These curves are used only when L/D > 20 and when the moment generated by the ultimate lateral load is greater than the yield moment of the pile. For short piles embedded in cohesionless soils, Broms' method provides the curves given in figure 2.3a, which relate the pile's embedment length-to-diameter ratio L/D to the normalized ultimate lateral force $Q_u/K_pD^3\gamma$ for various e/D ratios. Note that K_p is the passive lateral earth pressure coefficient and γ is the unit weight of the soil around the pile. Figure 2.3b used for long piles embedded in cohesionless soils. The curves in this figure relate the normalized ultimate lateral force $Q_u/K_pD^3\gamma$ to the normalized yield moment of the pile $M_{yield}/K_pD^4\gamma$ for various e/D ratios. These curves are used only when L/D > 20 and when the moment generated by the ultimate lateral load is greater than the yield moment of the pile.

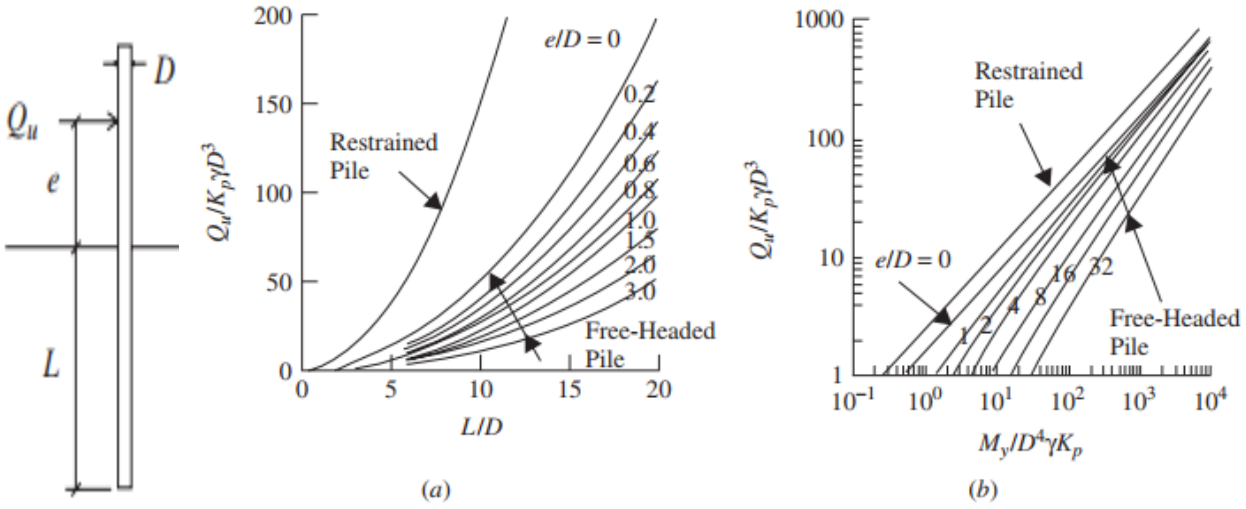

a) Short (b) long piles

Figure 2-4: Broms' method solution for piles embedded in cohesionless soils:

Therefore, Broms method is suitable to calculate the lateral deflection when using calculating the ultimate lateral resistance.

Calculating acceptable deflection at working lateral load

In most situations, the design of pile to resist lateral load based on acceptable lateral deflection rather than the ultimate lateral capacity.

Modulus of subgrade reaction approach (Rees and Matlock, 1956)

This approach assume a soil acts as a series of independent elastic springs. The method is relatively simple and it can incorporate factors such as non-linearity, variation of subgrade reaction with depth, and layered systems. The stiffness of the spring k_h (modulus of horizontal subgrade reaction) is the ratio of the soil reaction per unit length of the pile and the pile deformation.

Modulus of horizontal subgrade reaction: $k_h = \frac{p}{y}$ (2.2)

Palmer and Thompson (1948) employed the horizontal subgrade reaction throughout the depth of the pile as: $k_x = k_h(\frac{x}{L})^n$, where k_h =values of k_x at x=L or tip of the pile

x= any point along the pile depth and n = a coefficient equal to or greater than zero

According to Davisson and Prakash **(1963),** a more appropriate value of n will be 1.5 for sands and 0.15 for clays under undrained conditions.

The behavior of a pile can be analyzed using the equation of an elastic beam supported on an elastic foundation and it is given by:

$EI\frac{d^4y}{dx^4} + p = 0$ we can write as $EI\frac{d^4y}{dx^4} + \frac{k_h y}{EI} = 0$ (2.3)

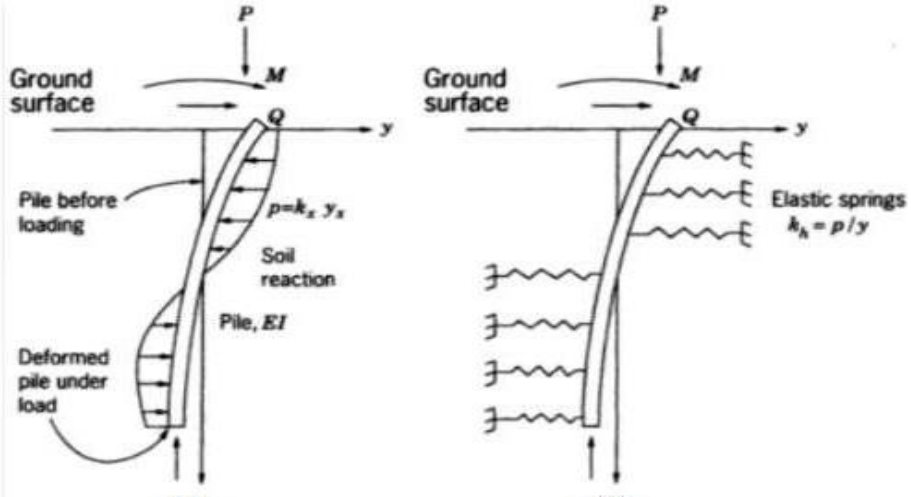

Figure 2-5: Laterally loaded pile in soil and spring

Elastic Continuum Approach (Poulos, 1971a and b)

In this approach, the soil assumed as an ideal elastic continuum. The method is theoretically more realistic approach and it can give solutions for varying modulus with depth and layered system. The determination of deflection and moment of pile subjected to lateral load and moment is based on the theory of subgrade reaction is un-satisfactory, as the continuity of the soil mass is not taken in to account. The behavior of elastic continuum explained by Poulos (1971a and b) is theoretically more realistic, one of the major obstacles in its application to the practical problem is the realistic determination of soil modulus Es^* (k_h used interchangeably). In addition, the approach needs more field verification by applying the theoretical concept to practical problems.

2.2.3Vertical pile with inclined load

According to Meyerhof and Ranjan (1972), the ultimate central inclined load, $Q_{\alpha u}$ on the pile head at inclination "α" obtained using a semi empirical equation:

$$\left(\frac{Q_{\alpha u}\cos\alpha}{P_u}\right)^2+\left(\frac{Q_{\alpha u}\sin\alpha}{Q_u}\right)^2=1 \qquad (2.4)$$

Where, Pu = ultimate axial vertical load capacity

$P_u=\gamma L N_q A_t+K_s\gamma L\tan\alpha(A_s/2)$ for cohesionless soil

$P_u=9c_U A_t+\alpha c_U A_s$ for cohesive soil

Qu = ultimate pile capacity under horizontal load ($\theta = 90^0$)

This can be theoretically obtained from the triangular pressure distribution for $\delta_1=\delta_2=0$.

- For cohesionless soils the value of Q_u can be obtained from the relationship:

$$Q_u=0.125\gamma BL^2k_b \qquad (2.5)$$

Where, γ = unit weight of soil; L = pile length; δ = angle of skin friction; k_b = lateral earth pressure coefficient; B = pile diameter; A_t = area of the pile toe; A_s = area of the pile shaft; K_s =average earth pressure coefficient of the shaft

- For cohesive soils the ultimate pile capacity under horizontal load ($\alpha = 90^0$) is theoretically estimated using zero adhesion. For a fully embedded pile the following expression is obtained by Meyerhof et al. (1981) to calculate the value of $Q_{u:}$

$$Q_u = 0.4 C_{us} BL\ K_c \tag{2.6}$$

Where, C_{us} = average undrained shear strength of a clay along pile shaft

$K_c = 2\tan(45 + \phi/2) S_{cu}$, S_{cu} = is the shape factor obtained from the graph

P-y curves

Lateral capacity of pile calculated by the subgrade reaction approach extended beyond the elastic range where soil yields plastically. This can be done by employing p-y curves (Matlock, 1970; Rees et al 1974). The differential equation for laterally loaded piles, assuming that the pile is linearly elastic beam; $EI\frac{d^4y}{dx^4} + p\frac{d^2y}{dx^2} - p = 0$, Where, p = ky, where y is the lateral deflection of x along the pile length, k is the soil modulus

A family of curves that shows the soil reaction p as a function of deflection y best accomplishes the numerical description of the soil modulus. In general, these curves are nonlinear and depend on several parameters, including depth, soil shear strength and number of load cycles. The curves are assumed to have the following characteristics (Shamsher Prakash and Hari D. Sharma 1990).

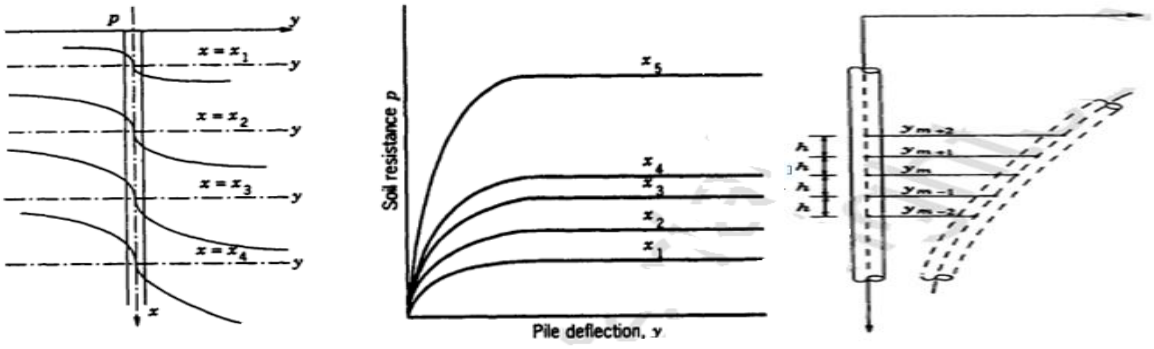

Figure 2-6: Set of p-y curves and representation of deflected pile

Once sets of p-y curves established for a soil pile system, the problem of laterally loaded pile solved by an iterative procedure.

2.2.4Batter pile with inclined load

The equivalent behaviour of batter pile and vertical pile indicates that, a vertical pile subjected to at inclined load at angle α is equivalent to the behavior to a batter pile inclined at angle β and subjected to vertical load (Shamsher prakash and Hari D. Sharma 1990).

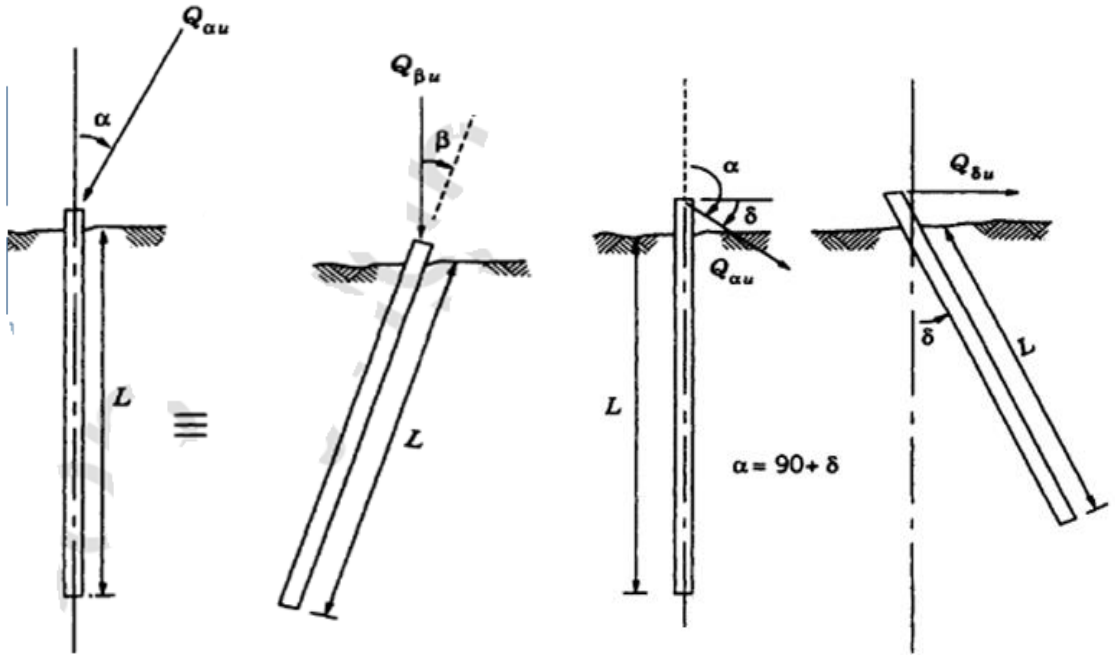

Figure 2-7: Equivalent behavior of vertical batter pile

The equivalent behavior of batter and vertical pile is presented by (Shamsher Prakash and Hari D. Sharma 1990) and satisfactory result were obtained with some factors stands for inclination of pile and load as a reference of vertical pile and load as shown in table 2.1below.

Table 2-1: Comparison between load capacity of vertical and batter piles

α or β (degree)	$\frac{Q_{\alpha u}}{(Q_{vu})}$	$\frac{Q_{\beta u}}{(Q_{vu})}$
0	1	1
7.5	1.14	1.04
15	1.25	1.20
22.5	1.35	1.34
30	1.28	1.31

α = inclination of load on vertical pile

β = inclination of batter pile

$Q_{\alpha u}$ = ultimate inclined load on vertical pile

$Q_{\beta u}$ = ultimate vertical load battered pile

Q_{vu} = ultimate vertical load on vertical pile

This exhibits that ultimate inclined load capacity of a vertical pile ($Q_{\alpha u}$) is equivalent to the ultimate vertical load capacity ($Q_{\beta u}$) of the batter pile inclined at an angle $\beta = \alpha$. Thus, in this research the behavior of the batter pile analyzed by considering the equivalent vertical pile subjected to inclined loads. The ultimate capacity $Q_{\beta u}$ of a single batter pile therefore calculated after the ultimate inclined load of an equivalent vertical pile is determined.

2.3 Finite Element Equation Derivations

2.3.1.Basic equations in elasticity

In theory of elasticity, usually right hand rule used for selecting the coordinate system. Equations derived for any one such orientation hold good for all other orientations of coordinate system with right hand rule.

A. Stress in a Typical Element

The direct stress σ and the shearing stress τ acting on the negative face show suitable face subscript. The first subscript of shearing stress is the plane face and the second subscript is the direction.

Table 2-2: Element stress distribution component

Face	Stress on negative face	Stress on positive face
x	σ_x	$\sigma_x^+ = \sigma_x + \frac{\sigma_x}{\partial x} dx$
	τ_{xy}	$\gamma_{xy}^+ = \gamma_{xy} + \frac{\gamma_{xy}}{\partial x} dx$
	τ_{xz}	$\gamma_{xz}^+ = \gamma_{xz} + \frac{\gamma_{xz}}{\partial x} dx$
y	σ_y	$\sigma_y^+ = \sigma_y + \frac{\sigma_y}{\partial y} dy$
	τ_{yx}	$\gamma_{yx}^+ = \gamma_{yx} + \frac{\gamma_{yx}}{\partial y} dy$
	τ_{yz}	$\gamma_{yz}^+ = \gamma_{yz} + \frac{\gamma_{yz}}{\partial y} dy$
z	σ_z	$\sigma_z^+ = \sigma_z + \frac{\sigma_z}{\partial z} dz$
	τ_{zx}	$\gamma_{zx}^+ = \gamma_{zx} + \frac{\gamma_{zx}}{\partial z} dz$
	τ_{zy}	$\gamma_{zy}^+ = \gamma_{zy} + \frac{\gamma_{zy}}{\partial z} dz$

Thus, the τ_{xy} means the shearing stress on the plane where x value constant and y is the direction. A stress is positive when it is on positive face in positive direction or on negative face in negative direction.

Note that stress on positive face is equal to the stress on negative face plus rate of change of that stress multiplied by the distance between the faces. The intensity of body force acting on the element along x, y, z direction is X, Y, Z respectively and those forces are uniform over the entire body. Hence, the total body force in x, y, z direction on the element given by:

(i) X dx dy dz in x – direction

(ii) Y dx dy dz in y – direction and

(iii) Z dx dy dz in z – direction

Equations of Equilibrium

Considering all the forces acting, it can write the equations of equilibrium for the element.

$\Sigma Fx = 0$, $\Sigma Fy = 0$, $\Sigma Fz = 0$, we obtain:

$$\begin{aligned}
\frac{\partial \sigma_x}{\partial x} + \frac{\tau_{yx}}{\partial y} + \frac{\partial \tau_{zx}}{\partial z} + X = 0 \\
\frac{\partial \tau_{xz}}{\partial x} + \frac{\partial \tau_{yz}}{\partial y} + \frac{\partial \sigma_z}{\partial z} + Z = 0 \\
\frac{\partial \tau_{xy}}{\partial x} + \frac{\partial \sigma_y}{\partial y} + \frac{\partial \tau_{zy}}{\partial z} + Y = 0
\end{aligned} \tag{2.7}$$

Now again by taking summation of moment about x-axis is zero and neglecting the 4th order and dividing by dx dy dz it is obtained: $\tau_{yz} = \tau_{zy}$ similarly $\tau_{xz} = \tau_{zx}$ and $\tau_{xy} = \tau_{yx}$

Thus the stress vector is:

$$\left|\sigma\right|^T = \left[\sigma_x \quad \sigma_x \quad \sigma_x \quad \tau_{xy} \quad \tau_{yz} \quad \tau_{xz}\right] \tag{2.8}$$

B. Strain displacement equations

Corresponding to the six stress components given equation 2.8, the state of strain at a point divided in to six strain components:

$$\{\varepsilon\}^T = \begin{bmatrix} \varepsilon_x & \varepsilon_y & \varepsilon_z & \gamma_{xy} & \gamma_{yz} & \gamma_{xz} \end{bmatrix} \tag{2.9}$$

Taking displacement components in the x, y, z directions as u, v and w respectively, the relations among components of strain and components of displacement are:

$$\begin{aligned} \varepsilon_x &= \frac{\partial u}{\partial x} + \frac{1}{2}\left[\left(\frac{\partial u}{\partial x}\right)^2 + \left(\frac{\partial v}{\partial x}\right)^2 + \left(\frac{\partial w}{\partial x}\right)^2\right] \\ \varepsilon_y &= \frac{\partial v}{\partial y} + \frac{1}{2}\left[\left(\frac{\partial u}{\partial y}\right)^2 + \left(\frac{\partial v}{\partial y}\right)^2 + \left(\frac{\partial w}{\partial y}\right)^2\right] \\ \varepsilon_z &= \frac{\partial w}{\partial z} + \frac{1}{2}\left[\left(\frac{\partial u}{\partial z}\right)^2 + \left(\frac{\partial v}{\partial z}\right)^2 + \left(\frac{\partial w}{\partial z}\right)^2\right] \end{aligned} \tag{2.10}$$

$$\begin{aligned} \gamma_{xy} &= \frac{\partial v}{\partial x} + \frac{\partial u}{\partial y} + \frac{\partial u}{\partial x}\cdot\frac{\partial u}{\partial y} + \frac{\partial v}{\partial x}\cdot\frac{\partial v}{\partial y} + \frac{\partial w}{\partial x}\cdot\frac{\partial w}{\partial y} \\ \gamma_{yz} &= \frac{\partial w}{\partial y} + \frac{\partial v}{\partial z} + \frac{\partial u}{\partial y}\cdot\frac{\partial u}{\partial z} + \frac{\partial v}{\partial y}\cdot\frac{\partial v}{\partial z} + \frac{\partial w}{\partial y}\cdot\frac{\partial w}{\partial z} \\ \gamma_{xz} &= \frac{\partial u}{\partial z} + \frac{\partial w}{\partial x} + \frac{\partial u}{\partial x}\cdot\frac{\partial u}{\partial z} + \frac{\partial v}{\partial x}\cdot\frac{\partial v}{\partial z} + \frac{\partial w}{\partial x}\cdot\frac{\partial w}{\partial z} \end{aligned} \tag{2.11}$$

In equation 2.10 and 2.11 above strains are expressed up to the accuracy of second order (quadratic) changes in displacements. These equation may be simplified to the first (linear) order accuracy only by dropping the second order changes terms. Then linear strain - displacement equation obtained as:

$$\varepsilon_x = \frac{\partial u}{\partial x} \qquad \varepsilon_y = \frac{\partial v}{\partial y} \qquad \varepsilon_z = \frac{\partial w}{\partial z} \tag{2.12}$$

$$\gamma_{xz} = \frac{\partial u}{\partial z} + \frac{\partial w}{\partial x} \qquad \gamma_{xy} = \frac{\partial v}{\partial x} + \frac{\partial u}{\partial y} \qquad \gamma_{yz} = \frac{\partial w}{\partial y} + \frac{\partial v}{\partial z}$$

C. Linear – Elastic Constitutive Equations

In order to relate the stress components, we theoretically need thirty-six material constants. The 'Generalized Hook's low' stated as:

$$\begin{Bmatrix}\sigma_x\\ \sigma_y\\ \sigma_z\\ \tau_{xy}\\ \tau_{yz}\\ \tau_{zx}\end{Bmatrix}=\begin{bmatrix}D_{11} & D_{12} & D_{13} & D_{14} & D_{15} & D_{16}\\ D_{21} & D_{22} & D_{23} & D_{24} & D_{25} & D_{26}\\ D_{31} & D_{32} & D_{33} & D_{34} & D_{35} & D_{36}\\ D_{41} & D_{42} & D_{43} & D_{44} & D_{45} & D_{46}\\ D_{51} & D_{52} & D_{53} & D_{54} & D_{55} & D_{56}\\ D_{61} & D_{62} & D_{63} & D_{64} & D_{65} & D_{66}\end{bmatrix}\begin{Bmatrix}\varepsilon_x\\ \varepsilon_y\\ \varepsilon_z\\ \gamma_{xy}\\ \gamma_{yz}\\ \gamma_{zx}\end{Bmatrix} \tag{2.13}$$

Alternatively, in matrix form:- $\{\sigma\}=[D]\{\varepsilon\}$**,**

Where D is '6x6' matrix of constants of elasticity to be determined by experimental investigations for each material, as D is symmetric matrix [$D_{ij} = D_{ji}$], there are 21 material properties for linear elastic an isotropic material.

However, for an isotropic elastic material, it can be shown that only two constants are sufficient to characterize the continuum and relate the strains and stresses. These material constants are elastic (Young's) modulus, *E*, and Poisson's ratio, *v*. There also certain materials (orthotropic materials) exhibit symmetry with respect to planes with in the body. Hence, the number of material constants reduces to 9 as shown below.

$$\begin{Bmatrix}\sigma_x\\ \sigma_y\\ \sigma_z\\ \tau_{xy}\\ \tau_{yz}\\ \tau_{zx}\end{Bmatrix}=\begin{bmatrix}D_{11} & D_{12} & D_{13} & 0 & 0 & 0\\ & D_{22} & D_{23} & 0 & 0 & 0\\ & & D_{33} & 0 & 0 & 0\\ & sym & & D_{44} & 0 & 0\\ & & & & D_{55} & 0\\ & & & & & D_{66}\end{bmatrix}\begin{Bmatrix}\varepsilon_x\\ \varepsilon_y\\ \varepsilon_z\\ \gamma_{xy}\\ \gamma_{yz}\\ \gamma_{zx}\end{Bmatrix} \tag{2.14}$$

Thus for three dimensional problem, the stress strain relation for isotropic material is,

$$\begin{Bmatrix}\varepsilon_x\\ \varepsilon_y\\ \varepsilon_z\\ \gamma_{xy}\\ \gamma_{yz}\\ \gamma_{zx}\end{Bmatrix}=\begin{bmatrix}\frac{1}{E} & \frac{-\nu}{E} & \frac{-\nu}{E} & 0 & 0 & 0\\ & \frac{1}{E} & \frac{-\nu}{E} & 0 & 0 & 0\\ & & \frac{1}{E} & 0 & 0 & 0\\ & sym & & \frac{1-\nu}{2} & 0 & 0\\ & & & & \frac{1-\nu}{2} & 0\\ & & & & & \frac{1-\nu}{2}\end{bmatrix}\begin{Bmatrix}\sigma_x\\ \sigma_y\\ \sigma_z\\ \tau_{xy}\\ \tau_{yz}\\ \tau_{zx}\end{Bmatrix} \quad (2.15)$$

By taking $G=\frac{E}{2(1+\nu)}$, where G is the shear modulus of a material and the material constants are determined from appropriate laboratory tests.

$$\gamma_{xy}=\frac{1}{G}\tau_{xy},\gamma_{xz}=\frac{1}{G}\tau_{xz},\gamma_{yz}=\frac{1}{G}\tau_{yz}$$

$$\begin{Bmatrix}\sigma_x\\ \sigma_y\\ \sigma_z\\ \tau_{xy}\\ \tau_{yz}\\ \tau_{zx}\end{Bmatrix}=\frac{E}{(1+\nu)(1-2\nu)}\begin{bmatrix}1-\nu & \nu & \nu & 0 & 0 & 0\\ & 1-\nu & \nu & 0 & 0 & 0\\ & & 1-\nu & 0 & 0 & 0\\ & sym & & \frac{1-2\nu}{2} & 0 & 0\\ & & & & \frac{1-2\nu}{2} & 0\\ & & & & & \frac{1-2\nu}{2}\end{bmatrix}\begin{Bmatrix}\varepsilon_x\\ \varepsilon_y\\ \varepsilon_z\\ \gamma_{xy}\\ \gamma_{yz}\\ \gamma_{zx}\end{Bmatrix} \quad (2.16)$$

With the six additional linear relationships between strain components in equation below, an equal number of equations and number of unknowns are in a position to tackle specific elasticity problems.

$$\varepsilon_{xx}=\tfrac{1}{E}\left[\sigma_{xx}-\nu(\sigma_{yy}+\sigma_{zz})\right] \qquad \gamma_{xy}=\tfrac{1}{G}\tau_{xy};$$
$$\varepsilon_{yy}=\tfrac{1}{E}\left[\sigma_{yy}-\nu(\sigma_{xx}+\sigma_{zz})\right] \qquad \gamma_{yz}=\tfrac{1}{G}\tau_{yz};$$
$$\varepsilon_{zz}=\tfrac{1}{E}\left[\sigma_{zz}-\nu(\sigma_{xx}+\sigma_{yy})\right] \quad \text{shear} \quad \gamma_{zx}=\tfrac{1}{G}\tau_{zx}$$

2.3.2. Formulation of Finite Element Method (FEM)

The first step in FEM analysis is to define the problem domain, which usually includes all the materials enclosed by a set of restraints or boundary conditions. The problem domain can be broken (discretized) into a series of continuum elements to form a mesh. The elements in the problem domain are connected together by nodes that transfer forces and displacements between elements. The force applied on the element is represented by a load vector act of the forces that at the nodes.

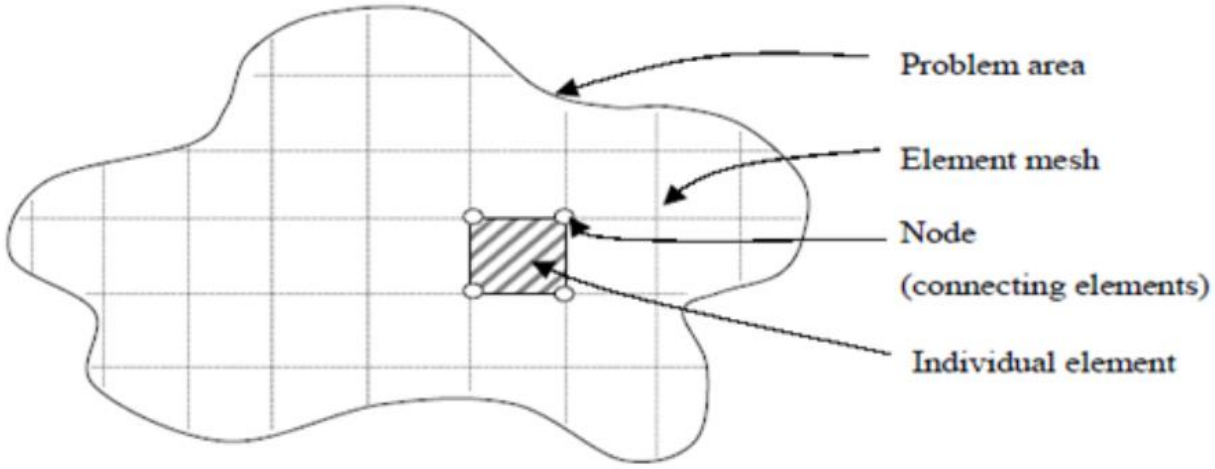

Figure 2-8: Typical mesh problem domain for FEM (Kate 2005)

Once the problem domain is defined and the element type is chosen, then individual element matrices can be formed. The individual elements have an element property matrix, a vector of unknown degree of freedom, and a resultant vector of element nodal forces. This relationship for static loading is described in the simple form of

$$[k]\{d\} = \{f\} \quad \textbf{where,}$$

$[k]$ = element property matrix, commonly stiffness or general property matrix

$\{d\}$ = vector of unknown degree of freedom (nodal displacement)

$\{f\}$ = vector of element nodal forces

The element functions are gathered in the global equation system containing material and geometric data. The unknown nodal displacement is solved from the global equation system and the values between the nodes are determined either by linear or polynomial approximated shape (or interpolation) functions. The accuracy of a finite element analysis result depends on the

element type, mesh size, boundary conditions, interface elements and constitutive models employed. Therefore, proper selection of these parameters is required for accurate results. Some of the parameters used for this study are reviewed as follows.

2.3.3. Constitutive models

In the model, it assumed that the soil behaved linear elastically, until a Mohr Coulomb plastic failure envelope reached. Once the stress state at any location reaches the failure surface it will undergo plastic deformation. The constitutive parameters and initial stresses state imposed on to the model before the analysis started. The initial stress accounted for the in situ stresses due to the self-weight of the system before the load is applied.

Mohr-coulomb model

Soil behaves elasto-plastically; when it subjected to loads, the displacement will contain both a recoverable and non-recoverable component. Hence, a failure criterion needs to be included in the elastic models to define the stress states that cause plastic deformation. One possible failure criterion is the Mohr-Coulomb line.

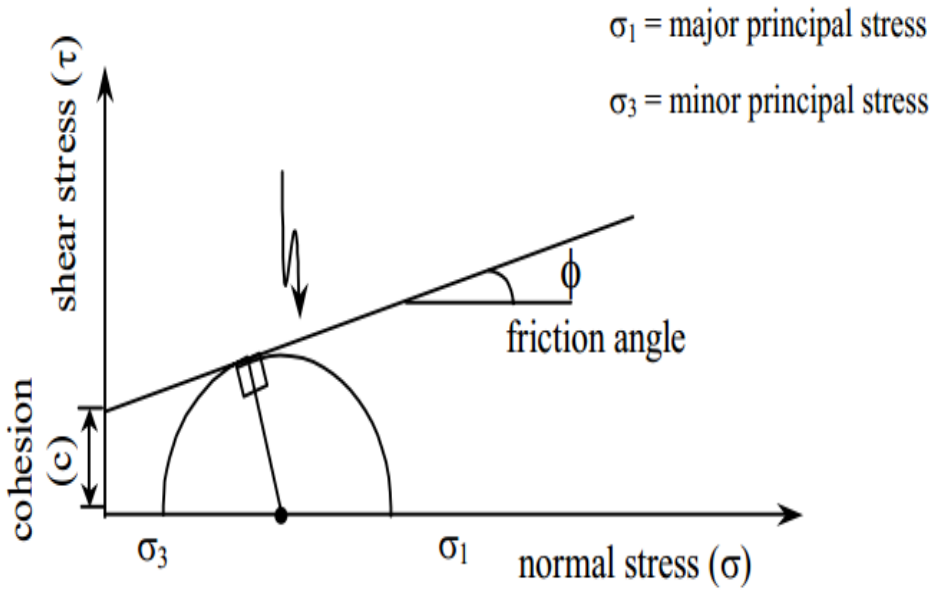

Figure 2-9: Mohr–Coulomb failure surfaces

The Mohr-coulomb failure surface in τ-σ space defined by:

$\tau_f = C + \sigma f \tan \phi$ Where, τ_f = failure shear stress

C = cohesion

σ_f = failure normal stress

ϕ = friction angle

The failure surface is only dependent on the major and minor principal stresses (σ_1, σ_3), and is independent of the intermediate principal stress (σ_2). Mohr-Coulomb criterion resolves in to an irregular hexagonal pyramid once mapped in to three-dimensional stress as follows.

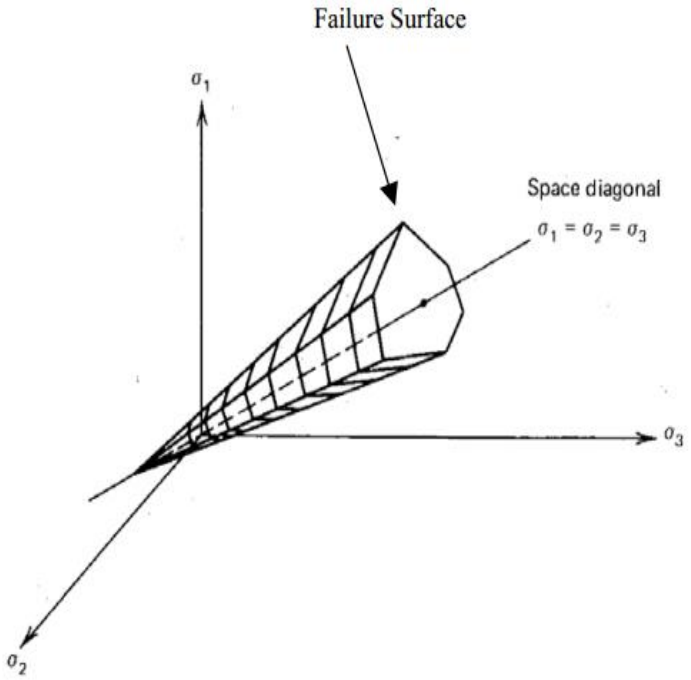

Figure 2-10: Mohr-Coulomb failure surface (Chen and Saleeb, 1983)

The above pyramid forms a failure yield surface that intern governs how the soil behave. The material behave either linear or non-linear elastically if the stress point lies within the failure envelope. However if the stress point reaches the yield surface of the material it undergo a degree of plastic deformation. It noted that several researchers have utilized Mohr-Coulomb failure criterion, and found it to be sufficiently accurate for most geotechnical applications (Chen and Saleeb 1983).

Drucker-Prager model

Fundamental modeling of soil behavior under general loading and different site condition is the important factor to achieve accurate numerical outcomes. A linear elastic basic relationship has been widely utilized to depict soils in early numerical researches; but most soil behavior is highly nonlinear.

PLAXIS 3D provides a large number of plasticity models to incorporate soil nonlinearity in the analysis. These include the extended Modified Drucker Prager models, the Mohr-Coulomb plasticity model and the critical state (clay) plasticity model. This plasticity model is recommended by Drucker-Prager (1952) for frictional soils.

Plasticity approach

Soil deformation includes elastic and plastic strains relating to loading and unloading was (Shamsher Prakash and Hari D. Sharma 1990). Plastic behavior taken into account as soil irrecoverable deformation and elastic behaviour considered when the deformation is recoverable. Incremental approach of plasticity utilize successfully in depicting a wide range of materials such as soils.

Soil failure surface

Many experiments carried out on different sands at various confining pressures showed the general shape of the failure surface as presented in Figure below. In numerical soil model, the shape of the failure surface is the same as shown below.

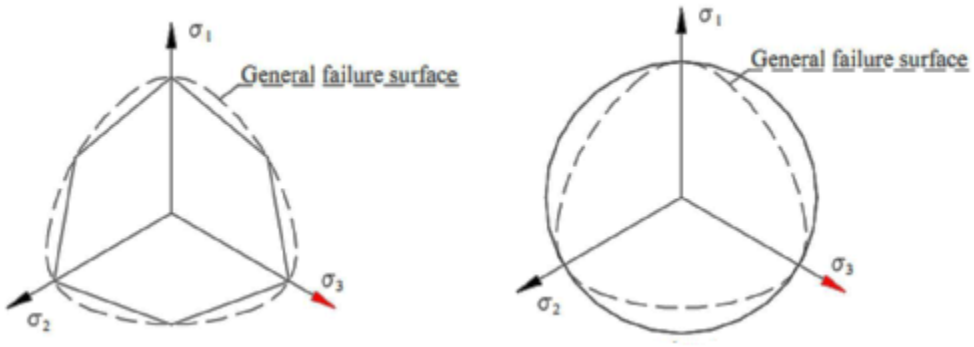

A) Mohr's Coulomb surface B) Drucker Pragar surface

Figure 2-11: Deviator plane surface for two parameter models (PLAXIS 3D)

Soil constitutive properties

The accuracy and reliability of estimating a foundation of soil response dependent on the constitutive and failure models used to represent the stress strain behaviour. Several models developed for estimating the stress strain behaviour of sands and soils. Constitutive and failure models are dependent on a number of variables, which estimated from standard field and laboratory testing of soils.

Friction angle of soil

Soil in real life is a collection of discrete particles that interact with each other to form an overall continuum. Soil particles interact with surrounding particles via friction at particle surface. This friction effect forms the interlocking along shear lines that result from load placed on to the soil. The roughness, particle shape, particle density and overburden pressure of soil influences its shearing capacity. The interlocking capacity or shear strength of soil is represented by an angle of internal friction, which is commonly referred to as effective friction angle, ϕ'. This friction angle effectively represents the inclination of the ultimate shear stress failure line, as defined by Mohr-Coulomb. In general, sandy soils have higher friction angle up to 50^0 for pure sand and clay soils have low friction angle up to 0^0 for pure clay.

Young's modulus of soil

PLAXIS uses the Young's modulus as the basic stiffness modulus in the elastic model and the Mohr-Coulomb model, but some alternative stiffness moduli displayed as well. The soil commonly said to be a nonlinear elasto plastic material that stress history dependent. The constitutive behaviour of soil in general is very complex. Therefore, approximations and simplifications have made when estimating constitutive parameters such as Young's modulus. It is dependent on the confining stresses, foundation type and different loading scenarios. From this, it expect that the method of pile installation would have a vast impact on the soil properties.

In soil mechanics, the initial slope is usually indicated as E_0 and the secant modulus at 50% strength is denoted as E_{50} (Figure 2-12). For highly over-consolidated clays and some rocks with

a large linear elastic range, it is realistic to use E_0 whereas for sands and near normally consolidated clays it is more appropriate to use E_{50}, at least for loading conditions.

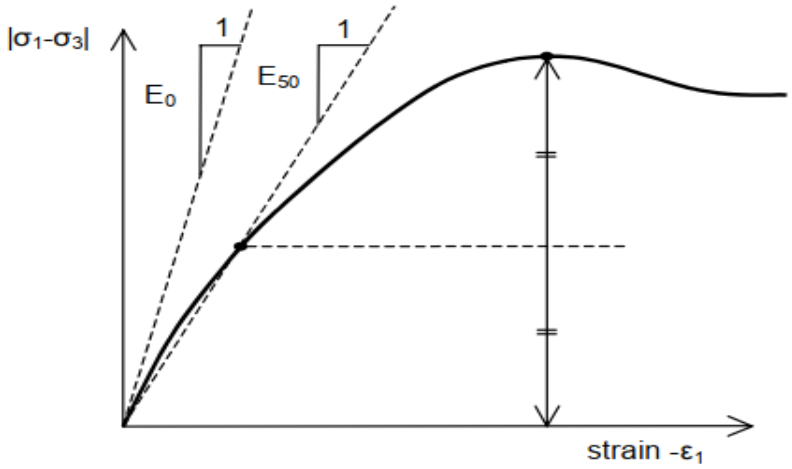

Figure 2-12: Determination of modulus of elasticity

For soils, both the initial modulus and the secant modulus tend to increase with the confining pressure. Hence, deep soil layers tend to have greater stiffness than shallow layers. Moreover, the observed stiffness depends on the stress path that is followed. The stiffness is much higher for unloading and reloading than for primary loading. In addition, the observed soil stiffness in terms of a Young's modulus is generally lower for drained compression than for shearing. Hence, when using a constant stiffness modulus to represent soil behaviour one should choose a value that is consistent with the stress level and the expected stress path. Note that some stress-dependency of soil behaviour is taken into account in the advanced models in PLAXIS, which are described in the Material Models manual. For the Mohr-Coulomb model, PLAXIS offers a special option for the input of a stiffness increasing with depth.

Poison ratio of soil

Soils in real life exhibit an isotropic behavior. However, assumptions and simplifications required to achieve a closed form of solution that used to estimate footing and soil response. For this reason, many researchers have idealized soil behaviour as an elastic isotropic material, which allows approximations for the footing displacement behaviour to be determined. Young's modulus and Poisson's ratio needed to define the sand behaviour under load, when assuming the soil is an elastic medium.

Poisson's ratio typically represents the relationship between axial and lateral strain components. As general, poison's ratio for an elastic isotropic material given by the following equation:

$\nu = \varepsilon_{lateral}/\varepsilon_{axial}$, where, $\varepsilon_{lateral}$ = latral strain and ε_{axial}= axial strain

This equation is complicated further if the material is considered to be an isotropic. For isotropic elastic material Poisson's ratio varies from o to 0.5.

For the model, the soil property is taken from Krishna M V Ratnam D. Neelima Satyyam (2017).

Alternative stiffness parameters

In addition to Young's modulus, PLAXIS allows for the input of alternative stiffness moduli, such as the shear modulus, *G*, and the Oedometer modulus, *Eoed*. These stiffness moduli are related to the Young's modulus according to Hooke's law of isotropic elasticity, which involves Poisson's ratio, ν:

$$G = \frac{E}{2(1+\nu)} \qquad E_{oed} = \frac{(1-\nu)E}{(1-2\nu)(1+\nu)}$$

When entering one of the alternative stiffness parameters, PLAXIS will calculate the corresponding Young's modulus and retain the entered Poisson's ratio.

2.3.4.Contact behaviour and Interface criteria in the model

Sometimes in geotechnical engineering problems, it is necessary to simulate the interaction between two material types. As the load in the pile increased, the shear stress at the pile soil interface reach a critical mobilized value. Once the critical shear stress exceed, the pile move relative to the soil.

In addition to the soil properties, the data set also contains parameters to derive interface properties from the soil model parameters in the case that interface elements are located in the corresponding soil layer. The main interface parameter is the strength reduction factor R_{inter}, which found on the third tab sheet of the material data set window.

An elastic-plastic model used to describe the behaviour of interfaces for the modelling of soil-structure interaction. The Coulomb criterion used to distinguish between elastic behaviour, where small displacements can occur within the interface, and plastic interface behaviour when permanent slip may occur. For the interface to remain elastic, the shear stress τ given by:

$$|\tau| < \sigma_n \tan\varphi_i + c_i \quad \text{Where} \quad |\tau| = \sqrt{\tau_{S1}^2 + \tau_{S2}^2}$$

Where, τ_{s1} and τ_{s2} are shearing stresses in the two (perpendicular) shear directions and σ_n is the effective normal stress. For plastic behaviour, τ is given by:

$|\tau| = \sigma_n \tan\varphi_i + c_i$ Where, φ_i and Ci are the friction angle and cohesion of the interface. The strength properties of interfaces are linked to the strength properties of a soil layer. Each data set has an associated strength reduction factor for interfaces (R_{inter}). The interface properties are calculated from the soil properties in the associated data set and the strength reduction factor by applying the following rules:

$$c_i = R_{inter}\, c_{soil}$$

$$\tan\varphi_i = R_{inter} \tan\varphi_{soil} \leq \tan\varphi_{soil}$$

$$\psi_i = 0° \text{ for } R_{inter} < 1, \text{ otherwise } \psi_i = \psi_{soil}$$

In this research, rigid option is used when the interface should not have a reduced strength with respect to the surrounding soil. These interfaces should be assigned the Rigid setting (which corresponds to Rinter = 1.0). As a result, the interface properties, including the dilatancy angle ψi, are the same as the soil properties in the data set, except for Poisson's ratio ν.

Initial stress states

The stress state in the soil pile before a static load placed on the pile head can have a significant effect on a piles response under load. The Mohr coulomb diagram can be used as an illustrative how initial stresses affect the response of a pile. The initial stress state causes a shift along a normal stress axis. Hence, the Mohr Coulomb failure circle has an increase in radius, and then larger loads are required to induce shear failure with in the soil mass.

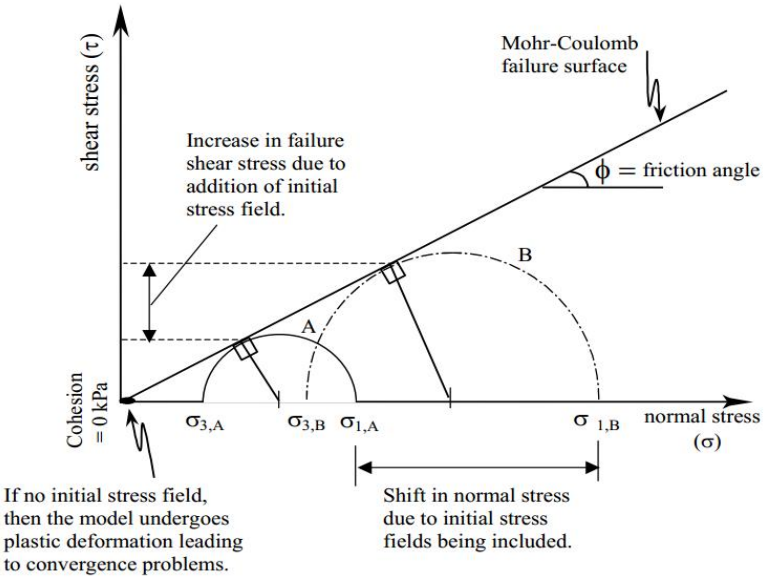

Figure 2-13: Influence of initial stress in Mohr – Coulomb failure criterion

The initial stress state with in the soil depends up on many factors. Soil in general said to have a memory of past events such as pre loading, vibration and compaction. In this research, generally consist of a normal gravity field from the self-weight of soil and pile. The initial vertical stress in cast in place pile soil system model given by:

$\sigma'_v = \rho gh - u$, Where: σ'_v = effective vertical stress (it is noted that this work is based on an effective stress analysis)

ρ = density of soil and pile g = gravity

h = depth below the ground surface u = pore water pressure (the influence of the water table was not investigated as part of this research, u=0).

For a given effective vertical stress field there is effective horizontal stress field. The horizontal stress field at any depth approximated as equal to the vertical stress at the same depth times by the effective earth coefficient (K). For piles constructed in a region where the ground surface is relatively flat, the earth coefficient is at rest K_0 employed. The inclusion of horizontal stress resist movement in the horizontal direction. As shown by Das (1999) the effective at rest earth coefficient may be approximated by $K_0 = 1 - \sin\phi$ for bored and cast in place piles, or $K_0 = 1.8*(1-\sin\phi)$ for high displacement driven piles.

2.4 Related Research Works

2.4.1.Laboratory test researches

Research done on battered pile by Mohammed et al. (2017), examines the effect of batter angle on a single pile model on its ultimate vertical load capacity. The test conducted in laboratory and pile used in this study is circular pile with a model size shown in figure 2.14 (a) below. The test performed according to ASTM specifications on sand with three different densities; loose, medium, and dense sand. Pile load capacity highly affected by relative density and less affected by L/D ratio observed during the result of the test.

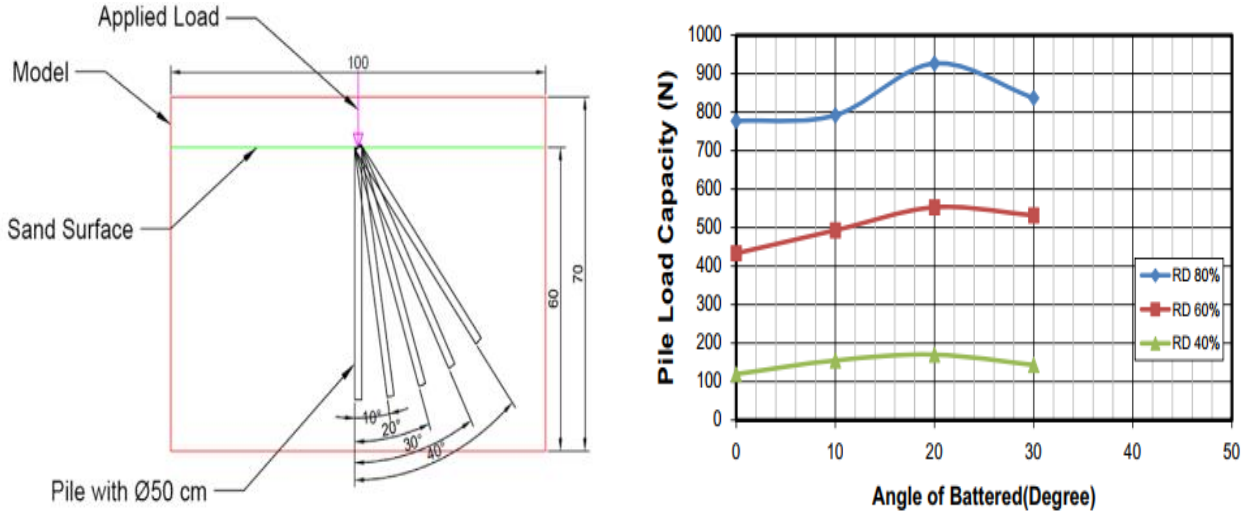

a) model of pile soil system b)Results of pile load capacity with batter angle

Figure 2-14 Model and result of pile and soil system (Mohammed & Neami 2016)

Based on the results of 32 monotonic test models carried out on a single batter and vertical piles embedded in sand, the following conclusions are drawn.

- The batter angle 20° give a higher load capacity
- The variation in relative density has a higher impact on pile load capacity. When the increase percent of the pile load capacity for the 20º batter piles decreasing as relative density increases
- The batter pile load capacity is less affected by embedded ratio (*L/D*)

Thekadi et al (2009), Conduct a laboratory test on the model study of vertical pile subjected to central inclined loads.

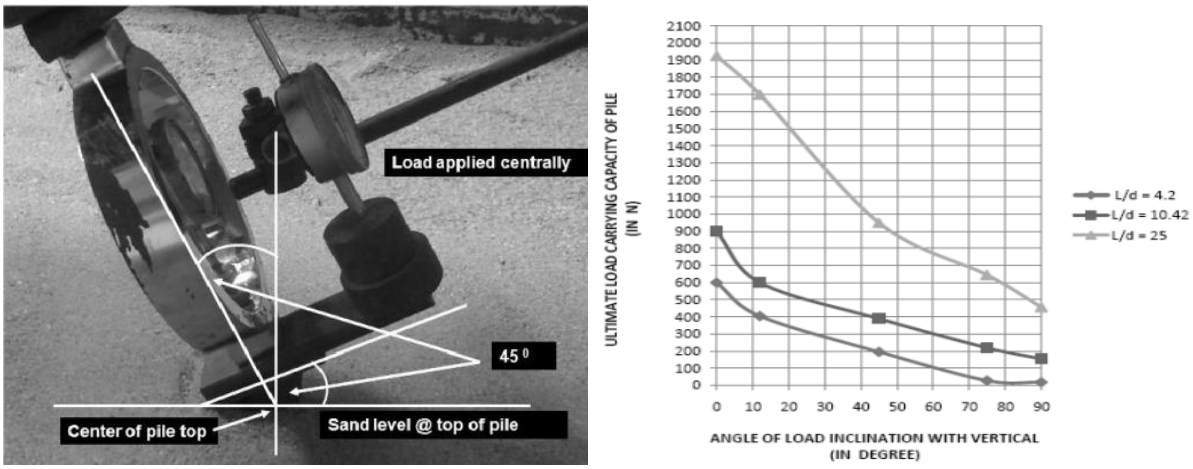

a) Concept of setup for load inclination b) Ultimate load caring capacity

Figure 2-15: Concept of setup and ultimate load caring capacity of battered pile (Thekadi, 2009)

The result shows that, ultimate load carrying capacity of pile decreases when the angle of load inclination from the vertical decreases. There also a decrease ultimate load carrying capacity of vertical pile when L/D ratio decreases.

The conclusion made on research simplified as follows:

- As L/d ratio of pile, relative density of sand, flexural rigidity of pile increases the ultimate load carrying capacity of pile increases.
- As the load inclination with vertical increases from 0° to 12°, there is a little decrease in the carrying capacity of pile.
- With further increase in inclination, carrying capacity decreases considerably up to 90° load inclination. At smaller L/d ratios, the reduction in the load carrying capacity of the pile is more substantial.
- As the load inclination with vertical increases from 0° to 90°, the piles with pile material having higher flexural rigidity shows lesser reduction in load carrying capacity.
- Results obtained using suggested equation for reduction factor reasonably agree with model test results, for L/d of pile at 25.

Research also done by NIT Kurukshetra and Haryana (2017), conducted on sandy soil, laboratory test carried out on rectangle steel tank and it was kept large enough to avoid the boundary effect. The tank was filled using rainfall method of sand filling. Experimental test on sandy soil showed that, the effect of batter angle is parabolic, that is batter angle increases from 20^0 to 25^0 pile capacity increases and beyond 25^0 batters angle the load carrying capacity decreases. Negative batter piles offer more resistance to deformation as compared to positive batter piles.

Another researcher, MIET Mohri et al. (2016) have done the lateral load capacity of pile foundation. Model tests conducted to determine the lateral load capacity of vertical and batter piles. The tests conducted in uniform fine sand. For batter piles and angle of pile kept 25˚. After conducted the test it was observed that the negative batter pile showed more resistance as compared to that of a vertical pile for a constant deflection subjected to lateral loads and similarly positive batter piles showed less resistance as compared to vertical piles.

2.4.2.Numerical modeling researches

H. Mroueh and I. Shahrour (2008), the research conducted on numerical analysis response of battered piles to inclined pullout loads using finite difference FLAC^{3D} software. The numerical concerns with the analysis of the response of a battered pile to inclined uplift load. The soil behaviour is an elastic perfectly plastic constitutive relation based on the non-associated Mohr–Coulomb criterion. Pile with a square cross section considered in the analysis. Furthermore, investigations showed that the response of piles to lateral and axial loads moderately affected by the shape of the cross section (circular or square cross section). The soil mass dimension depends on the pile diameter and length. The lateral extension of the soil mass is equal to 50Bp (Bp is pile width). The height of soil mass is L p+10Bp (Lp is the length of pile). The displacement at the base is restricted in all directions, while the displacement at the lateral boundaries is restricted in the normal direction.

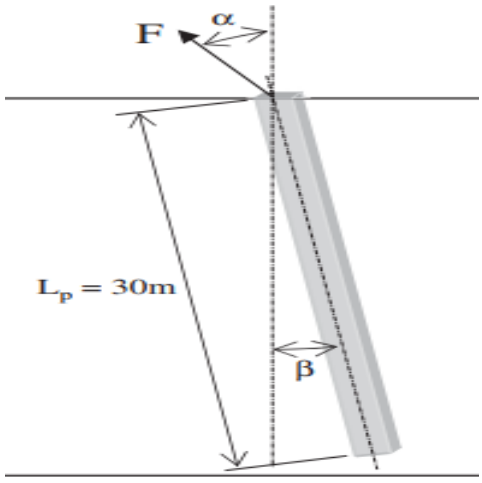

Figure 2-16: Model of batter pile to inclined uplift loads (Mroueh and &Shahrour, 2008)

Results show that the load inclination affects the response of battered piles in both the lateral and axial directions. The pile pullout capacity for forward load is higher than the reverse load. This result attributed to the upward soil movement induced in front of the pile by the forward loading. When the load acts on the direction of the pile, the horizontal movement of the pile induces an increase in the vertical stress at the soil–pile interface and consequently leads to an increase in the pile's pullout capacity in the horizontal direction.

Research done by Hussein and Isam (2008), presents a three-dimensional finite element analysis to the response of battered piles combined lateral and vertical pullout loads. Analyses carried out using an elasto-plastic constitutive law based on the non-associated Mohr–Coulomb criterion. The influence of the contact condition at the pile–soil interface was investigated. Analyses show that the load's inclination with regard to the pile's axis affects both the lateral and axial response the battered piles. Analyses also show that the pullout capacity of battered piles affected by the pile inclination regarding the vertical axis as well as the load's inclination regarding the pile axis. The pile pullout capacity decreases with load inclination, in particular at the low values of load inclination regarding the pile axis. The result shows that pile pullout capacity for forward load is higher than that for reverse load. This result attributed to the upward soil movement induced in front of the pile by the forward loading. The investigation of the contact condition at the soil–pile interface shows that the possibility of sliding at the soil–pile interface affects the response of battered piles subjected to loads with low inclination regarding

the pile's axis. The influence of the contact condition at the soil–pile interface neglected when the load inclination regarding the pile's axis exceeds 10◦.

Similar research done by Hazzar et al. (2017), three-dimensional finite difference parametric analyses is carried out to investigate the influence of vertical load on the lateral performance of battered piles in both sandy and clayey soils. Different batter angles and soil stiffness considered to examine the salient features of this complex soil–structure interaction problem. Numerical results show that the lateral response of battered piles embedded in sands influenced by the value and the direction of the pile inclination, the presence of vertical loads as well as the soil state of density. The response of piles at positive batter angles, however, does not appear to vary considerably with the batter angle or sand density. The effect of vertical load on lateral response of battered pile in sand found to be very pronounced. On the other hand, the lateral response of pile embedded in a clayey soil at negative batter angles increase greatly with increase inclination angle. The lateral response of the piles with positive inclination angles is independent of the batter angle and the soil stiffness. Moreover, the presence of a vertical load prior to the application of a lateral load to a battered pile does not alter its lateral capacity.

CHAPTER THREE

3 SITE GEOLOGY AND ASSESMENT OF BEARING CAPACITY

3.1. General description of the study area

The study area is chosen for two selected sites in Addis Ababa simply to take the soil properties for the input of the software. The first one is Wegagen Bank site soil properties around stadium and secondly the new headquarter building of commercial bank of Ethiopia around the national theatre sites.

Wogagen Bank (WB) site is located in Addis Ababa adjacent to Lalibela restaurant around stadium. The building consists of three basement floors, one ground floor and twenty four floors for shop and office purpose. The existed pile has a diameter of 600 mm with estimated design load on the foundation 905 N per pile. The length of the pile is 21 m and it is located below 10 m from natural ground level. Then the study wants to see the effectiveness of the existed vertical pile, if an imaginary batter pile is replaced and compare the results to know the applicability of batter in geotechnical fields.

The New Headquarter Building of Commercial Bank of Ethiopia (CBE) project is located in central Addis Ababa, Kirkos sub city, around the national theatre. The building complex consists of mainly office buildings, including 1 tower building of 46 floors, 2 podiums of 5 floors (business center and conference center) and 1 underground parking. The foundation is founded at the depth of 21 m under the ground surface. The estimated load on the foundation is **21** KN per pile and average pile diameter of 2 m with proposed length of 10 m.

3.2. Site geology

3.2.1. Site geology of Wegagen Bank

Backfill materials characterize the top most part of the project site with maximum depth of 1.45 below existing ground level. Underlying the back fill layer, dark to reddish brown, soft to firm, highly plastic clay silt was encountered maximum thickness of 2.55 m. Reddish brown to yellowish grey, stiff to very stiff, high plastic clay silt was encountered. Following the high

plastic clay soil layer, yellowish grey to reddish brown, very stiff, low plastic clay silt was encounter having a maximum thickness of 9.7 m yellowish grey to brown, very stiff hard, high plastic clay silt was encountered underlying the above low plastic clay silt layer having a maximum thickness of 10.45m. Underlying the soil layers in all the boreholes alternating layers of slightly to moderately weathered basalt layer and relatively thin layers of dark grey to yellowish, low to medium plastic clayey silt/sandy silt soil layers were encountered.

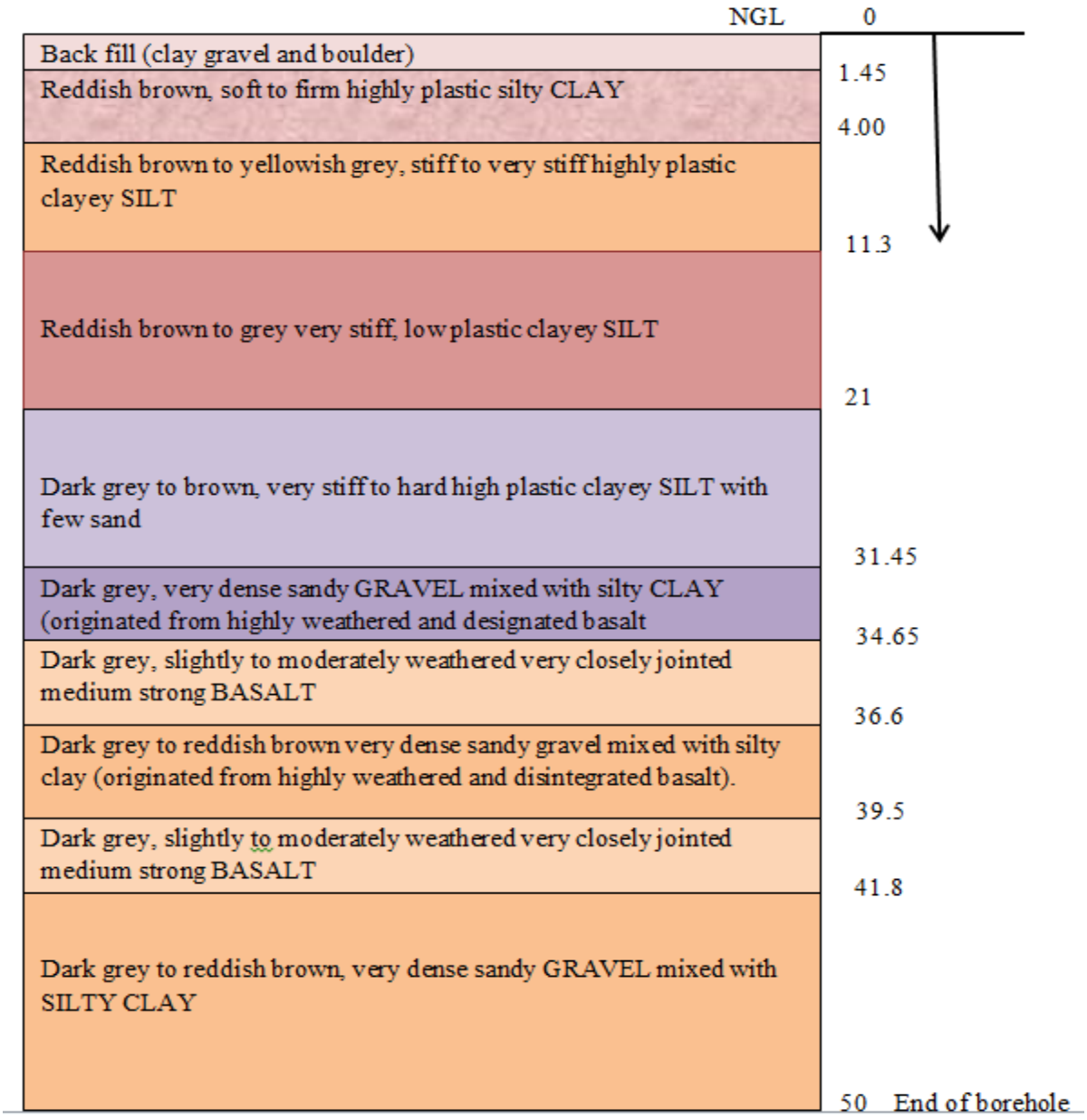

Figure 3-1: Soil profile for Wegagen Bank

One pile is chosen to deal the effect of single batter pile for resistance and deformation behaviour.

3.2.2. Site geology of Commercial Bank of Ethiopia (CBE)

Subsurface profile of the site and the engineering properties of the soil strata are investigated by Construction Design Share Company. The company carried out Core drilling of ten (10) boreholes with a maximum drilling depth of 90m along with in situ and laboratory tests. The following geological layers have been identified by the company.

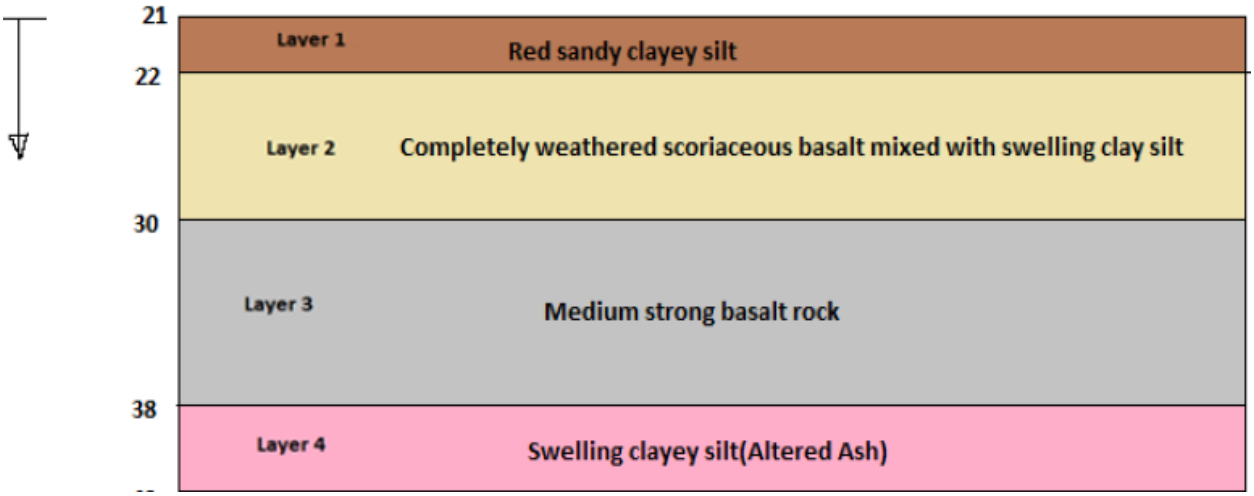

Figure 3-2: Soil profile for Commercial Bank of Ethiopia

Determination of soil parameter for model

Almost all of the soil parameters used for the analysis of the foundation is obtained from geotechnical reports; however some necessary data are not included in the investigation report. Therefore the parameters which could not be obtained directly from the laboratory tests, have been indirectly derived by using empirical correlations based on the recommendations of different literature, international geotechnical codes and standards. The data used for this study can be categorized in the following group;

1) Stiffness parameters; modulus of elasticity (**Es)** and Poisson‟s ratio (**v**)

2) Shear strength parameters; angle of internal friction (ϕ) and soil cohesion(**c**)

3) Unit weight or density of the soil (γ)

1) Stiffness parameters

a) Stiffness Modulus (Es)

The stiffness modulus Es is a basic parameter that describes the load-settlement behavior of soils and governs the results of settlement related problems.

Several methods are available for estimating the stiffness modulus of a soil as described by (Bowles 1996). Unconfined compression tests, tri-axial compression tests and in situ tests are among the test methods. The geotechnical investigation report has included stiffness modulus of values for different layers but some of them are not conducted. The elastic modulus of layers has been determined using German code (DIN4094-1&2 2002) and literature recommendations given by (Gu 2008).

b) Poisson's Ratio, v

Poisson's ratio is property of materials that describes volume change of the material in a direction perpendicular to application of a load. It is defined as the ratio of the lateral expansion to the axial compression of soils. (Bowles 1996) recommend a range of values of Poison's ratio between 0.4 and 0.5 for most clay and 0.2 to 0.4 for medium to dense cohesion less soil.

2) Shear Strength Parameters

Shear strength parameters, namely, angle of internal friction (Ø') and cohesion (c') are taken from literature recommendation given by (Braiud 2013). The shear parameters of the of some type of soil is taken by assuming the worst case layer

3. Unit weight or density of the soil

The Soil density is another soil property that the software takes as in put data. Therefore, the saturated and unsaturated unit weight of the soil is used in doing software modelling.

3.3. Assessment for Bearing Capacity

Prior to the detailed geotechnical design, a feasibility assessment is necessary by considering various foundation schemes. This is to investigate the adequacy of the batter pile on its ultimate bearing capacity. To deal with this capacity assessment, first the pile is taken as a vertical pile and second it is compared to a batter pile by varying the load from vertical to horizontal with different angles. Two broad modelling are considered in this research. First taking constant inclination of batter and varying application of loads with different angles and second by taking the loads constant and varying the batter angle. From this, a good resistance capacity of soil is chosen for the design and practical applications.

3.3.1. Bearing capacity of an existing pile for WB

Soil parameters are determined from soil investigation report. However, some parameters like Young's modulus and poison ratio are not obtained directly from soil investigation; those are correlated with soil parameter determination manuals simply by observing the physical properties of the soil.

ETG designers and consultants were done the soil investigation report for wegagen bank site in 2009. Standing from this report all soil parameters are determined which are necessary for the input for PLAXIS 3D foundation software. The foundation profile report is shown in figure 3.3 below starting from 10 m depth below OGL, because pile embedment starts at this depth.

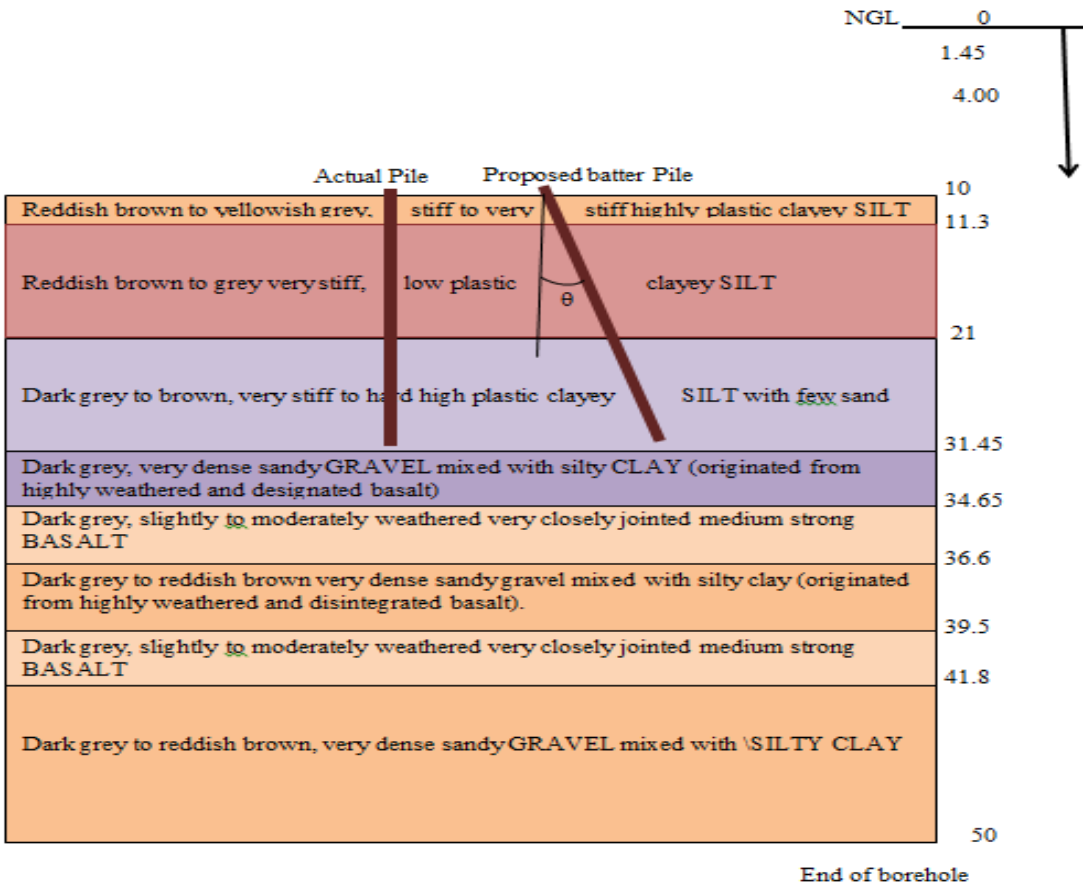

Figure 3-3: Pile and foundation profile Wegagen Bank

Table 3-1: Soil and pile properties Wogagen Bank

Soil Property	Wogagen Bank soil investigation report							
	Layer 1	Layer 2	Layer 3	Layer 4	Layer 5	Layer 6	Layer 7	pile
γ_{unsat}	17.29	16.66	12.7	16	20	16	20	-
γ_{sat}	20	20	18	18	20	18	20	24
Young's modulus E (N/m^2)	27000	39000	30000	60000	200000	60000	200000	2.62e7
Poisson ratio (v)	0.3	0.3	0.3	0.3	0.25	0.3	0.25	0.22
Cohesion (N/m2)	51.33	73.33	5	5	25	5	25	-
Friction angle	0	0	12	12	35	12	35	-

A. Axial compression capacity

The ultimate capacity of pile is derived from both its side and tip resistance. The side or shaft resistance of the pile is calculated using the method, whereas the tip resistance is taken from the compressive strength test result of the investigation report.

$Q_U = Q_p + Q_f = A_p q_p$ Where, $Q_p = A_p(CNc + 0.5\gamma BN_\gamma + \gamma D_f N_q)$

$Q_f = P\sum_{L=0}^{L=L} f_s \Delta L = \sum As\ f\ s,$ Where, A_p = area of the pile tip

C = cohesion of the soil supporting the pile tip q_p = unit point resistance

q' = effective vertical stress at the level of the pile tip, N_c, N_q = the bearing capacity factors

P = perimeter of the pile length f_s = unit frictional resistance at any depth z

ΔL = incremental pile length over which p and fs are taken to be constant

1) Skin frictional resistance

For computing skin friction, α method is used to calculate the bearing capacity of the shaft. $Qs = \sum As\ f\ s$, $fs = \alpha c + qk\tan\delta$,

it is assumed that only 21 meter of the pile is would have contribution for the skin friction from the clayey silt layers. From previous soil investigation and worsts value of c = 72 kpa and $\gamma = 17\ N/m^2$ is taken.

Taking α = 0.55 based on c = c = 72 kpa, the ultimate pile friction resistance capacity is calculated as:

$Qs = \sum As\ (\alpha c + qk\tan\delta)$

Qs = (3.46*0.6*21) [(0.55*72) + ((17 – 9.81) *21/2)*)0.33*0.49)] = 2049.69 N

Taking factor of safety 3, the sum of the skin friction contribution shall be

Qs/SF = 2049.69 N/3 = 683 N

2) End bearing capacty

Qp = Ap q, Ap = $3.14(0.6)^2/4 = 0.2826\ m^2$

q= compressive strength of highly weathered and decomposed basalt and slightly weathered basalt (8 kg/cm^2) is taken as allowable bearing pressure.

Qall = 8 kg/cm^2* 2826 cm^2 * 9.81m/s^2 = 2260 kg * 9.82 m/s^2 = 222 N

Therefore allowable bearing capacity of a pile:

Qall = (683 + 222) N = 905N for a single pile.

B. Lateral capacity

Brom's (1964 a) analyzed free head and fixed head piles separately. In this research, free head single pile is considered with lateral loading. Basic theory and assumptions made to obtain the ultimate resistance of piles. Simply it is calculated using the following chart to determine the ultimate capacity of lateral loaded pile.

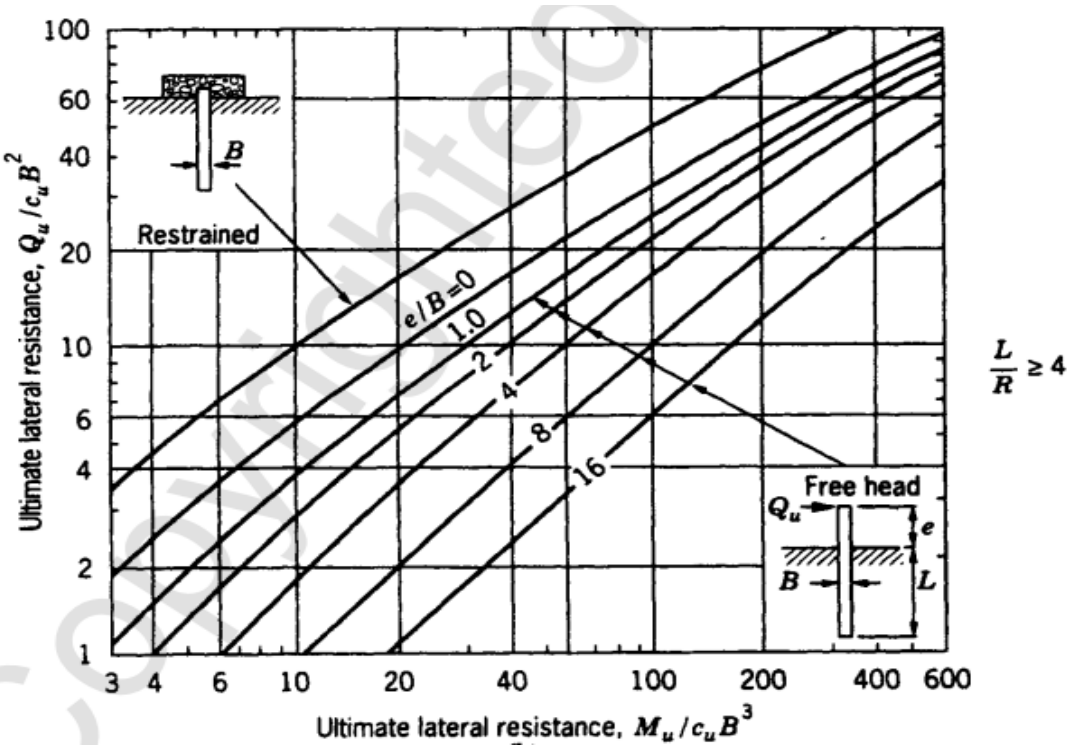

Figure 3-4: Ultimate lateral load capacity of piles (Broms 1964)

M_u/C_uB^3 is calculated from the given soil investigation report, where

Mu = ultimate moment on the pile

= 0.6Zfy by taking the yield strength of pile reinforcement fy = 450 Mpa

and Z = I/(B/2) where I = moment of inertia for circular pile, B = pile diameter

$Z = ((3.14*0.6^4)/64)^4/(0.6/2) = 0.0212\ m^3$ then,

Mu = 0.6*0.0212 m^3 * 450 Mpa = 5724 KN-m, Taking C=Cu = 72 Kpa

$M_u/C_uB^3 = 368$, from the chart, $Q_u/C_uB^2 = 75$ then,

Qu = 1944 KN, taking factor of safety = 3 and

Qall = 1944/3 = 648 N

C. Proposed batter pile capacity for WB

The theory of ultimate bearing capacity Qult of batter pile computed using a theory suggested by Meyerhof and Ranjan et al 1981. It is based on the assumption that vertical pile with central inclined load is equivalent to batter pile inclined and subjected to vertical load. According to Meyerhof et al 1981, the normal capacity of pile given by the equation described in chapter 2:

$$\left(\frac{Q_{\alpha u}\cos\alpha}{P_u}\right)^2+\left(\frac{Q_{\alpha u}\sin\alpha}{Q_u}\right)^2=1$$

Where, Pu = ultimate axial vertical load capacity

$P_u = \gamma L N_q A_t + K_s \gamma L \tan\alpha (A_s/2)$, for cohesionless & $P_u = 9c_U A_t + \alpha c_U A_s$, cohesive soil

Qu = ultimate pile capacity under horizontal load ($\theta = 90^0$)

Axial and lateral capacity of the pile is calculated in the above section. Then,

$$\left(\frac{Q_{\alpha u}\cos 20}{905}\right)^2+\left(\frac{Q_{\alpha u}\sin 20}{648}\right)^2=1$$

$Q_{\alpha u}$ = 858.5 N allowable batter pile capacity

3.3.2. Bearing capacity of an existing pile for CBE

The bearing capacity of existed pile in Commercial Bank of Ethiopia first determined and later as it replaced by batter investigated.

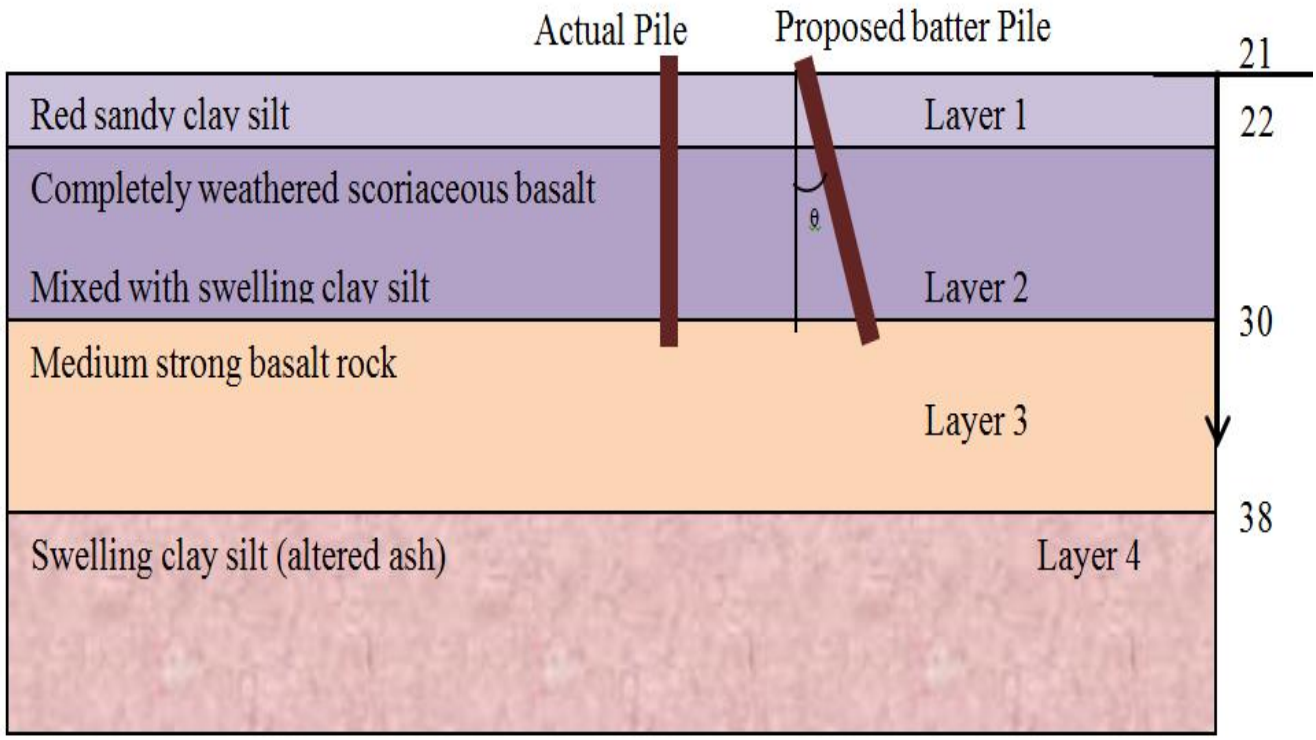

Figure 3-5: Pile and foundation profile of Commercial Bank of Ethiopia

Table 3-2: Soil and pile properties Commercial Bank of Ethiopia

Soil Property	Commercial Bank of Ethiopia soil investigation report				
	Layer 1	Layer 2	Layer 3	Layer 4	pile
γ_{unsat}	17.29	16.66	12.7	16	-
γ_{sat}	20	20	18	18	24
Young's modulus E (N/m^2)	27000	39000	30000	60000	2.91e7
Poisson ratio (v)	0.3	0.3	0.3	0.3	0.22
Cohesion (N/m2)	51.33	73.33	5	5	-
Friction angle	3	3	12	12	-

Axial Compression Capacity

1) Skin frictional resistance using α method (Qs):

$Qs = \sum As\ f\ s$

Where: $fs = \alpha c + q k \tan\delta$,

As = effective pile surface area c = average soil cohesion = 30kpa

q = effective vertical stress on the element α = adhesion factor = 0.55

k = coefficient of lateral earth pressure = $1-\sin\phi = 0.5$

δ = effective frictional angle between soil and pile material = 0.7ϕ

ϕ = angle internal friction of the soil = 37º

Qs = (3.14*2*10)*[(0.55*30) + ((166+(17.7-9.8)*10/2)*0.5*0.48)

= (62.83)*[16.5+167.73] = 12.06MN

Taking factor of safety (FS = 3), Qs Allowable = 12.06/3 = 4 MN

2) End bearing

Qp = Ap q

Where: Ap = Cross sectional Area of the pile

q = compressive strength of the medium strong basalt layer (q =quit/10 = 2.4 Mpa)

Qp = (3.14*22/4)*2.4 = 7.536MN

Allowable total bearing capacity of the pile (Q_T) is the summation of shaft resistance and end bearing resistance

$Q_T = 4+7.536 = 11.54MN$

Lateral capacity

Mu/CuB3 is calculated from the given soil investigation report, where

Mu = ultimate moment on the pile

= 0.6Zfy by taking the yield strength of pile reinforcement fy = 450 Mpa

and Z = I/(B/2) where I = moment of inertia for circular pile, B = pile diameter

$Z = ((3.14*2^4)/64))/(2/2) = 0.785$ m3 then,

Mu = 0.6*0.875 m3 * 450 Mpa = 236250 N-m

Taking C=Cu = 72 Kpa, similar to WB

Mu/CuB3 = 410, from the chart figure 4.1, $Qu/CuB^2 = 80$ then,

Qu = 2340 KN, taking factor of safety = 3 and

Qall = 23040/3 = 7680 N

3.3.3. Bearing capacity of a proposed batter pile for CBE

The theory of ultimate bearing capacity Qult of batter pile computed using a theory suggested by Meyerhof and Ranjan et al 1981. It based on the assumption that vertical pile with central inclined load is equivalent to batter pile inclined and subjected to vertical load.

Axial and lateral capacity of the pile is calculated in the above section. Then,

$$\left(\frac{Q_{\alpha u}\cos 20}{11540}\right)^2+\left(\frac{Q_{\alpha u}\sin 20}{7680}\right)^2=1$$

$Q_{\alpha u}$ = 10,774.5 N Allowable batter pile capacity

CHAPTER FOUR

4 FINITE ELEMENT MODELLING AND ANALYSIS OF A SINGLE BATTER PILE

4.1 Introduction

The use of numerical models to simulate complex problems has become more popular due to advances in technology and computer speed. Numerical models allow multiple simulations to explore and it allows researchers to gain a better understanding of the mechanisms involved.

The full-scale test for pile is a difficult task due to their size and cost. Researchers can explore the interaction of both pile and soil under various loading scenarios and soil properties by using numerical methods, such as finite element method. The research presented in this thesis uses the finite element computer package, PLAXIS 3D, to explore the interaction between different pile load combinations.

PLAXIS 3D is a multipurpose computer package that allows users to investigate mechanical, structural, and geotechnical problems under loading. It is an ideal package due to its capability in modelling complex interactions between several bodies, and the available constitutive models for both structural and geotechnical materials. The package also allows residual stress fields to define real situations. It is important to verify the numerical model to insure its predictions with in an acceptable limit when compared to real life situations. The following sections show the finite element model used to achieve the aims of this work, along with the verification cases used to test the developed pile model.

4.2 Soil and pile modelling

The model composed of three steps in the simulation. The first is keeping the vertical displacement constant and simulate it by varying the batter angle of the pile. The second step also simulated as keeping the lateral load constant to find the maximum failure effect by varying the batter angle.

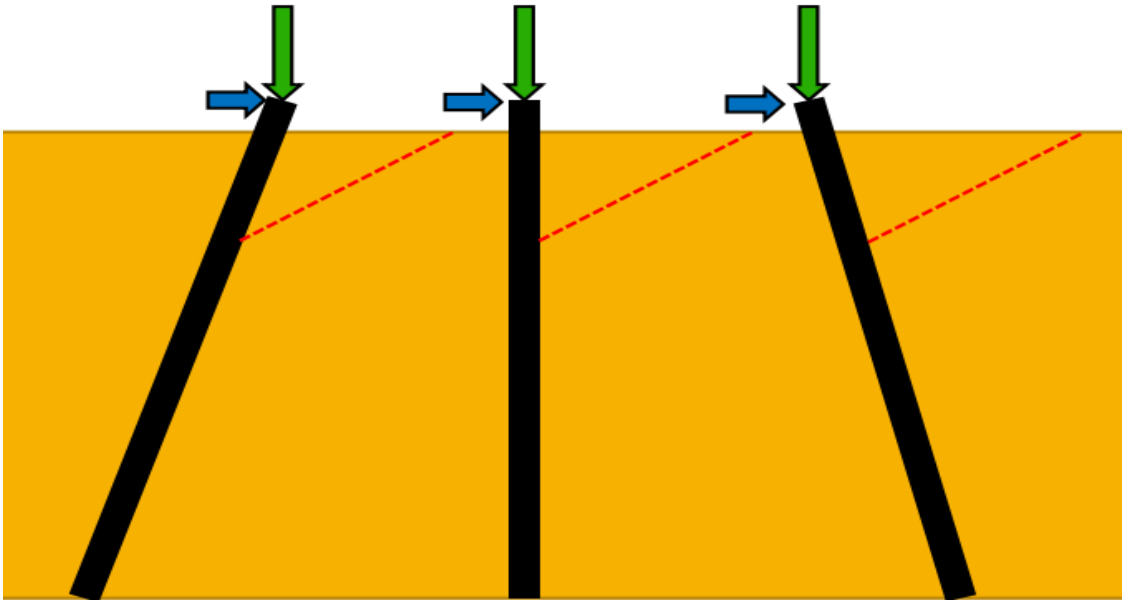

Figure 4-1: Load and pile inclination model

PLAXIS 3D is a complete environment that provides a simple consistent interface for creating, submitting, monitoring and evaluating results, which works on finite element method. Abaqus working window divided in to modules. Each module defines the logical aspect of the modelling process; defining geometry, defining material properties, and generating mesh, which constitute to form a finite element model.

4.3 Size of the soil model

As a soil is a continuum material, the size of a soil model should specify to analyze the effects of stress and deformations. Grid size and boundary conditions used in mesh are a crucial control factors that determine the efficiency of the numerical calculations. For example, a smaller grid size and larger study area increase the precision of the modelling compared to a coarse mesh used with boundary conditions, Chen and Hsu (2017). To avoid boundary effects sensitivity analysis carried out. The mesh is refined around the pile, in order to increase precision in areas of high strain gradient. According to Karthigeyan et. al (2018) the soil mass dimension depends on the pile width and length. The lateral extension of a soil mass is equal to 50B pile (B pile is pile width). The height of soil mass is Lp + 10B pile (Lp is the length of the pile. Whereas according to Hazzar et al (2017) for floating batter pile with a diameter “D” and length “L” embedded in soil stratum the total thickness corresponding to $L\cos\beta + 6D$, where β is batter angle. However, for the

lateral extension, the distance decided after performing a trial analysis with several horizontal distances until the displacements and stresses of the pile did not change significantly with further increasing of the distance. Taking of the above-published studies as a reference, the vertical extension of the soil mass calculated for the specified length, diameter and batter angle of the pile and made it constant and sensitivity analysis carried out for a variable lateral extension of the model.

4.3.1Boundary Conditions

Boundary condition defines the state condition of the model for its end faces. The nodes at the base of the mesh and far bound fixed against all displacements. The nodes on the plane of symmetry restrained from moving normal to the plane of symmetry, but can move along the plane of symmetry.

PLAXIS automatically imposes a set of general fixities to the boundaries of the geometry model. These conditions generated according to the following rules:

- Vertical model boundaries with their normal in *x*-direction (i.e. parallel to the *y*-*z* plane) are fixed in *x*-direction (*ux* = 0) and free in *y*- and *z*-direction.
- Vertical model boundaries with their normal in *z*-direction (i.e. parallel to the *x*-*y* plane) are fixed in *z*-direction (*uz* = 0) and free in *x*- and *y*-direction.
- Vertical model boundaries with their normal neither in *x*- nor in *z*-direction (skew boundary lines in a work plane) are fixed in *x*- and *z*-direction (*ux* = *uz* = 0) and free in *y*-direction.
- The model bottom boundary is fixed in all directions (*ux* = *uy* = *uz* = 0).
- The 'ground surface' of the model is free in all directions.

4.3.2Mesh Generation

To perform finite element calculations, the geometry divided into elements. When the geometry model is fully defined and material properties were assigned to all soil layers and structural objects, it is recommended to first generate a 2D mesh of work planes. The 2D mesh were made fully satisfactory including global and local refinements; before proceeding to the 3D mesh generation. It is advisable to avoid very fine meshes, since this will lead to excessive calculation

times. If the 2D mesh is satisfactory, 3D mesh generation can be performed. The 3D mesh generation process will take the information from the work planes at different levels as well the soil stratigraphy from the boreholes into account. The 3D FOUNDATION program allows for a fully automatic generation of 2D and 3D finite element meshes.

2D Mesh Generation

The generation of the 2D mesh is based on a robust triangulation procedure, which results in 'unstructured' meshes. These meshes may look disorderly, but the numerical performance of such meshes is usually better than for regular (structured) meshes.

The required input for the 2D mesh generator is a plane geometry model composed of points, lines and clusters. When creating structural elements or loadings, corresponding geometry lines are automatically created in each work plane. In this way, all work planes have the same composition of points and lines. Points and lines may also be used to influence the position and (local) distribution of elements.

Clusters are areas that fully enclosed by geometry lines. Clusters automatically generated during the creation of the geometry model. The generation of the mesh is started by clicking on the mesh generation button in the tool bar or by selecting the Generate option from the Mesh sub-menu. The generation also activated directly after the selection of a refinement option from the Mesh submenu. Before the actual 2D mesh generation is performed, possible crossings between soil layers and work planes are determined from the borehole data. If a soil layer crosses a work plane, additional geometry lines introduced in the geometry model. This is to make sure that a consistent 3D mesh can be generated, taking into account both the work plane data as well as the bore hole data. After the 2D mesh generation, the Output program started and a plot of the 2D mesh is displayed. Although interface elements have a zero thickness, the interfaces in the mesh are drawn with a certain thickness to show the connections between soil elements, structural elements and interface elements.

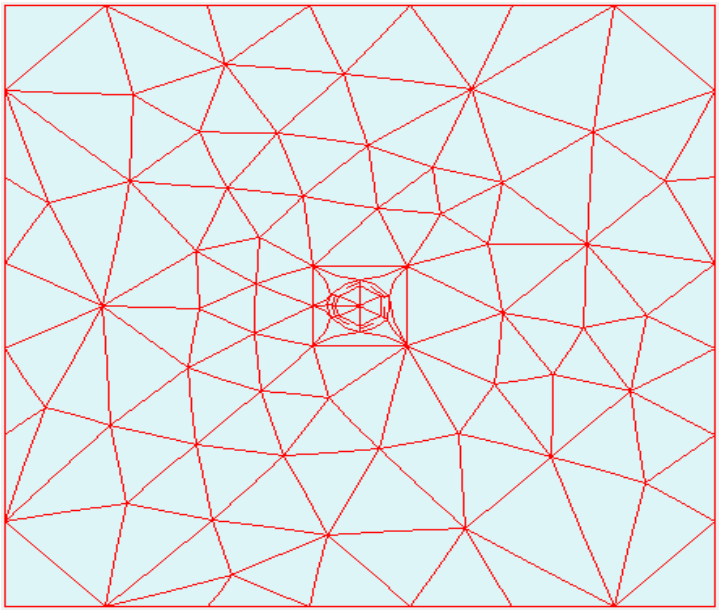

Figure 4-2: 2D mesh in PLAXIS

3D Mesh Generation

When the 2D mesh is satisfactory, a fully 3D mesh can be generated. This can be done by clicking on the 3D mesh generation button or selecting the corresponding option from the Mesh sub-menu. In fact, it is possible to generate a 3D mesh directly, i.e. without generating a 2D mesh first. The 3D FOUNDATION program will then automatically generate a 2D mesh using default or existing coarseness settings and subsequently generate a 3D mesh. However, in this case the user has less control over the accuracy of the mesh.

The 3D mesh is based on a system of horizontal and pseudo-horizontal planes in which the 2D mesh is used. The work planes and the soil layer boundaries as defined by the boreholes form these planes. A single borehole leads to soil layer boundaries that are true horizontal planes. When multiple boreholes are used, the soil layer boundaries may form non-horizontal planes. The precise vertical position of such planes in all mesh points is obtained by interpolation from the levels as defined in the various boreholes. When a non-horizontal plane crosses a work plane, a mesh line will be available in the 2D mesh to guarantee consistency of the 3D mesh at such crossings.

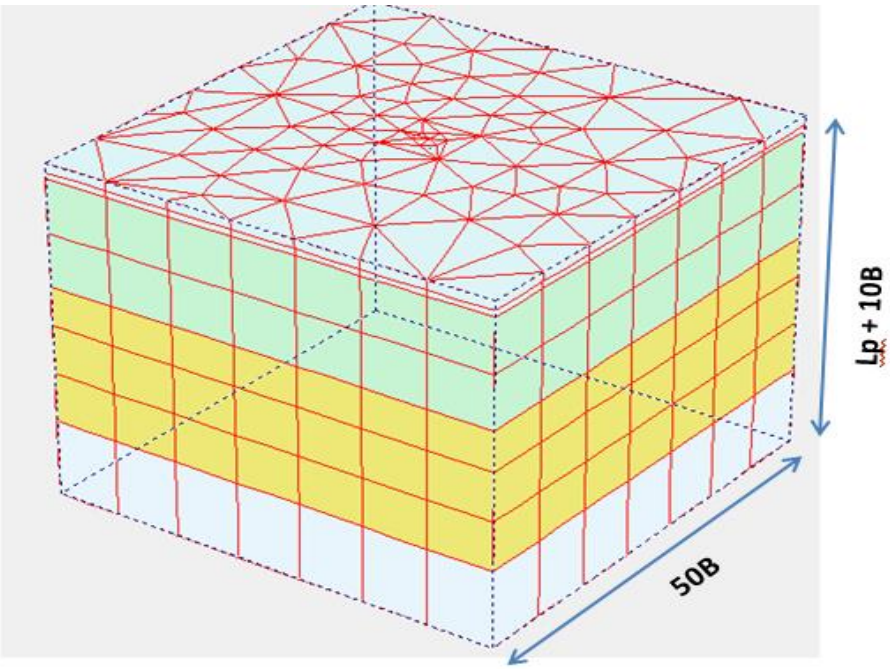

Figure 4-3: 3D mesh in PLAXIS

4.3.3Mesh Sensitivity analysis

Mesh size is one of the most common problems in finite element analysis. Bigger elements give bad results and very fine elements give long computing time. In order to establish a suitable mesh size:

- Perform chosen analysis for several different mesh sizes
- Notice where high deformation or high stress occur, perhaps it is worth to refine mesh in those regions
- Collect data from analysis of each mesh: outcome, number of nodes in the model, computing time.

Reduction of finite element size leads to more elements, which in turn leads to more nodes in the model. If the chart build showing the outcome (first eigenvalue) dependence on node count. It also just as easy use a number of elements on the width of the part of the typical element to obtain a good mesh.

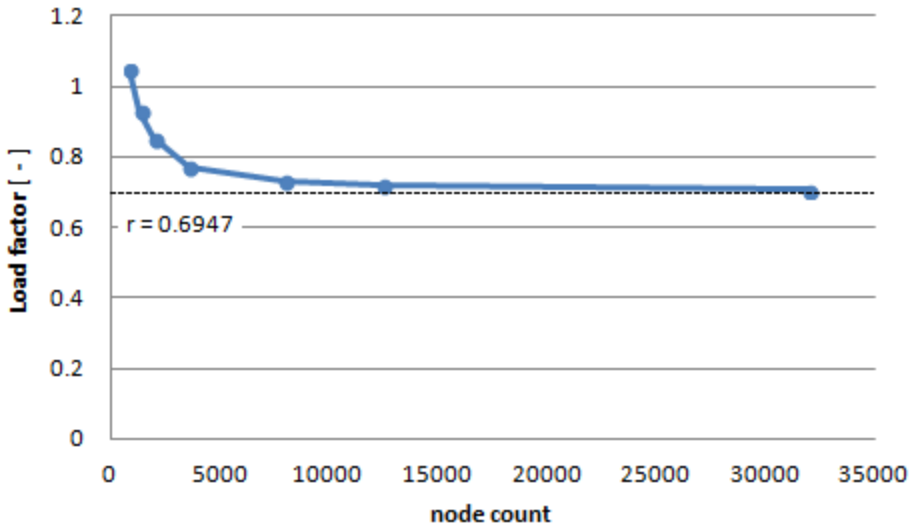

Figure 4-4: Sensitivity analyses for load factor and number of nodes

Therefore, it indicate good mesh at the beginning of the horizontal line in the curve. Since the correct mesh known, once can search how big errors made in the results for each element size. The following chart shows dependence between error and computing time, and between error and finite element size.

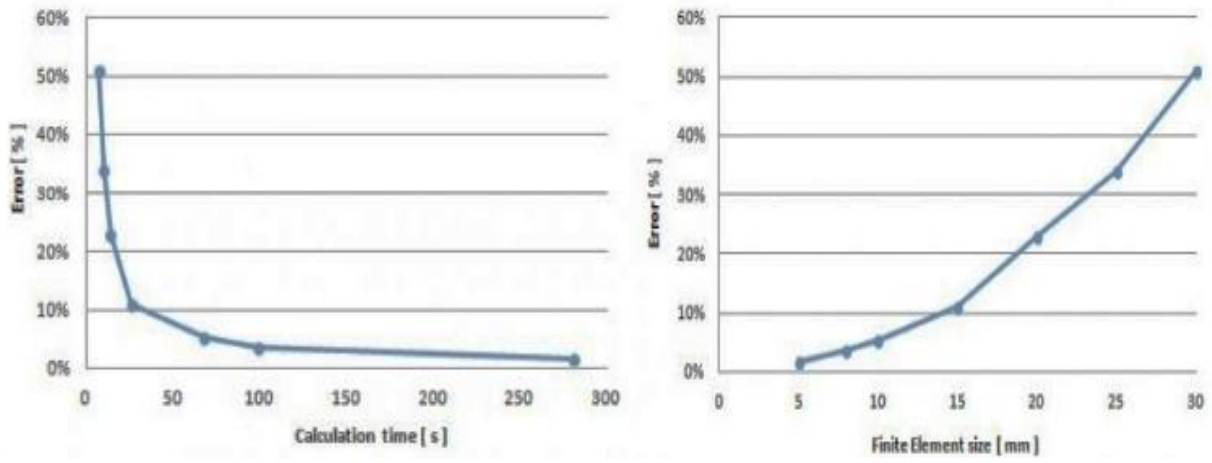

Figure 4-5: Sensitivity analysis for calculation time and element size

As shown in the above chart after a certain time accuracy decreasing is negligible even the time becomes larger and larger. As element size increases error increases and as element size decrease error become decrease due to the fact more discretization of the element become more accurate.

It should be smart on the selection of good meshes in the finite element mesh analysis. Using the above alternatives in sensitivity analysis I have choose the maximum stress versus number of elements in a single node.

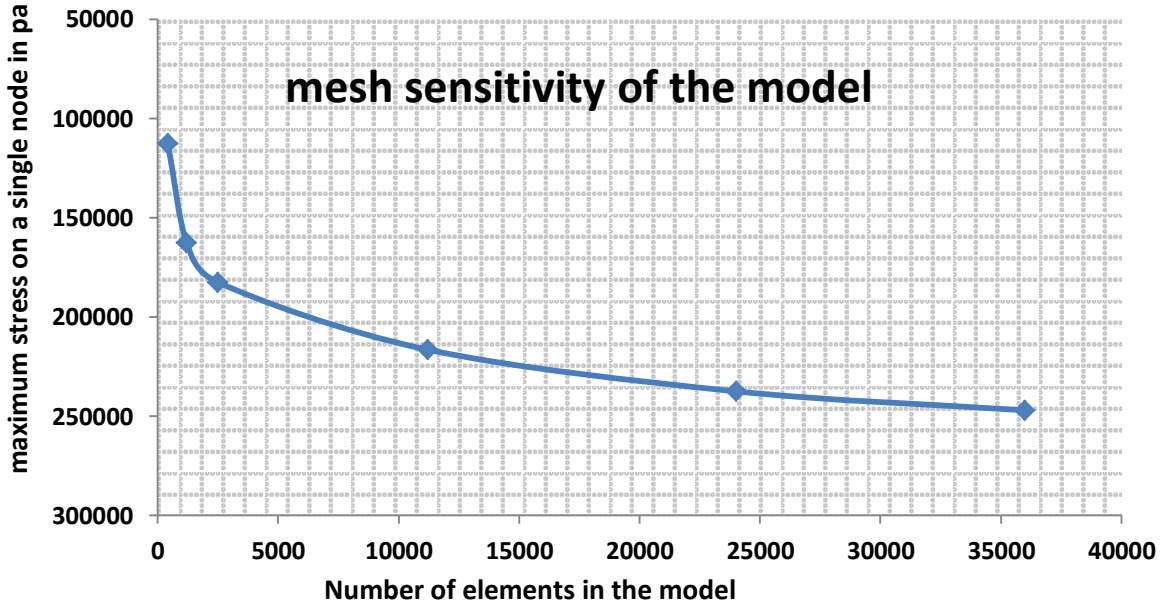

Figure 4-6: Sensitivity analysis between stress and number of elements in the model

From the graph, it decided that the mesh size of the model is appropriate about 36000 elements. After this, the increase of number of elements in the model it is less advantageous as compared to the computing time

4.3.4Model validation

The software, which is used for developing the model, must be validated before its result is accepted and applied to simulate the real world problems. Validation is the only way to justify the predictions of a numerical model to the true physics concerned (Sinha 2013).

To check the validity of the results the model (PLAXIS 3D), an example batter pile was analyzed. The model reported in the international journal of geotechnical engineering by (Mohammed Al-Neami- 2017), has been used in this thesis for validation purpose. The test was conduct in the laboratory using sandy soils with different inclination of batter angle.

As shown in figure 4.7 the pile has 50 cm diameter and it is tested with different inclination angles, which is 0^0, 10^0,20^0, 30^0, 40^0 degrees from the vertical axis. The soil used for the model is sandy soil with friction angle of 37 degree.

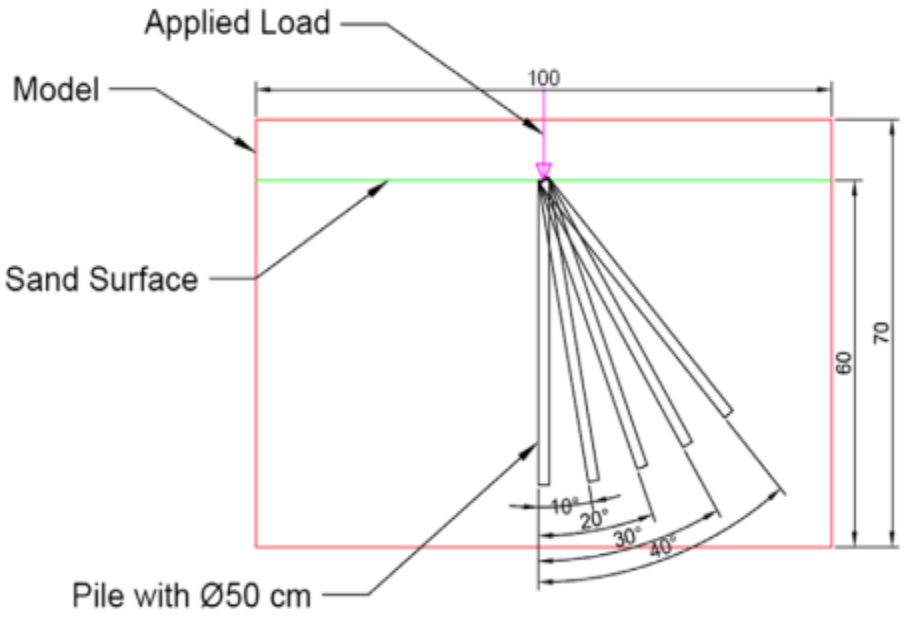

Figure 4-7: Model of Mohammed Al Neami (2017)

Table 4-1: Properties of model test

Material	γ_{unsat}(KN/m^3)	γ_{sat} (KN/m^3)	E (KN/m^2)	v	C (KN/m^2)	Φ (^{0})
Soil	17.8	17.8	13000	0.3	1	37
Pile	25	-	2.91e7	0.2	-	-

The PLAXIS 3D model result for validation purpose is described in figures 4.8 below. The load settlement predictions are compared to the model of Mohammed Al Neami etal 2017. From this, the result shows that a similarity of results with some differences due to the error occurred from material quality, measurement accuracy and software accuracy. As shown in figure 4.8 A the batter angle beyond 20^0 has smaller deformation as compared to 10^0 and plumb batter pile. This value has similar to the result obtained by Mohammed Al Neami 2017.

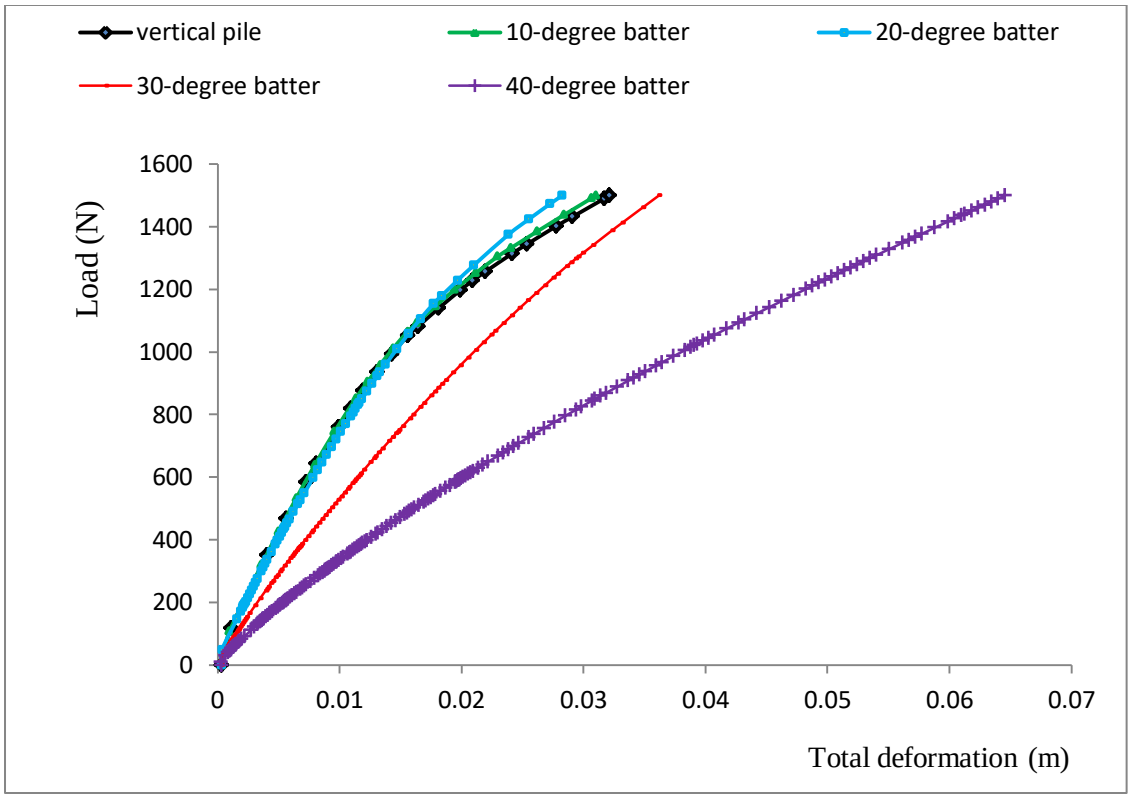
vertical pile
10-degree batter
20-degree batter
30-degree batter
40-degree batter
Load (N)
1600
1400
1200
1000
800
600
400
200
0
0
0.01
0.02
0.03
0.04
0.05
0.06
0.07
Total deformation (m)

A

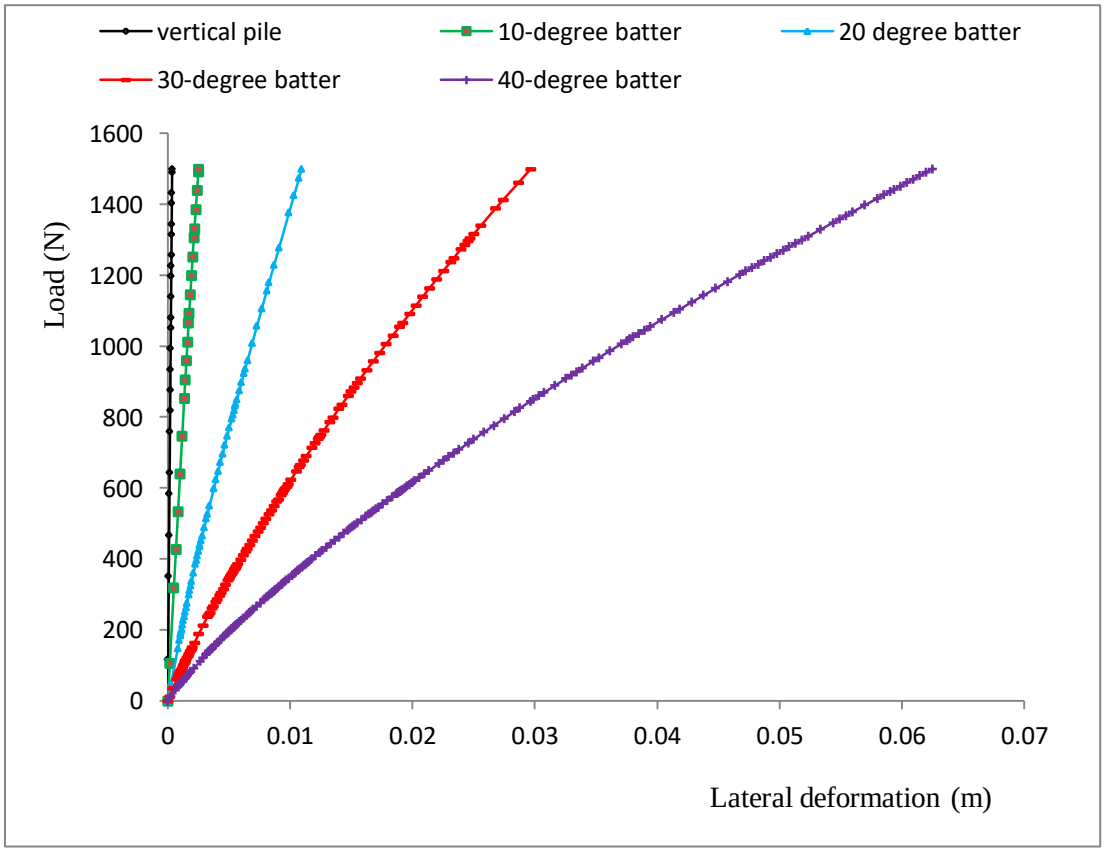
vertical pile
10-degree batter
20 degree batter
30-degree batter
40-degree batter
Load (N)
1600
1400
1200
1000
800
600
400
200
0
0
0.01
0.02
0.03
0.04
0.05
0.06
0.07
Lateral deformation (m)

B

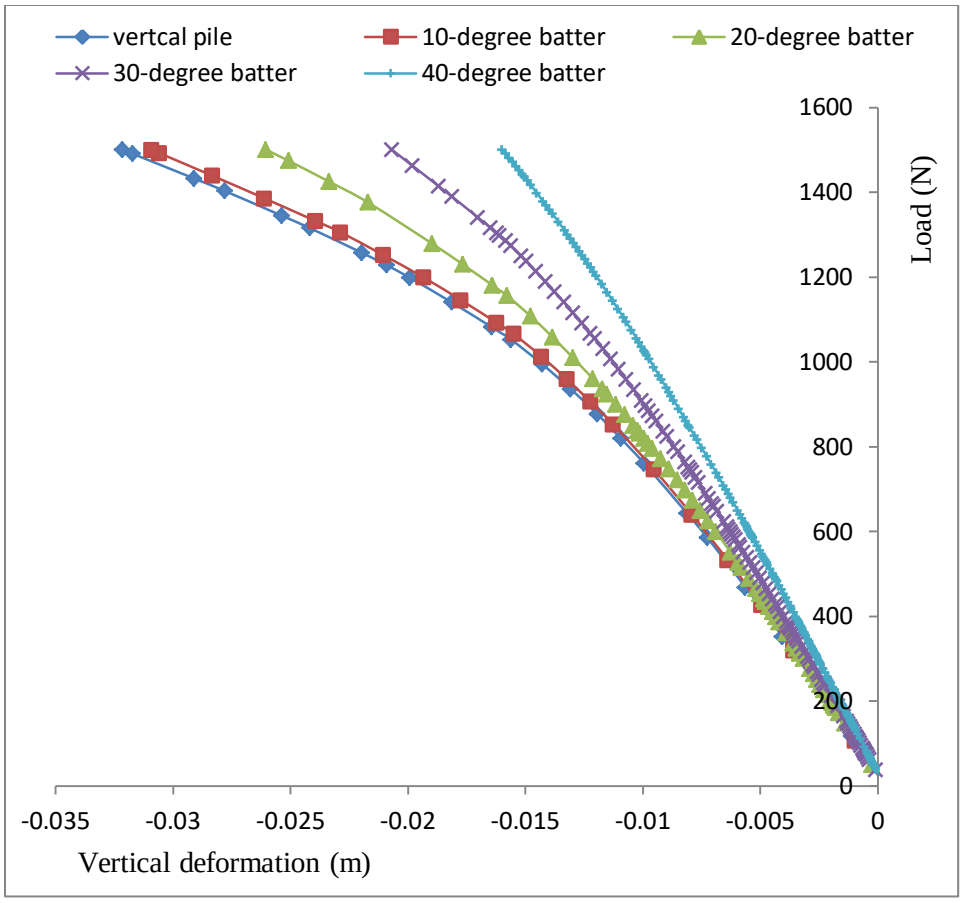

C

Figure 4-8: PLAXIS 3D model result A) Total B) Lateral C) Vertical deformations

Comparison of the two analysis results are described in table 4.2 below.

Table 4-2: Comparison of results

Batter angle (degree)	PLAXIS 3D model Load capacity (N)	Mohammed 2017 model Load capacity (N)
0 (plumb)	870	775
10	895	790
20	1010	925
30	840	830
40	570	660

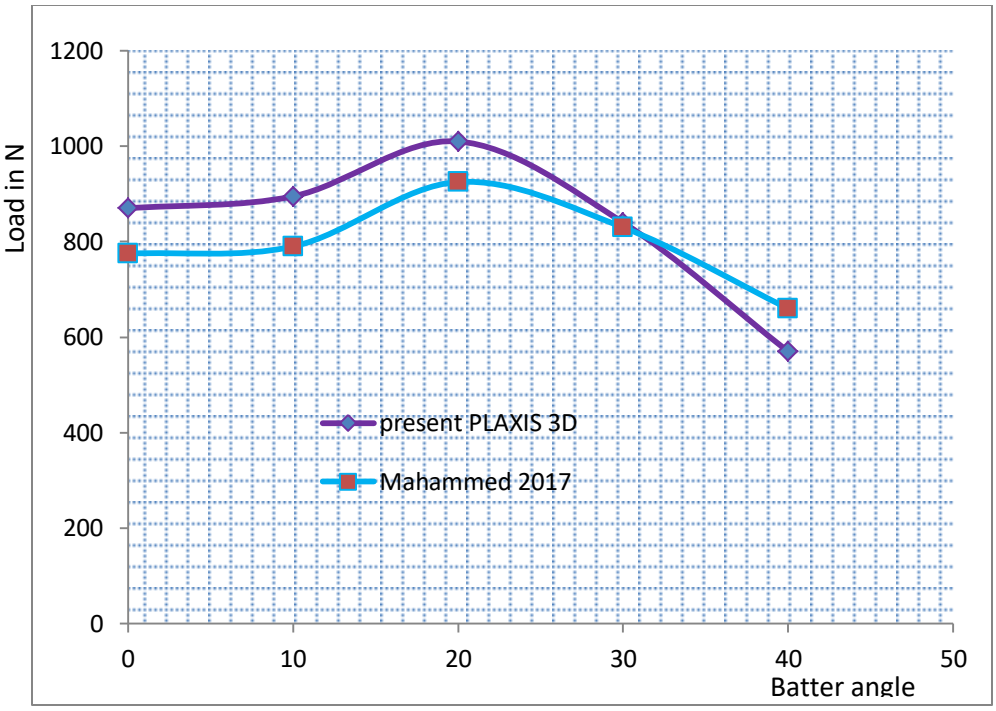

Figure 4-9: Comparison of PLAXIS 3D and Mohammed et al 2017 results

From the comparison result, load capacity on total deformation is increased until 20^0 for both models as shown figure 4-8 (A) above. After 20^0, the load capacity of batter pile is decreased for all cases. While the lateral component of deformation increases throughout when the batter angle increases in figure 4-8 (B). This shows lateral load capacity decreases when batter angle increases. Considerably the vertical component of deformation decreases as the equivalent batter angle increases from vertical.

CHAPTER FIVE

5 ANALYSIS RESULTS AND DISCUSSION

5.1 Introduction

The main objective of this study is to investigate the behaviour of batter pile to bearing behaviour of pile foundation. PLAXIS 3D model has been developed to study the behaviour of batter pile foundation with respect to vertical piles. In addition, to ensure the reliability of the results obtained by the developed model, comparison study was carried out between the results given by (Mohammed A. Al. Neami 2017) and those obtained from the current FE model with similar real structure geometry, loading and properties.

The scope of this study is to investigate the behaviour of piles under axial, lateral and inclined loads for the case of Addis Ababa soils (Wegagen Bank and Comercial Bank of Ethiopia sites). Therefore, the results obtained by the developed model are related with these parameters. Furthermore, discussions are made by considering comparisons to previous works related to the specific topic under consideration.

5.2 Behaviour of soil-pile model for WB

The pile modeled with PLAXIS 3D foundation software to simulate the existing pile and again model the pile if it is battered pile when the lateral loads on the structure is considered. As mentioned in chapter 3 the pile has a diameter of 0.6 meter with a length of 21 meter. Standing from this the proposed pile in Wegagen Bank building is long pile. The estimated design load taken from the soil investigation report is 905 N for single pile, but model is loaded until it fails which is the maximum value of 1700 N. First the pile is modeled as existing pile and lastly a single pile capacity is checked if it is better or not in resistance capacity. The deformations along load inclination has been simulated in this section. From model, maximum values of deformations are read from the analysis result. As shown in table 5.1 below with a constant values of applied load 1700 N in the soil pile system, there would be different extreme deformation values.

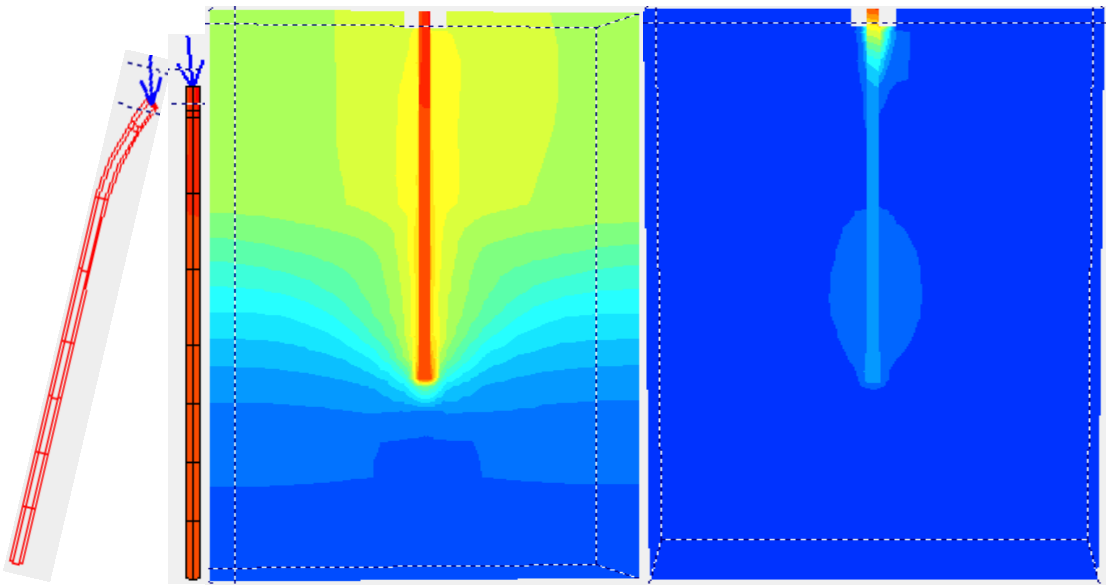

Figure 5-1: Deformation of soil and pile in PLAXIS 3D model

From the above figure 5.1, it is seen that deformation of soils around the pile higher and it decreases around the boundary of the soil. This shows stress is higher at the periphery of the pile, and it needs a special consideration for the design.

Table 5-1: Deformation according pile inclination angle for Wegagen Bank

Load direction	Symbol	Inclination from vertical (^{0})	Resultant Load (N)	Extreme total deformation (m)	Extreme lateral deformation (m)	Extreme vertical deformation (m)	Extreme trans deformation(m)
Vertical	WBV	0	1700	0.0442	0.00029	0.0442	0.000005
Inclined	WBI1	6.8	1700	0.0389	0.01590	0.0355	0.000065
Inclined	WBI2	13.6	1700	0.0516	0.04080	0.0316	0.000242
Inclined	WBI3	20.67	1700	0.0829	0.07740	0.0296	0.000105
Inclined	WBI4	28.1	1700	0.1350	0.13200	0.0279	0.00041
Inclined	WBI5	36	1700	0.2060	0.20400	0.0257	0.00129
Inclined	WBI6	55.44	1700	0.4150	0.41500	0.0177	0.0038
Lateral	WBL	90	1700	0.594	0.59400	0.0009	0.0046

WBV, WBI, WBL woegagen bank site pile vertical, inclined and lateral loads respectively.

As shown in figure 5.2 below the lateral and total deformation increases along the pile inclination increases from vertical to horizontal, while vertical deformation decreases when the load become laterally.

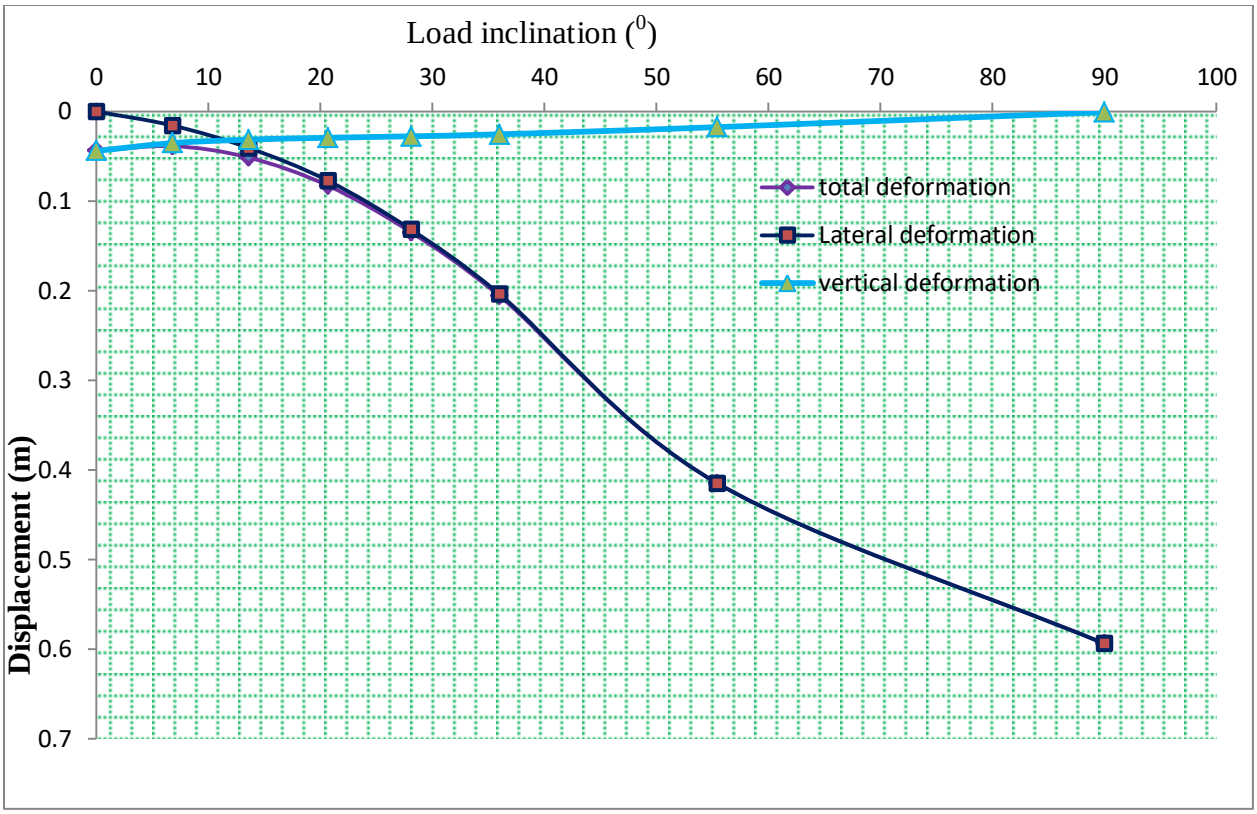

Figure 5-2: Extreme deformation of the model along load inclination with failure load

The graph shows that vertical deformation decreases smoothly but the lateral and total deformation increases for pile inclination angle increases until beyond 15^0 there is small deformation for all components.

From the figure 5.2 above, there is a comparative small deformation along the pile inclination within the range beyond 15^0. After 20-degree lateral and total deformations are much steper with a constant failure load of 1700 N. This shows as the load becomes horizontal from vertical the lateral and total deformation of the soil become higher and higher. While the vertical deformation decreases which is expected when vertical component of the load decreases in real situations. When the inclination angle greater than 40 degree the soil fails before the load reaches 1700 N. This shows for constant magnitude of the load, equal model size and similar soil properties the laterally loaded piles fail before axially loaded piles.

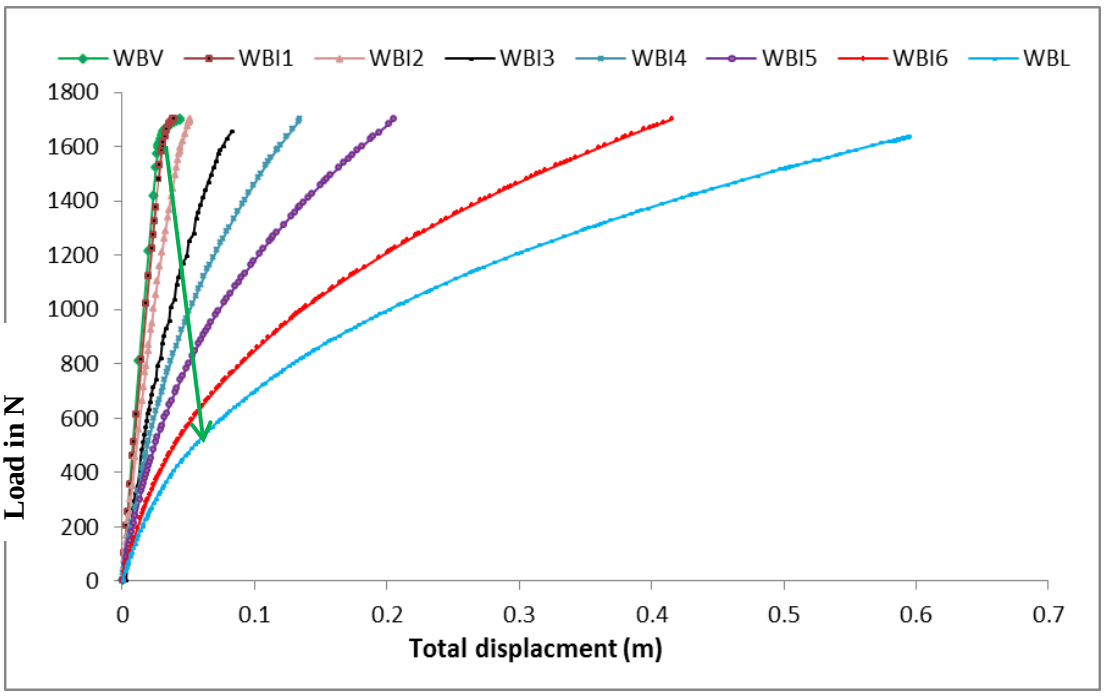

A

As shown in figure "A" above load inclination angle from the vertical increases **the total deformation** increases. Correspondingly, as angle increases the ultimate failure load decreases. This shows in the figure WBV is vertical load and it deforms (bends) around tips, which is 1650 N, load while WBL is lateral load and it deforms beyond 650 N

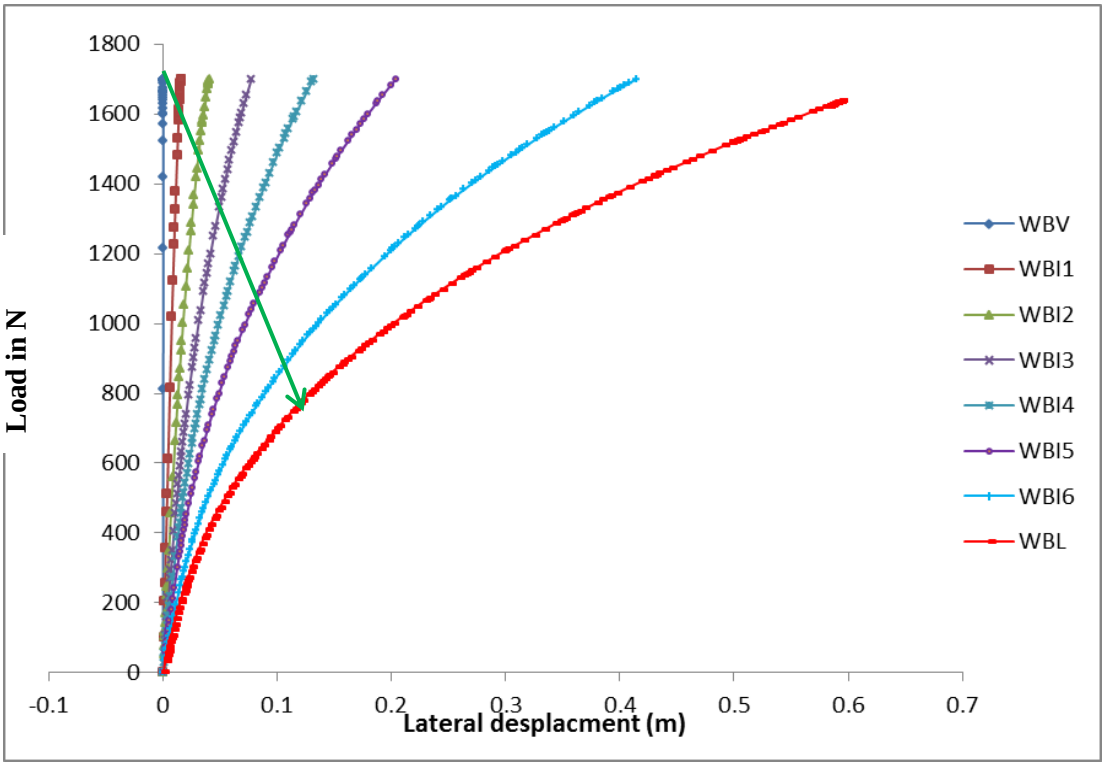

B

Similarly, for lateral component of deformation as load inclination angle increases from the vertical axis, the lateral deformation increases. Correspondingly, as angle increases the failure load decreases similar to the total deformation.

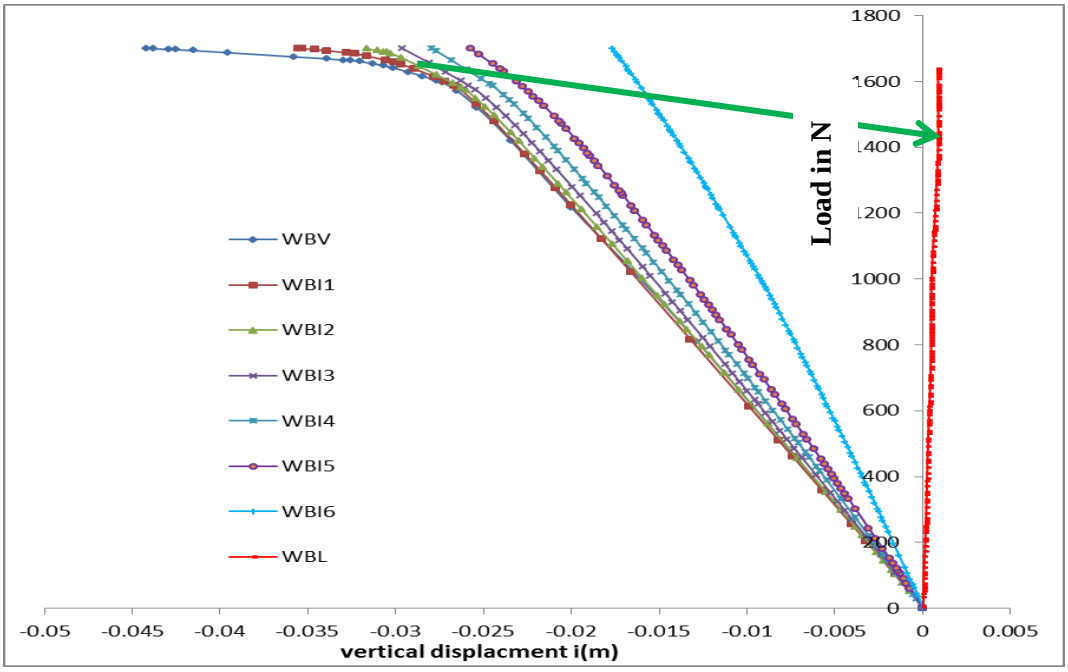

C

Vertical component deformation decreases as load inclination angle increases from vertical

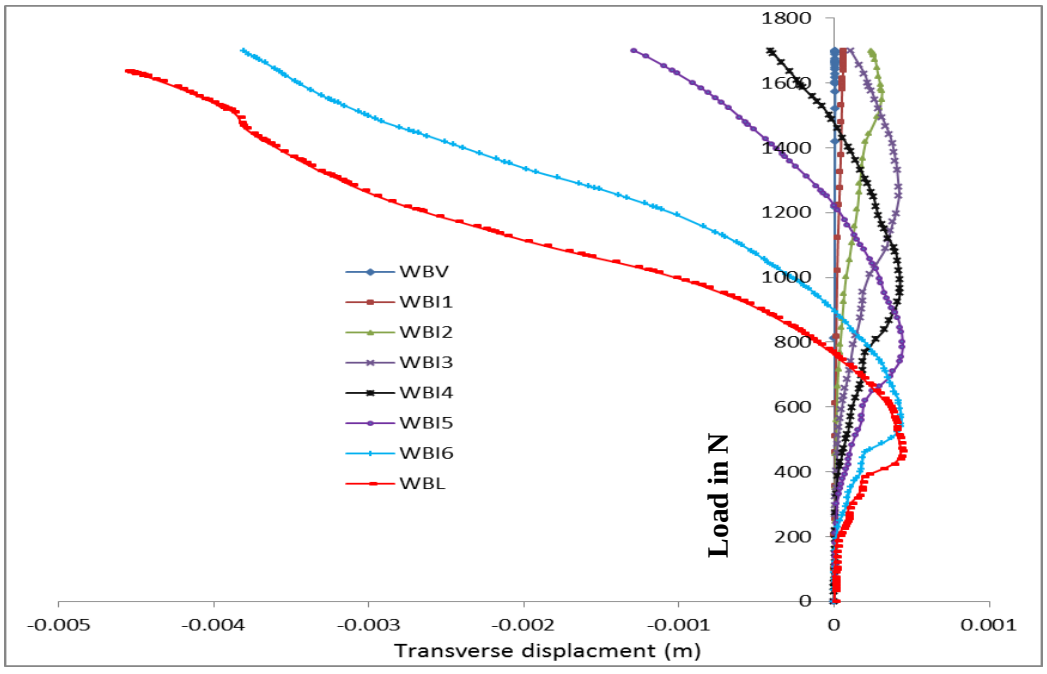

D

Figure 5-3: Deformation of a pile along pile load with different load inclination

A) Total B) Lateral C) Vertical D) transverse deformations

From the model analysis when the load becomes lateral from vertical for constant load, its deforms larger and larger. So deformation increases when pile inclination increases from vertical.

This shows the bearing capacity decreases when the load become lateral. As shown in the figure 5.3 (A, B, C), as the load becomes horizontal, ultimate capacity decreases; i.e. total deformation figure 5.3 A increases. When load is vertical symbolized by WBV, the curve bends on its ultimate load around 1650 N (figure 5.3 A), While the pile is loaded an angle of 55.4 degree (WBI5 figure 5.3 A) ultimate capacity becomes 650 N. This shows as the load inclination increases from vertical axis load capacity decreases and deformation increases.

In figure 5.3 C, when the pile load angle increases from the vertical axis, the vertical component deformation decreases as the load decreases. This is the same to the predictions that has been made in real situations. Even if it is very small, there is small deformation in transverse component of the load, which is perpendicular to the load direction as shown in figure 5.3 D.

It can be conclude that as the load inclination increases from the vertical axis, the total and lateral deformation increases and vertical component deformation decreases.

5.3 Behaviour of pile-soil model for CBE

The pile is modeled with PLAXIS 3D foundation software to simulate the existing pile and again model the pile if it is battered pile when the lateral loads on the structure is considered. As mentioned in chapter 3 the pile has a diameter of 2 meter with a length of 10 meter. Standing from this, the proposed pile in CBE is short pile. The estimated design load 11540 N is taken from the soil investigation report for a single pile but the model is loaded until it fails with a maximum load of 21000 N. First the pile is modeled as existing pile and lastly a single pile capacity is checked if it is better or not in resistance capacity. As compared to the vertical resistance, the lateral resistance is smaller than the vertical in real situations. Therefore, the lateral load is taken until it reaches one-half of the vertical loads.

Load direction	Symbol	Inclination from vertical (^{0})	Resultant Load (N)	Extreme total deformation (m)	Extreme lateral deformation (m)	Extreme vertical deformation (m)	Transverse deformation(m)
Vertical	CBEV	0	21000	0.0349	0.0001	0.0349	0.000028
Inclined	CBEVH1	13.77	21000	0.0313	0.0132	0.0291	0.000010
Inclined	CBEVH2	22.4	21000	0.0317	0.0318	0.0312	0.000129
Inclined	CBEVH3	31.6	21000	0.0377	0.0542	0.0203	0.000627
Inclined	CBEVH4	45.2	21000	0.0558	0.0449	0.0135	0.00026
Inclined*	CBEVH5	59	21000	0.0451	0.0512	0.00449	0.000579
Inclined*	CBEVH6	72.25	21000	0.0512	0.0459	0.00054	0.000728
Horizontal*	CBEH	90	21000	0.0388	0.0385	0.00463	0.000549

Table 5-2: Deformation according to pile inclination angle for Commercial Bank of Ethiopia

The upper script * shows soil fails before load reaches 21000 N

Commercial Bank of Ethiopia pile diameter is larger and the length is shorter than Wogagen Bank.

a)

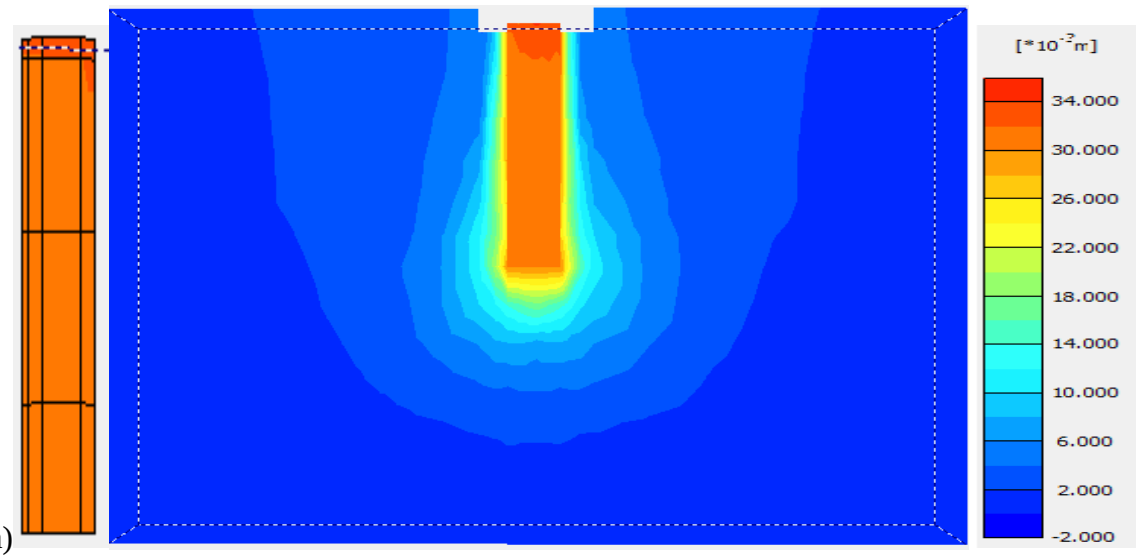

b)

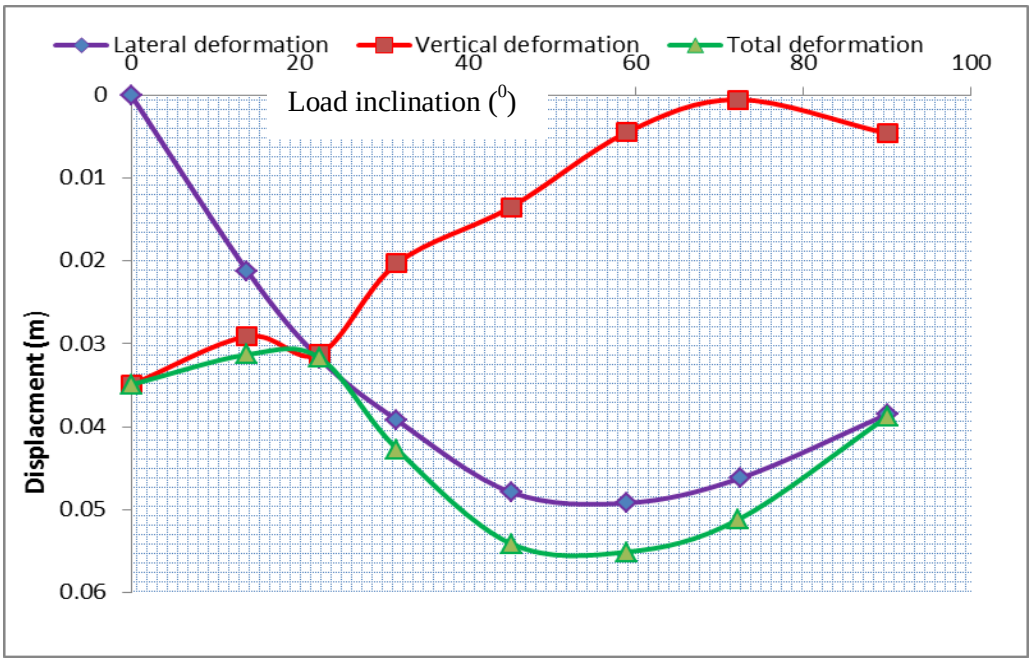

Figure 5-4: Deformation planes and extreme displacements

From the figure as load inclination angle increases lateral and total deformation increases while vertical deformation decreases. From figure 5.4 (a) above, deformation around the pile is larger and far away from the pile is become small. In figure (b) extreme deformation for vertical pile decreases when load inclination angle increases and lateral and total deformation increases. From the graph, figure 5.4 b, when the load inclination angle becomes 20^0; total, lateral and vertical deformation converges at a single point with an acceptable deformation. This shows for inclined loads 20^0 inclination gives more resistance when the pile is loaded in vertical and horizontal components.

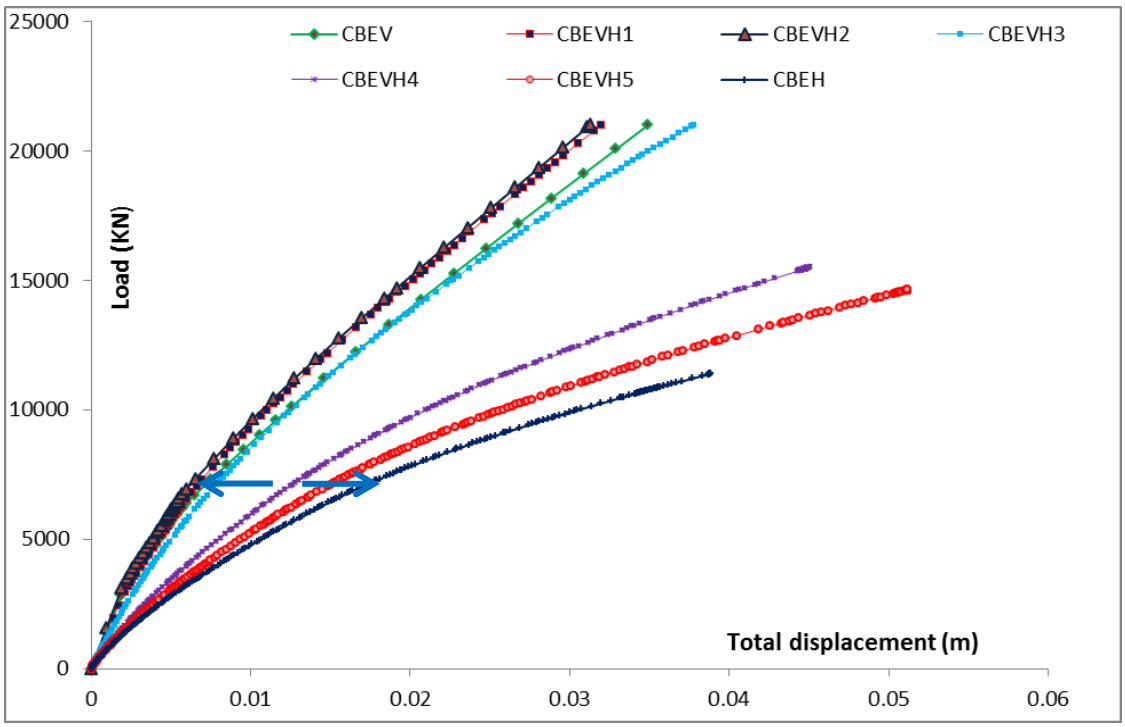

(A)

From figure "A" After CBEVH2, **total deformation** increases as load inclination angle increases from vertical axis. In contrast, the load inclination angle below CBEVH2 resistance increases and deformation decreases. This shows from equivalent behaviour of the batter pile, for the vertical pile around 20^0 has better resistance and small deformation as compared to the other modelling positions.

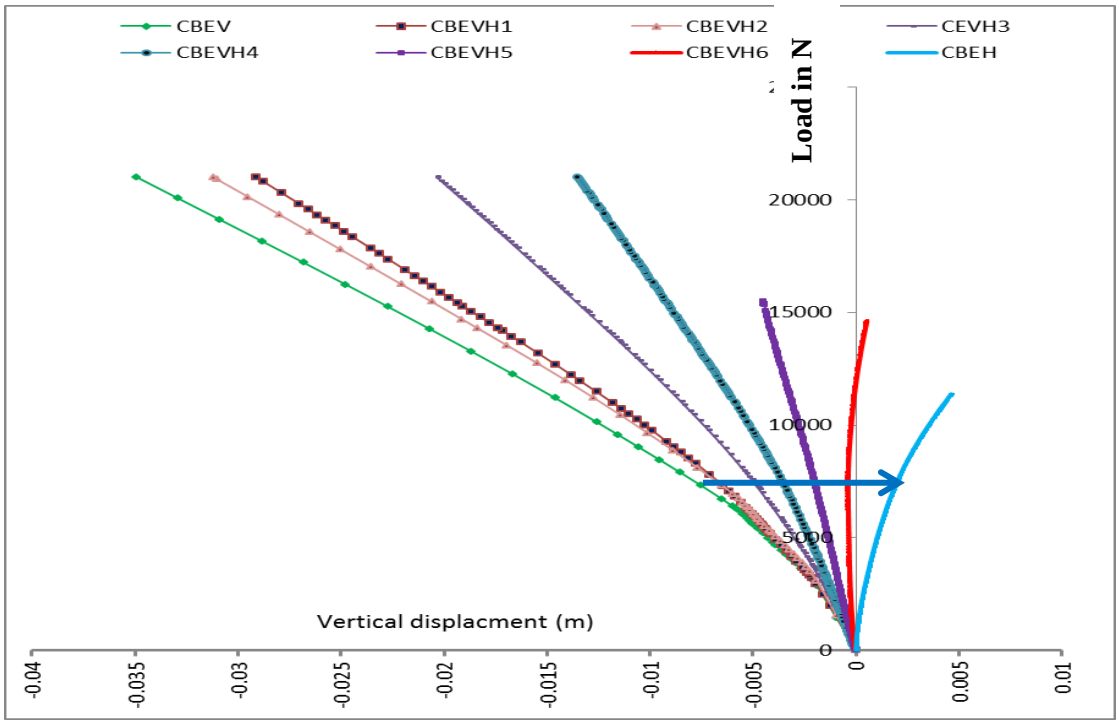

(B)

Vertical deformation decreases as load inclination angle increases from vertical axis.

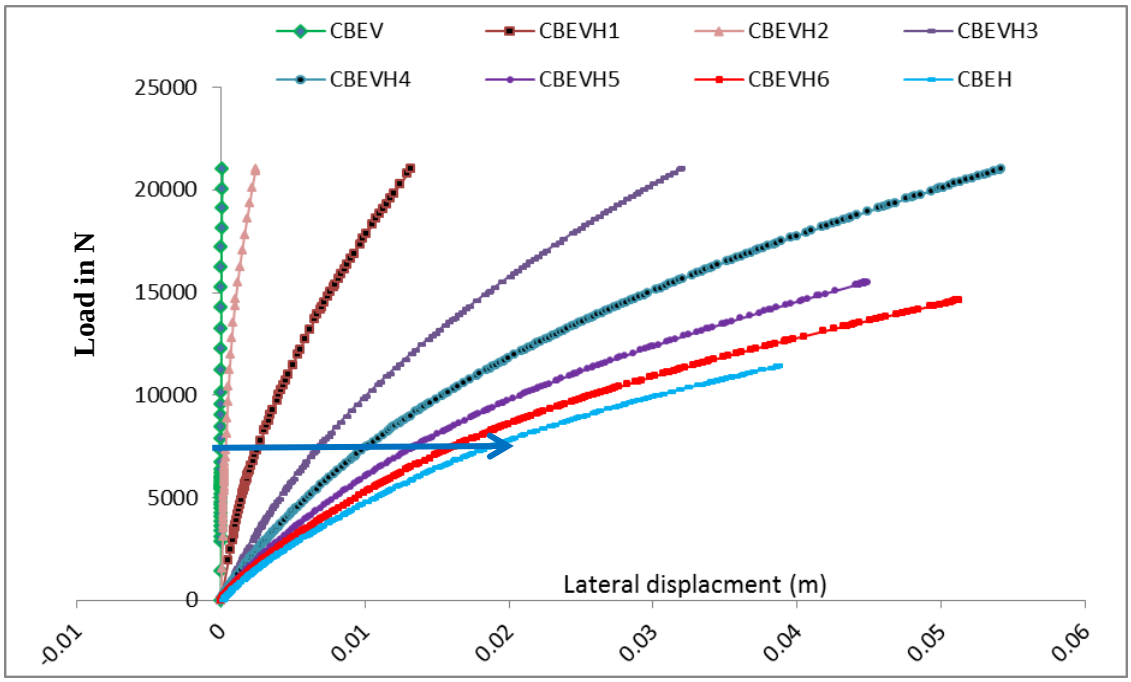

(C)

Lateral deformation increases as load inclination angle increases from vertical axis.

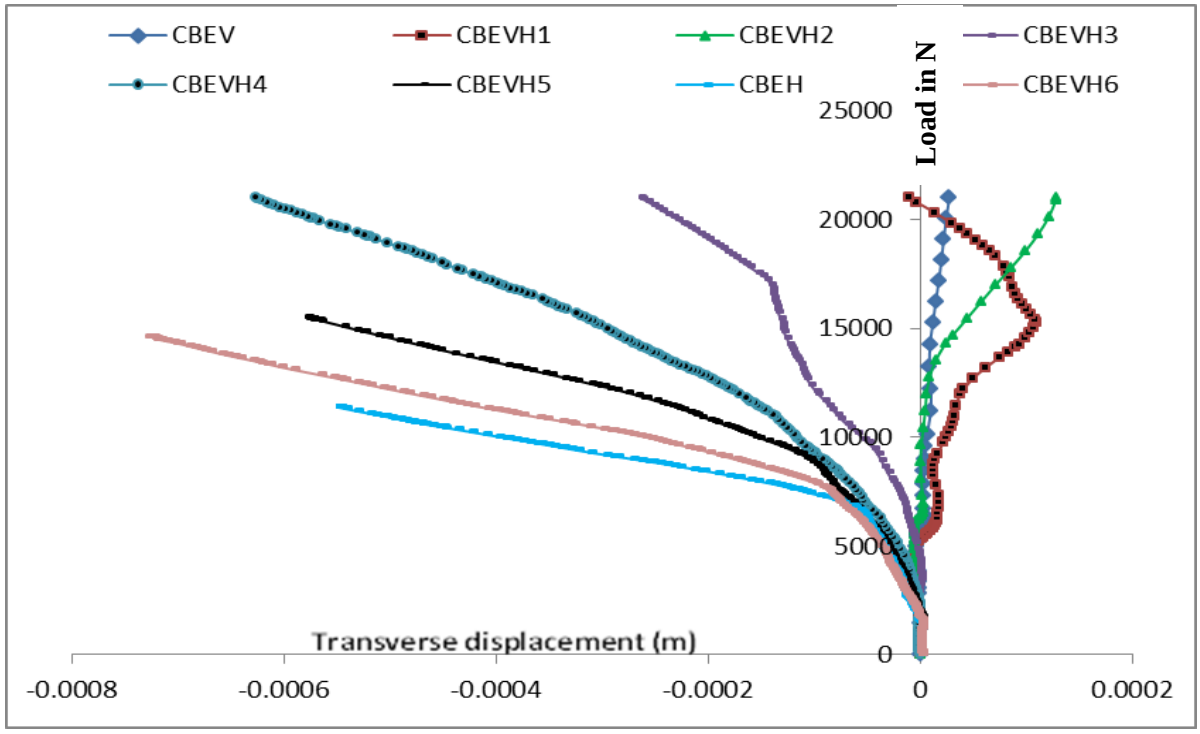

(D)

A) Total deformation B) Vertical C) Lateral and D) Transverse component deformations

Figure 5-5: Deformation of a pile along pile load with different load inclination

In figure "D" Transverse deformation increases with positive value until 22.4^0 (CBEVH2) after that decreases with negative value as load inclination angle increases from vertical axis.

From the analysis result it is shown in figure 5.5 A, the load inclined at beyond 20^0 (table 5.2) has smaller deformation. This shows lower deformation and higher bearing capacity is observed at 22.4^0 (CBEVH2) load inclination. From this result pile capacity increases when the load inclined is in the range of 0^0 to 25^0 after that its deformation increases bearing resistance decreases when the load becomes lateral. Taking vertical load as a reference deformation decreases by 10.3% and 9.17% for 13.77 degree and 22.4 degree respectively.

In figure 5.5 B, the vertical component deformation decreases, while lateral deformation increases when the load becomes lateral. As shown at CBEH for pure horizontal load, down ward deformation of the soil changes to vertical with small magnitude. There also a continuous increasing lateral component deformation when the load inclination angle increases from vertical.

5.4 Equivalent Batter Pile Analysis

Equivalent batter angle is taken as 20 degree inclined batter to replace equal magnitude of load inclination as described in chapter two section 2.2.4 proposed by Shamsher et al 1990. From vertical pile analysis, the load inclination is replaced by batter pile inclination. According to the load arrangement of the pile, it is necessary to distinguish positive or negative batter pile. In this research comparisons also made for deformation and resistance behaviour as shown in figure 5.6 below.

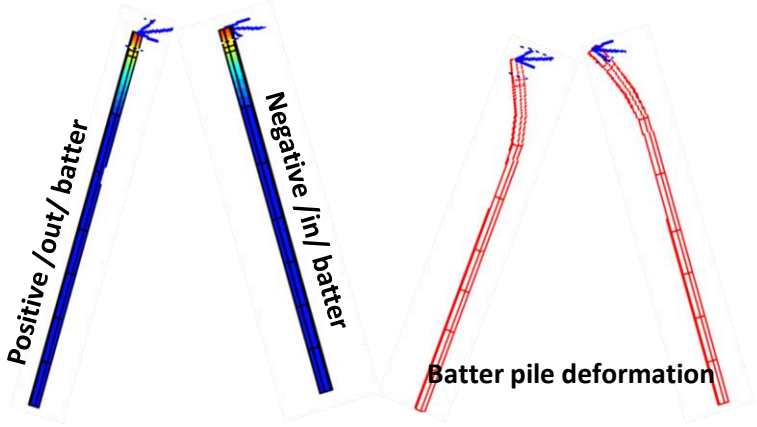

Figure 5-6: Batter pile position and deformation

(A)

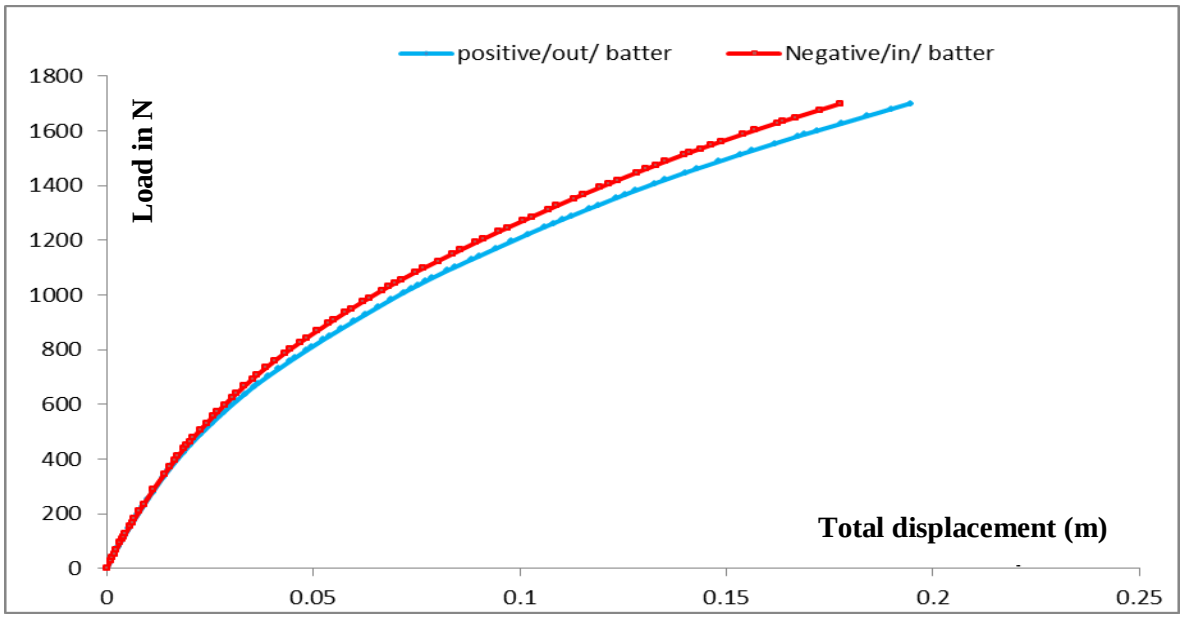

Negative batter has lesser total deformation than positive batter pile for equal load, similar material property and arrangement of the pile.

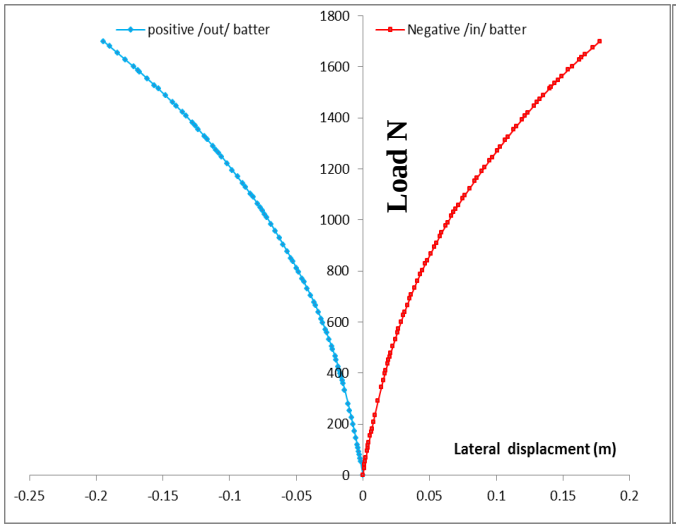

(B)

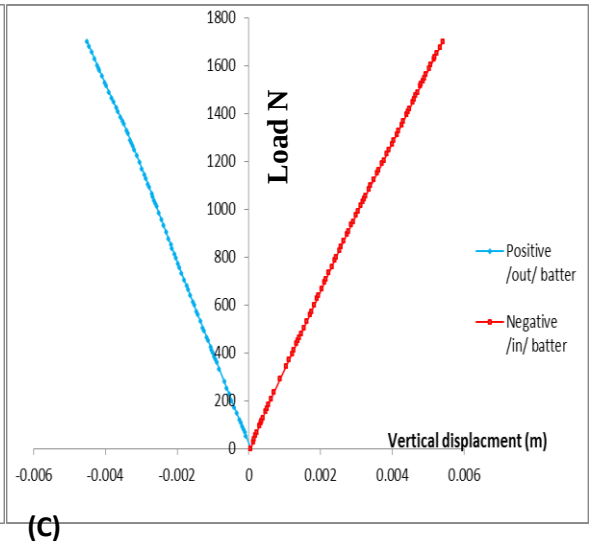

(C)

For figure "B" negative batter has lesser **lateral deformation** than positive batter pile for equal load and the same arrangement of the pile and for figure "C**"** negative batter has greater **vertical deformation** than positive batter for equal load, the same geometry of the pile and similar material properties

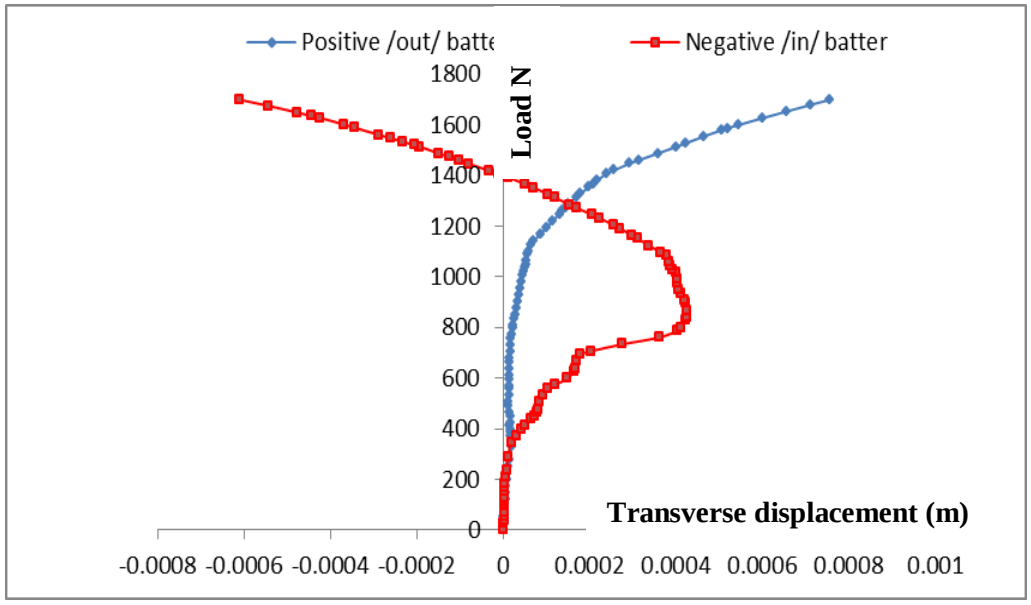

(D)

A) Total B) Lateral C) Vertical and D) Transverse deformation of batter pile

Figure 5-7: Positive and negative batter pile deformation

As shown clearly for equal magnitude of the load, the same geometry of pile and soil: negative batter has lower deformation than positive batter. This shows negative batter has higher bearing pressure than positive batter pile. Deformation of negative batter angle reduced by 8.25 %, 2.11% and 19.4 % for lateral, vertical and transverse components respectively.

CHAPTER SIX

6 CONCLUSION AND RECOMMENDATIONS

6.1 Conclusion

The main conclusions and recommendations drawn through the numerical modelling of batter pile foundation developed in this study are summarized in this chapter

As a general load inclination angle increases from the vertical axis, deformation increases and load carrying capacity decreases. Specifically short piles when the load inclined beyond 20^0 there is an increase in load carrying capacity with lesser deformation. As shown in the analysis of CBE taking the vertical pile result as a reference, deformation is reduced by 10.3% and 9.17 % for 13.77 degree and 22.4 degree respectively. However, for long piles in Wegagen Bank total deformation increases throughout when the load inclination angle increases from vertical.

The most important observations regarding the numerical modelling analysis are summarized below:

- It noted that increase batter angle would increase the pile load carrying capacity until reaching at angle -20^0, after that the resistance become decrease.
- Single positive batter pile is less resistance to lateral loads than negative batter pile for compression loads.
- Negative batter piles have more resistance to lateral load than vertical piles and inclined piles loaded in opposite direction (positive battered).
- The load inclined at an angle on the vertical pile has an equivalent effect to the pile inclined to the same degree of pile for lateral loading.
- The batter and load inclination angle significantly influence the ultimate bearing capacity of the piles.
- Deformation of negative batter reduced by 8.25 %, 2.11 % and 19.4 % for lateral, vertical and transverse deformation with equal load magnitude and material property of vertical pile.

6.2 Recommendation

Batter piles beyond -20^0 resist more bearing than vertical piles for the same material property, geometry and load magnitude for short piles. The cause is as short and larger diameter batter is installed, the periphery of the pile reacts as both shaft and end bearing resistance. It is better to use vertical pile subjected to inclined loading for the substitution of a batter to vertical loading. Batter piles shall be considered when the lateral loads exceeds the allowable limit for vertical piles. Therefore, it recommended that using a negative batter pile is great in resisting more lateral load than vertical and positive batter piles. The batter bearing capacity is relatively larger than vertical pile, it is better to use in our country Ethiopia. The cost of installation and casting mechanism is not more differ from the commonly known vertical piles but the cost of batter pile relative to the same capacity of vertical pile have considerably larger.

Some recommendations for further research on batter pile

- Due to batter piles are exposed to dynamic loads in practical situations, it is necessary to simulate batter piles with dynamic loads and it needs further study on its behaviour.
- Formulate an oblique interaction chart for that which differ from vertical piles.
- The work explored in this research is only on the effect of single piles, which have the basic behaviour on group batter, but a combination of batter and vertical pile may have more efficiency for the combination of vertical and lateral load effects on pile group.

Overall, this section of the research showed that the response of pile under combination loading is a complex problem. When modelling pile foundations it is important to model the pile soil system as close to the real situations as possible. Because pile exposed to varying combination of loads like static, dynamic loads in, down ward, uplift, lateral and inclined load directions.

References

[1] Arora, K.R. "*Soil Mechanics and Foundation.*" Kota (raj) India 1987

[2] Brinch Hansen J. "*The ultimate capacity of rigid piles against transversal forces.*" Journal of Danish geotechnical institute. Copenhagen, 1961.

[3] Bowles, J.E. "*Foundation Analysis and Design 5th Edition*." McGraw-Hill, 1996

[4] Braiud, J L. "*Geotechnical Engineering: Unsaturated and Saturated Soils*." 2013.

[5] Budhu, M. "*Soil Mechanics and Foundation 3rd Edition.*" 2011.

[6] Broms B. "*The lateral resistance of piles in cohesive piles cohesive soils.*" International journal of soil mechanics and foundation engineering. 123 – 15, 1964.

[7] Chen, L.T. and Saleeb A. "*Constitute of equations for engineering materials*" volume 1." Elasticity and modeling. Canada, 1983.

[8] Craig, R.F. S*oil mechanics and foundation engineering Fifth Edition*. London, 1992.

[9] Das. B. "*Principle of foundation engineering Fourth Edition*." Melbourne, 1999.

[10] Desai, c.s & Zman. M. *Advanced geotechnical engineering*: Soil structure interaction using computer and material models, 2013.

[11] "Ethiopian Building Code of Standard" EBCS - 7 EN 1997-1, Ethiopia 2013

[12] Gu, D.X. "*Effect of Weathering on Strength and Modulus of Basalt and Siltstone*." American Rock Mechanics Association, 2008.

[13] Hanna, A & Nguyen,T. "*Shaft resistance of single a single and vertical piles driven in sand*." Journal of Geotechnical and Geo environmental engineering 129:7, 601-607. 2003.

[14] Hussein Mroueh *et al*. *"Numerical analysis of the response of battered piles to inclined pullout loads.*" International Journal for Numerical and Analytical methods in Geomechanics. 33:1277–1288, 2008.

[15] Kate J. *"Load deformation behaviour of foundations under vertical and oblique loads."* Canada, 2005.

[16] Karsan R. Hirani and A. K. Verma. *"Lateral load carrying capacity of model pile groups".* National Conference on Recent Trends in Engineering & Technology, 2011.

[17] Krishna M.V Ratnam D.Neelima Satyam. "*Load carrying capacity of laterally loaded batter piles*." Journal of Geotechnical and Geo-environmental Engineering.14-16, 2017.

[18] Kurushekra, Haranya. "*Model study on vertical and batter pile groups subjected to lateral*

load in sandy soil." International Journal of Advanced research in engineering. ISSN:2349 – 2819, 2016.

[19] Lassaad Hazzar, Mahmoud N. Hussien, Mourad Karray. *Numerical investigation of the lateral response of battered pile foundations.* International Journal of Geotechnical Engineering 11:4, 376-392, 2017.

[20] Lassad Hazzar, .Mahamoud N. Hussien, Mmourad Karray. "*3D modeling laterally loaded battered piles in sand."* Korean Society Journal of Civil Engineering 18:7, 2051-2063. 2015.

[21] Lee, J. "*Three Dimensional Analysis of Bearing Behaviour of Piled Raft on Soft Clay."* Computers and Geotechnics, 2010.

[21] Meyerhof, G.G. "*Bearing capacity and settlement of pile foundation."* International journal of geotechnical division. 197 – 228, 1976.

[22] Meyerhof G.G, Mathur S.K. and Valsangkar A.J. "*Lateral resistance and deflection of rigid walls and piles in layered soil."* Journal of Canadian geotechnical engineering. 1959-197, 1981.

[23] Mohammed A. *"Bearing capacity of batter piles embedded in sandy soil."* International Journal of Geotechnical Engineering 10:5, 529-532, 2016.

[23] NIT Kurukshetra, Haryana. *"Influence of Pile Inclination on Batter Pile Groups subjected To Lateral Loading in Sand."* Proceedings of 29th Research World International Conference, 13-15, 2017.

*[*24] PLAXIS 3D FOUNDATION, "*Material Models Manual*", Version 1

[25] PLAXIS 3D FOUNDATION, "*Reference Manual*", Version 1

[26] PLAXIS 3D FOUNDATION, "*Tutorial Manual*", Version 1

[27] Poulos H.G. and Davis E.H. "*Pile foundation analysis and design.*" John wiley and sons INC Toronto, 1980

[28] Rees L.C & Matlock H. "*Non-dimensional solutions for laterally loaded piles preceding 8th."* Taxas conference on on soil mechanics and foundation engineering.1-41, 1956.

[29] Sam (Helwany, 2007). "*Applied soil mechanics with ABAQUS applications*." Published by John Wiley & Sons, Inc in Canada.

[30] Visc A.S. "*Design of pile foundation*." Transportation research board, national research council Washington D.C. 1992.

APPENDIX A

Borehole Data for Wegagen Bank

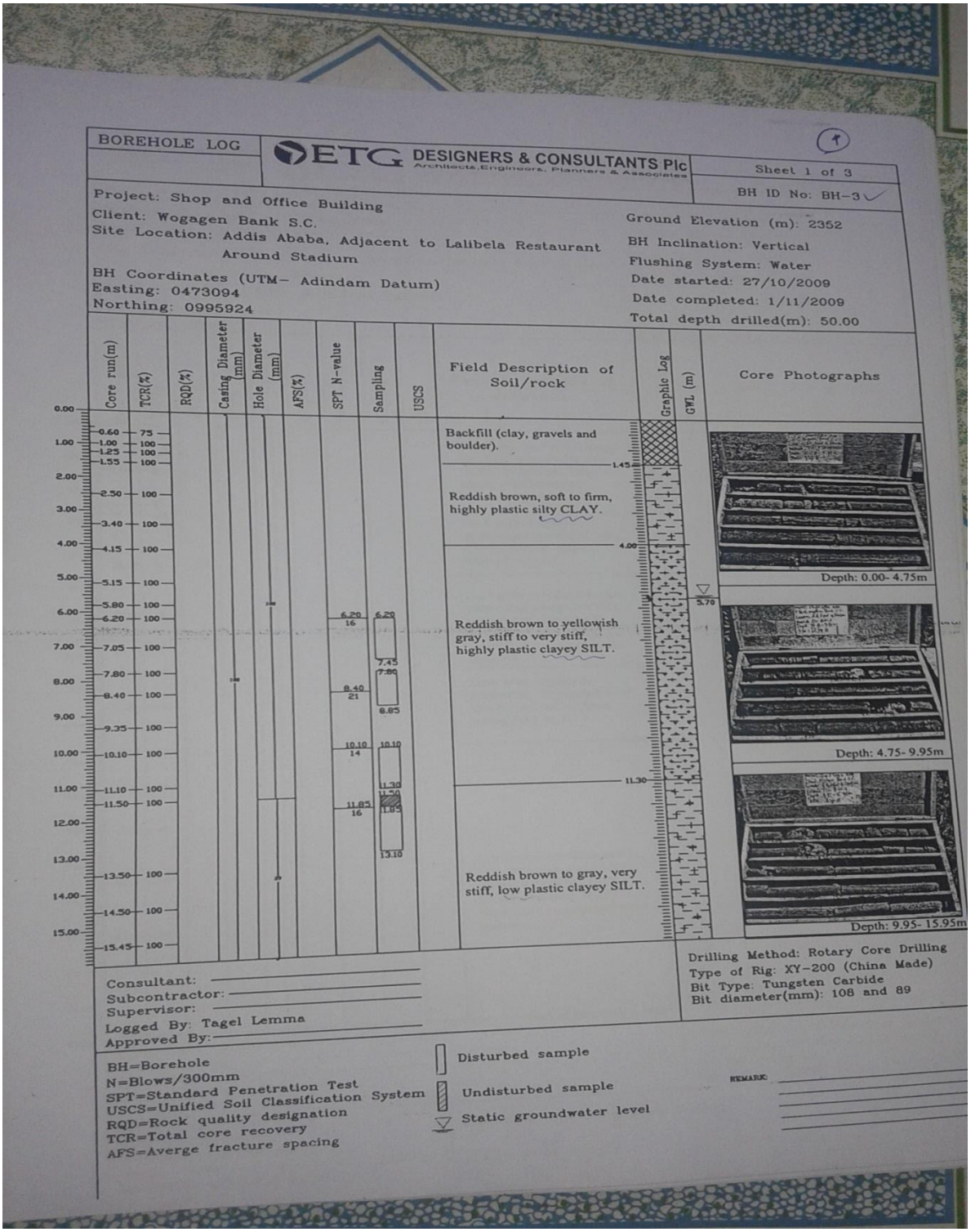

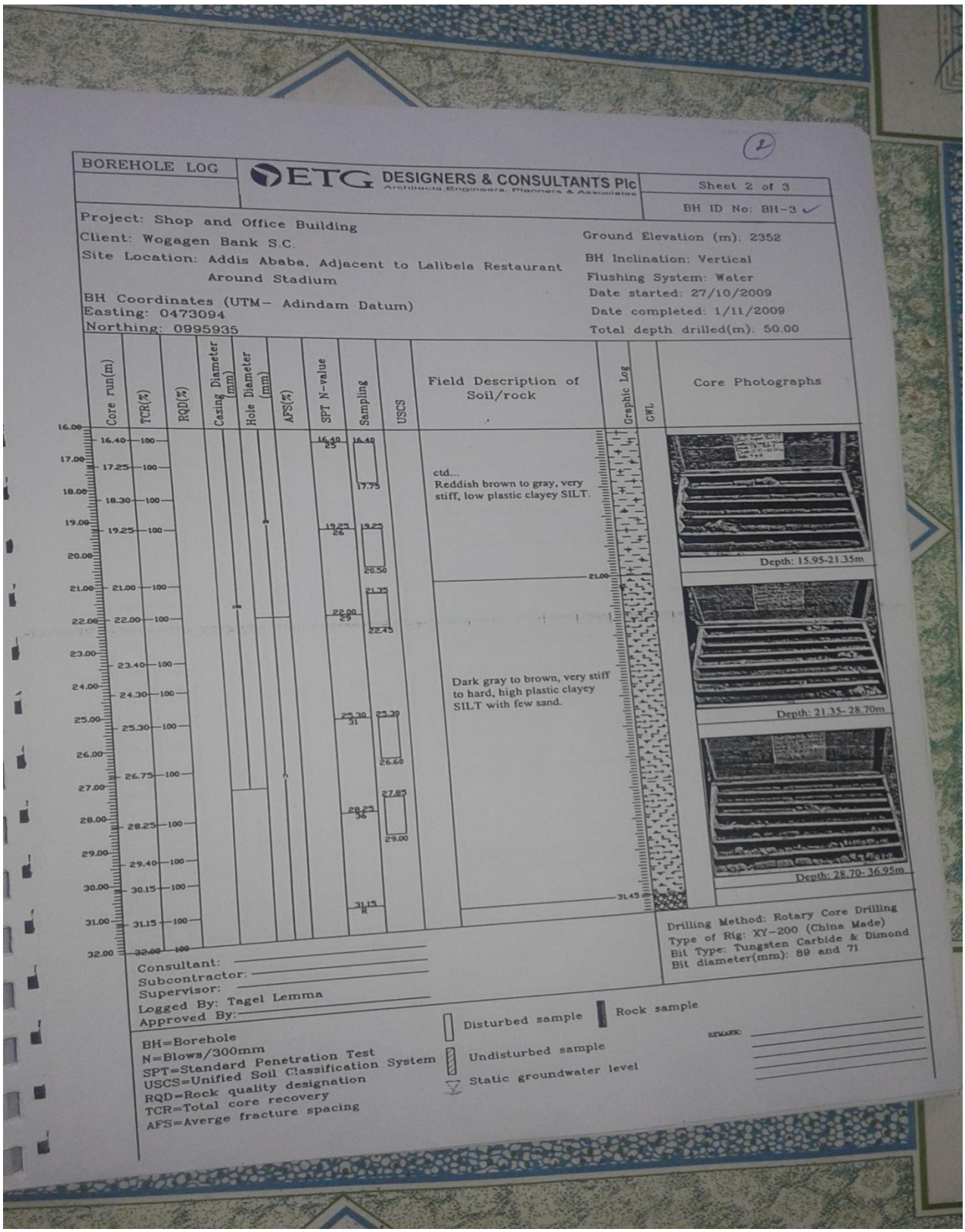

BOREHOLE LOG

ETG DESIGNERS & CONSULTANTS Plc
Architects, Engineers, Planners & Associates

Sheet 2 of 3
BH ID No: BH-3

Project: Shop and Office Building
Client: Wogagen Bank S.C.
Site Location: Addis Ababa, Adjacent to Lalibela Restaurant Around Stadium

BH Coordinates (UTM- Adindam Datum)
Easting: 0473094
Northing: 0995935

Ground Elevation (m): 2352
BH Inclination: Vertical
Flushing System: Water
Date started: 27/10/2009
Date completed: 1/11/2009
Total depth drilled(m): 50.00

Core run(m)	TCR(%)	RQD(%)	Casing Diameter (mm)	Hole Diameter (mm)	AFS(%)	SPT N-value	Sampling	USCS	Field Description of Soil/rock	Graphic Log	GWL	Core Photographs
16.00	16.40 100					16.40 25	16.40 17.75		ctd... Reddish brown to gray, very stiff, low plastic clayey SILT.			Depth: 15.95-21.35m
17.00	17.25 100											
18.00	18.30 100											
19.00	19.25 100					19.25 26	19.25 20.50					
20.00												
21.00	21.00 100						21.35					
22.00	22.00 100					22.00 29	22.45					Depth: 21.35- 28.70m
23.00	23.40 100								Dark gray to brown, very stiff to hard, high plastic clayey SILT with few sand.			
24.00	24.30 100											
25.00	25.30 100					25.30 31	25.30 26.60					
26.00	26.75 100											
27.00							27.05					
28.00	28.25 100					28.25 36	29.00					
29.00	29.40 100											
30.00	30.15 100											
31.00	31.15 100						31.15 R					
32.00	32.00 100											Depth: 28.70- 36.95m

Consultant:
Subcontractor:
Supervisor:
Logged By: Tagel Lemma
Approved By:

Drilling Method: Rotary Core Drilling
Type of Rig: XY-200 (China Made)
Bit Type: Tungsten Carbide & Dimond
Bit diameter(mm): 89 and 71

BH=Borehole
N=Blows/300mm
SPT=Standard Penetration Test
USCS=Unified Soil Classification System
RQD=Rock quality designation
TCR=Total core recovery
AFS=Averge fracture spacing

Disturbed sample
Rock sample
Undisturbed sample
Static groundwater level

REMARK:

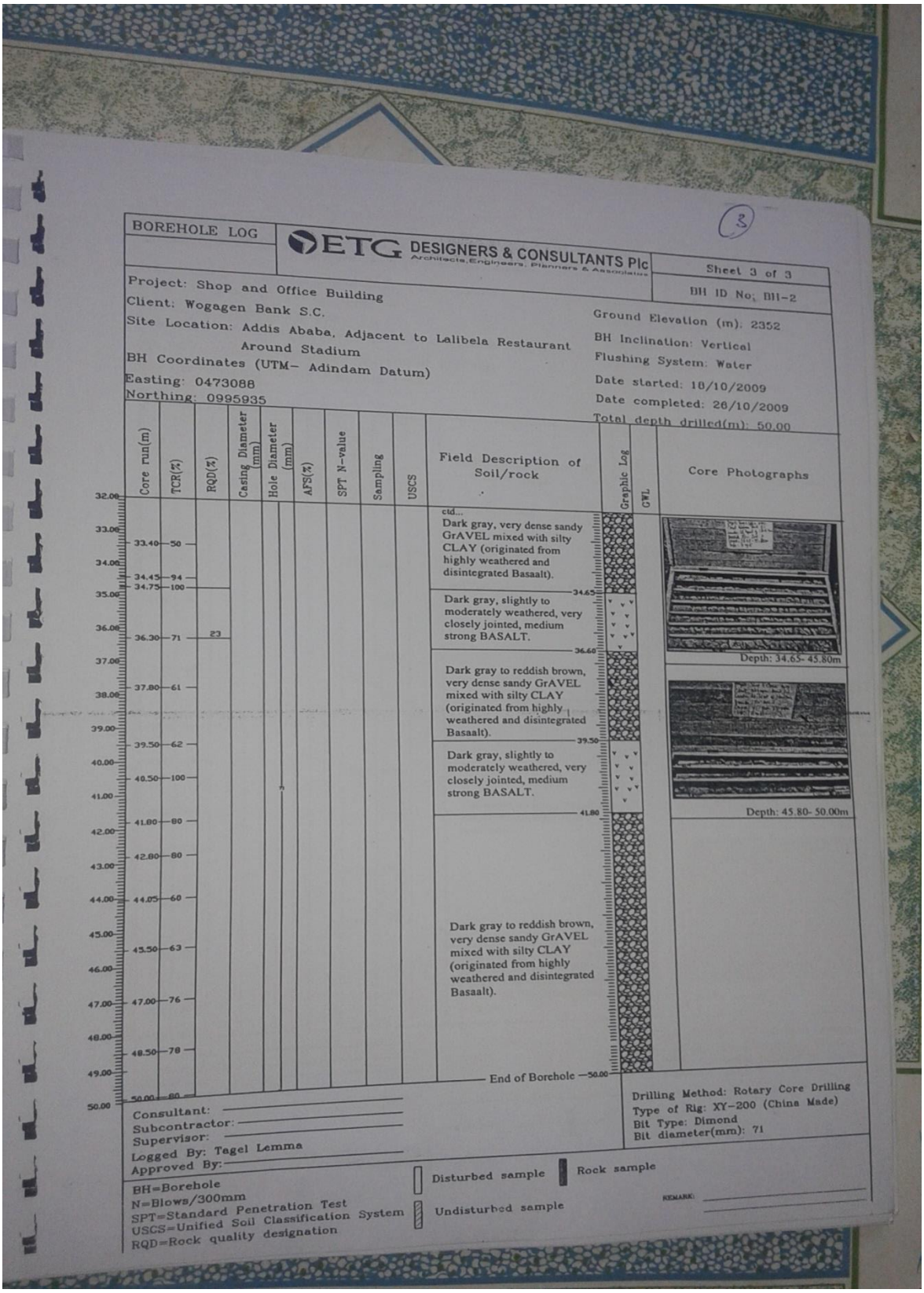

BOREHOLE LOG

ETG DESIGNERS & CONSULTANTS Plc
Architects, Engineers, Planners & Associates

(3)

Sheet 3 of 3

BH ID No; BH-2

Project: Shop and Office Building
Client: Wogagen Bank S.C.
Site Location: Addis Ababa, Adjacent to Lalibela Restaurant Around Stadium
BH Coordinates (UTM- Adindam Datum)
Easting: 0473088
Northing: 0995935

Ground Elevation (m): 2352
BH Inclination: Vertical
Flushing System: Water
Date started: 18/10/2009
Date completed: 26/10/2009
Total depth drilled(m): 50.00

Core run(m)	TCR(%)	RQD(%)	Casing Diameter (mm)	Hole Diameter (mm)	AFS(%)	SPT N-value	Sampling	USCS	Field Description of Soil/rock	Graphic Log	GWL	Core Photographs
33.40	50								ctd... Dark gray, very dense sandy GrAVEL mixed with silty CLAY (originated from highly weathered and disintegrated Basaalt).			
34.45	94											
34.75	100											
									34.65			
36.30	71	23							Dark gray, slightly to moderately weathered, very closely jointed, medium strong BASALT.			Depth: 34.65- 45.80m
									36.60			
37.80	61								Dark gray to reddish brown, very dense sandy GrAVEL mixed with silty CLAY (originated from highly weathered and disintegrated Basaalt).			
39.50	62											
									39.50			
40.50	100								Dark gray, slightly to moderately weathered, very closely jointed, medium strong BASALT.			
									41.80			Depth: 45.80- 50.00m
41.80	80											
42.80	80											
44.05	60											
45.50	63								Dark gray to reddish brown, very dense sandy GrAVEL mixed with silty CLAY (originated from highly weathered and disintegrated Basaalt).			
47.00	76											
48.50	78											
									End of Borehole 50.00			
50.00	80											

Consultant:
Subcontractor:
Supervisor:
Logged By: Tagel Lemma
Approved By:

Drilling Method: Rotary Core Drilling
Type of Rig: XY-200 (China Made)
Bit Type: Dimond
Bit diameter(mm): 71

BH=Borehole
N=Blows/300mm
SPT=Standard Penetration Test
USCS=Unified Soil Classification System
RQD=Rock quality designation

Disturbed sample
Undisturbed sample
Rock sample

REMARK:

Borehole Data for Commercial Bank of Ethiopia

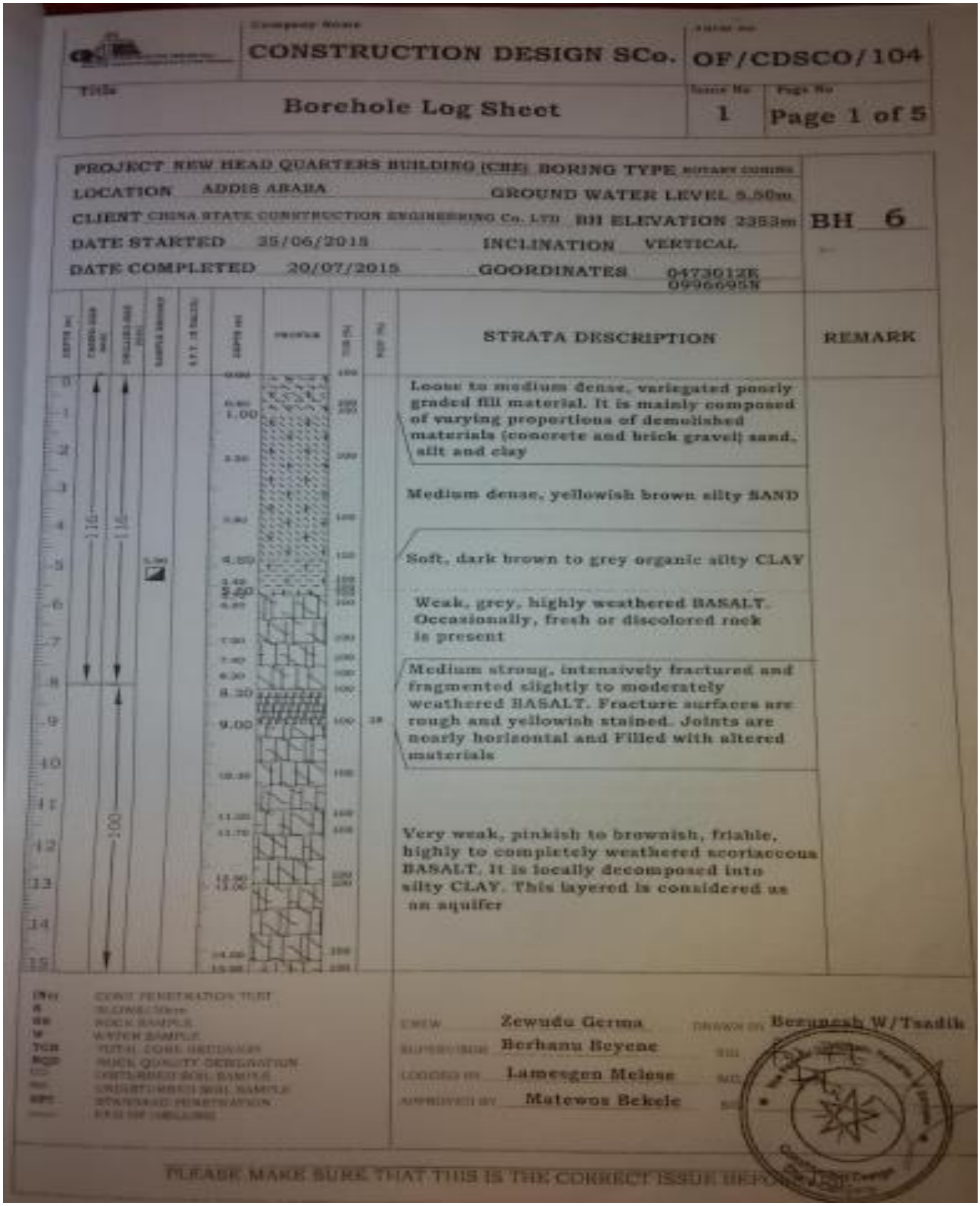

CONSTRUCTION DESIGN SCo.

OF/CDSCO/104

Borehole Log Sheet

1

Page 1 of 5

PROJECT NEW HEAD QUARTERS BUILDING (CBE) BORING TYPE ROTARY CORING

LOCATION ADDIS ABABA GROUND WATER LEVEL 5.50m

CLIENT CHINA STATE CONSTRUCTION ENGINEERING Co. LTD BH ELEVATION 2353m BH 6

DATE STARTED 25/06/2015 INCLINATION VERTICAL

DATE COMPLETED 20/07/2015 GOORDINATES 0473012E 0996095N

STRATA DESCRIPTION	REMARK
Loose to medium dense, variegated poorly graded fill material. It is mainly composed of varying proportions of demolished materials (concrete and brick gravel) sand, silt and clay	
Medium dense, yellowish brown silty SAND	
Soft, dark brown to grey organic silty CLAY	
Weak, grey, highly weathered BASALT. Occasionally, fresh or discolored rock is present	
Medium strong, intensively fractured and fragmented slightly to moderately weathered BASALT. Fracture surfaces are rough and yellowish stained. Joints are nearly horizontal and Filled with altered materials	
Very weak, pinkish to brownish, friable, highly to completely weathered scoriaceous BASALT. It is locally decomposed into silty CLAY. This layered is considered as an aquifer	

CREW Zewudu Germa DRAWN BY Bezunesh W/Tsadik

SUPERVISOR Berhanu Beyene

LOGGED BY Lamesgen Melese

APPROVED BY Matewos Bekele

PLEASE MAKE SURE THAT THIS IS THE CORRECT ISSUE BEFORE USE

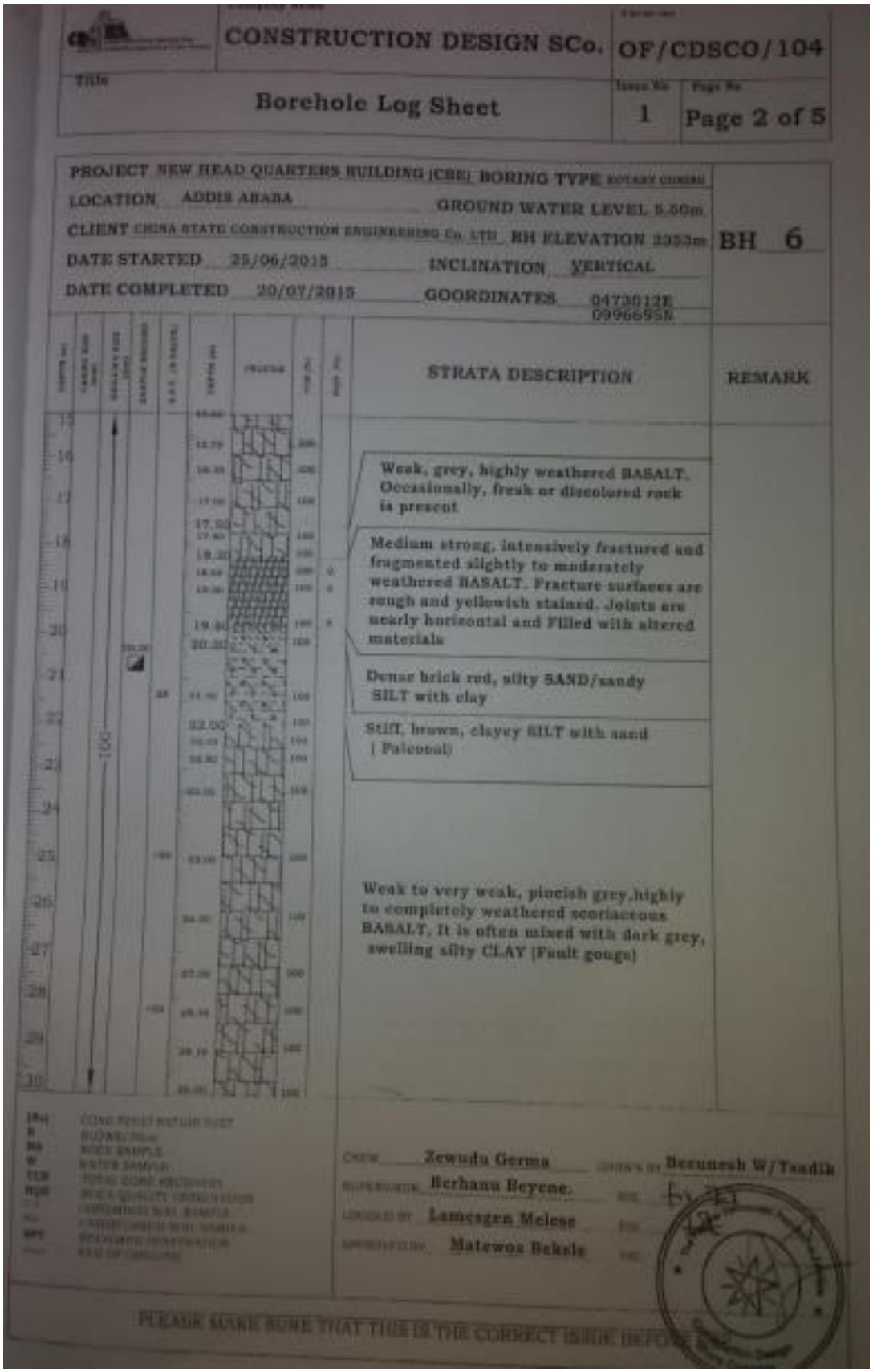

CONSTRUCTION DESIGN SCo.

OF/CDSCO/104

Title: Borehole Log Sheet

Issue No: 1

Page No: Page 2 of 5

PROJECT NEW HEAD QUARTERS BUILDING (CBE) BORING TYPE ROTARY CORING

LOCATION ADDIS ABABA GROUND WATER LEVEL 5.50m

CLIENT CHINA STATE CONSTRUCTION ENGINEERING Co. LTD BH ELEVATION 2353m

BH 6

DATE STARTED 25/06/2015 INCLINATION VERTICAL

DATE COMPLETED 20/07/2015 GOORDINATES 0473012E 0996695N

STRATA DESCRIPTION	REMARK
Weak, grey, highly weathered BASALT. Occasionally, fresh or discolored rock is present	
Medium strong, intensively fractured and fragmented slightly to moderately weathered BASALT. Fracture surfaces are rough and yellowish stained. Joints are nearly horizontal and Filled with altered materials	
Dense brick red, silty SAND/sandy SILT with clay	
Stiff, brown, clayey SILT with sand (Paleosol)	
Weak to very weak, pinckish grey,highly to completely weathered scoriaceous BASALT, It is often mixed with dark grey, swelling silty CLAY (Fault gouge)	

CHKD Zewudu Germa DRWN BY Berunesh W/Tsadik

SUPERVISOR Berhanu Beyene

LOGGED BY Lamesgen Melese

APPROVED BY Matewos Bekele

PLEASE MAKE SURE THAT THIS IS THE CORRECT ISSUE BEFORE

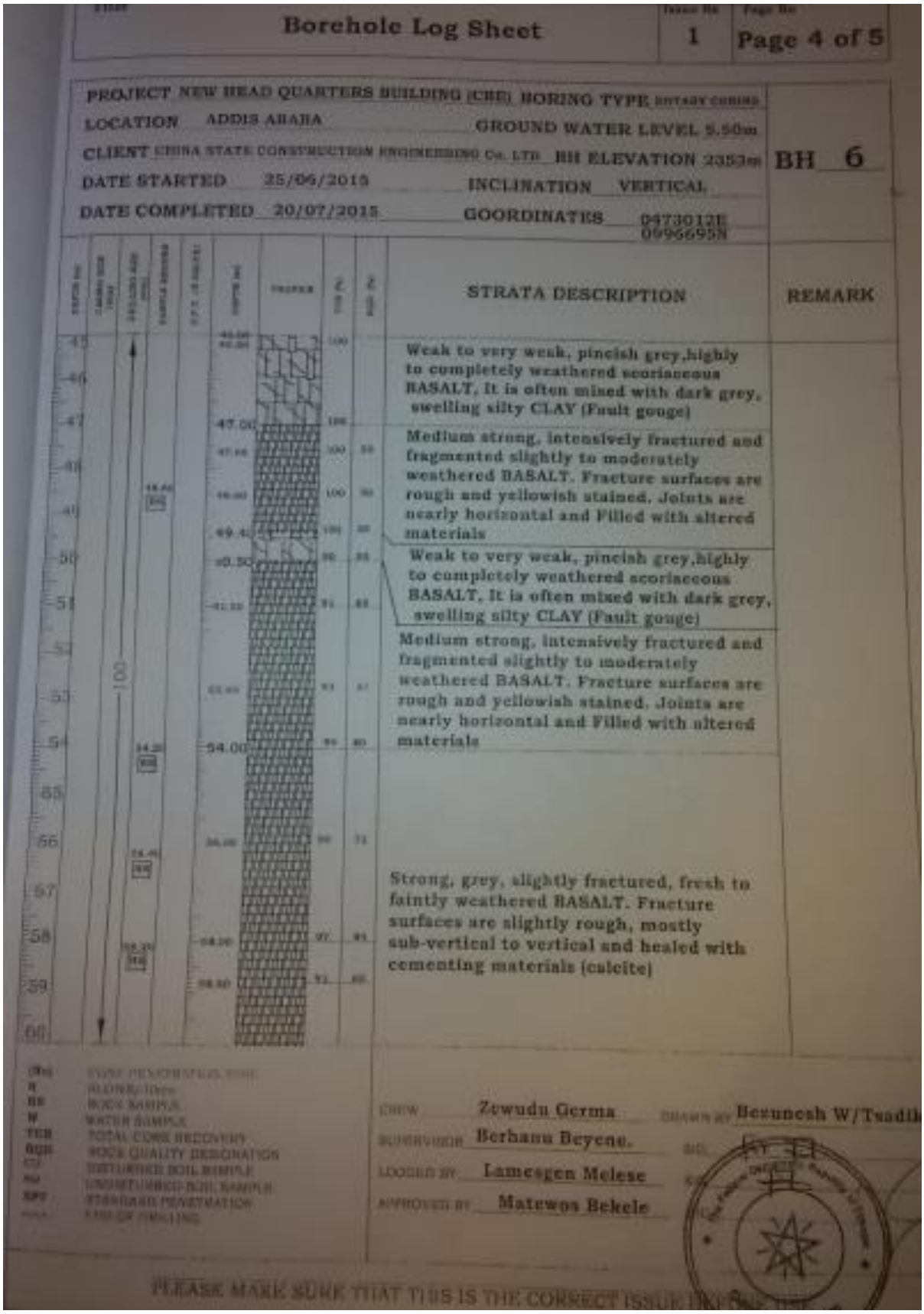

Borehole Log Sheet

Issue No: 1 | Page No: Page 4 of 5

PROJECT NEW HEAD QUARTERS BUILDING (CHE) BORING TYPE ROTARY CORING
LOCATION ADDIS ABABA GROUND WATER LEVEL 5.50m
CLIENT CHINA STATE CONSTRUCTION ENGINEERING Co. LTD BH ELEVATION 2353m
DATE STARTED 25/06/2015 INCLINATION VERTICAL
DATE COMPLETED 20/07/2015 GOORDINATES 0473012E 0996695N

BH 6

STRATA DESCRIPTION	REMARK
Weak to very weak, pincish grey,highly to completely weathered scoriaceous BASALT, It is often mixed with dark grey, swelling silty CLAY (Fault gouge)	
Medium strong, intensively fractured and fragmented slightly to moderately weathered BASALT. Fracture surfaces are rough and yellowish stained. Joints are nearly horizontal and Filled with altered materials	
Weak to very weak, pincish grey,highly to completely weathered scoriaceous BASALT, It is often mixed with dark grey, swelling silty CLAY (Fault gouge)	
Medium strong, intensively fractured and fragmented slightly to moderately weathered BASALT. Fracture surfaces are rough and yellowish stained. Joints are nearly horizontal and Filled with altered materials	
Strong, grey, slightly fractured, fresh to faintly weathered BASALT. Fracture surfaces are slightly rough, mostly sub-vertical to vertical and healed with cementing materials (calcite)	

CORE PENETRATION ZONE
BLOWS/10cm
ROCK SAMPLE
WATER SAMPLE
TOTAL CORE RECOVERY
ROCK QUALITY DESIGNATION
DISTURBED SOIL SAMPLE
UNDISTURBED SOIL SAMPLE
STANDARD PENETRATION
END OF DRILLING

DRILLED BY Zewudu Germa DRAWN BY Bezunesh W/Tsadik
SUPERVISOR Berhanu Beyene.
LOGGED BY Lamesgen Melese
APPROVED BY Matewos Bekele

PLEASE MAKE SURE THAT THIS IS THE CORRECT ISSUE

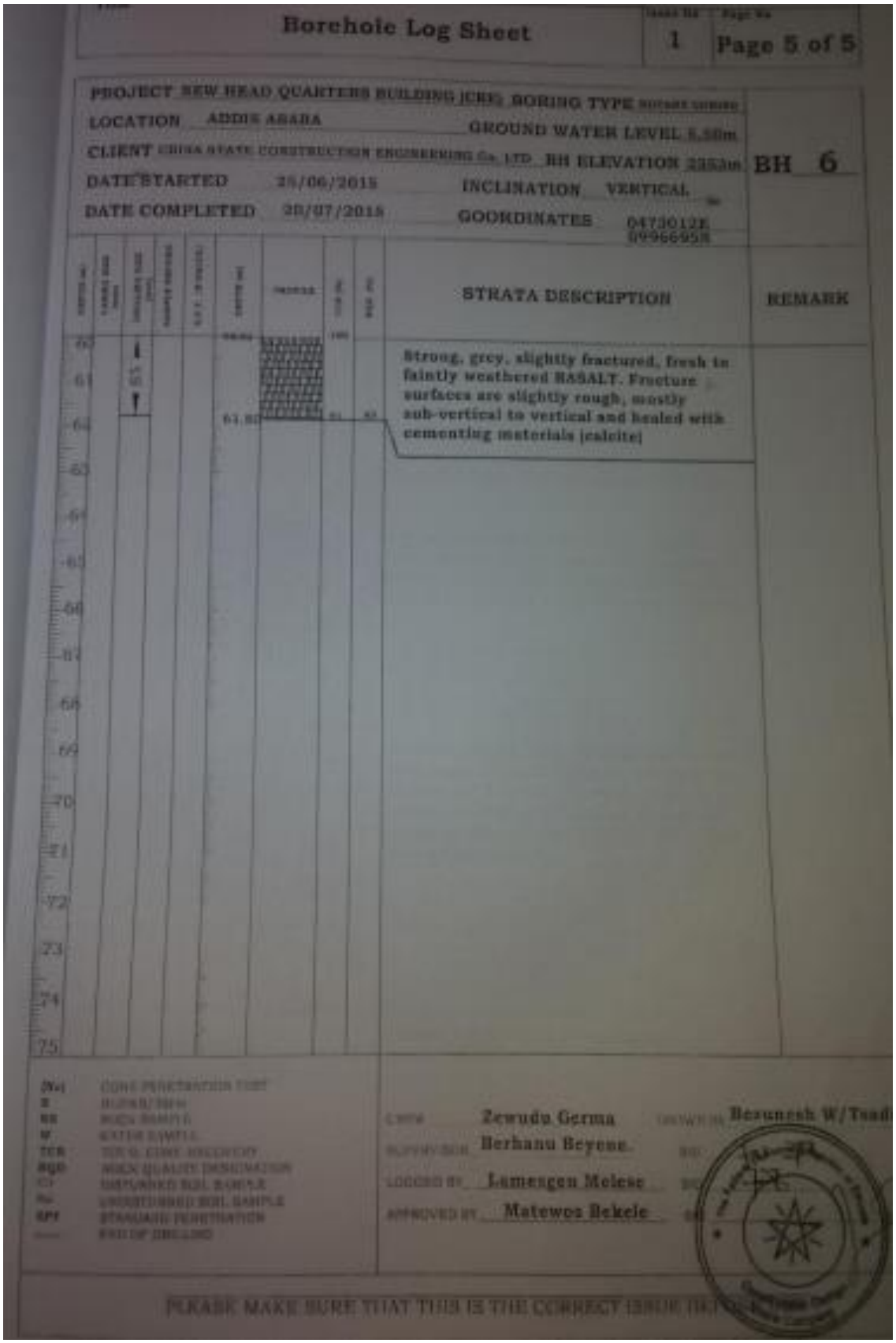

Borehole Log Sheet

1 | Page 5 of 5

PROJECT NEW HEAD QUARTERS BUILDING (CB3) BORING TYPE ROTARY DRILLING

LOCATION ADDIS ABABA GROUND WATER LEVEL 5.50m

CLIENT CHINA STATE CONSTRUCTION ENGINEERING Co. LTD BH ELEVATION 2353m BH 6

DATE STARTED 25/06/2015 INCLINATION VERTICAL

DATE COMPLETED 20/07/2015 COORDINATES 0473012E 09966958

STRATA DESCRIPTION	REMARK
Strong, grey, slightly fractured, fresh to faintly weathered BASALT. Fracture surfaces are slightly rough, mostly sub-vertical to vertical and healed with cementing materials (calcite)	

LOGGED BY Lamengen Melese

APPROVED BY Matewos Bekele

PLEASE MAKE SURE THAT THIS IS THE CORRECT ISSUE

CONSTRUCTION DESIGN SHARE CO.

LABORATORY TEST RESULT

Project :- Head Quarter Building Of CRE
Client :- China State Construction Engineering Ethiopia PLC
Location :- A.A (Ambassador)
Object :- Nineteen Undisturbed Soil Samples

N°	BH N°	Depth (m)	Atterberg Limit			Free Swell (%)	Organic Content (%)	Swelling Pressure (KN/m²)	Natural Moisture Content (%)	Natural Unit Weight (Kg/m³)	UnconFined Compressive Strength (KN/m²)	Triaxial Shear Test		Direct Shear Test	
			LL (%)	PL (%)	PI (%)							C (KN/m²)	ϕ Degree	C (KN/m²)	ϕ Degree
1	1	4.00	-	-	-	-	-	-	20.50	1670	64	-	-	14	21
2	1	18.00	75.48	48.35	26.13	-	-	-	54.22	1519	-	12	10	-	-
3	1	43.00	109.17	48.29	60.88	238	-	-	30.11	1643	-	-	-	15	17
4	3	8.50	43.89	25.82	20.27	78	-	-	18.87	1558	-	-	-	17	20
5	5	8.40	92.88	60.88	30.17	170	-	400	38.17	1674	344	-	-	35	35
6	5	23.00	144.58	49.99	94.51	240	-	-	38.03	1774	61	-	-	29	7
7	6	8.00	78.94	35.45	37.49	138	-	268	36.18	1598	138	-	-	30	19
8	6	20.50	118.50	52.23	67.23	-	-	-	84.25	1444	-	93	8	29	23
9	6	28.20	-	-	-	-	-	-	31.45	1658	341	84	5	-	-
10	6	42.00	-	-	-	-	-	-	38.96	1599	254	-	-	36	17
11	6	47.80	-	-	-	-	-	-	38.92	1963	385	84	18	-	-
12	7	3.00	76.83	38.91	37.12	110	-	-	20.50	1823	-	-	-	32	23
13	7	28.50	-	-	-	-	-	-	31.12	1563	306	-	-	29	16
14	7	38.50	77.51	29.25	48.26	240	8.28	-	39.82	1685	-	-	-	34	23
15	7	41.50	88.90	33.30	55.56	-	-	-	29.61	1747	-	65	18	-	-
16	8	48.00	84.89	34.68	49.45	-	-	-	33.36	1760	-	51	12	-	-
17	8	47.50	64.64	21.31	43.13	110	4.28	-	34.29	1790	-	-	-	32	18
18	9	19.00	93.55	55.49	38.06	-	-	-	46.27	1409	-	-	-	1	30
19	9	3.50	-	-	-	-	-	-	23.68	1649	132	-	-	23	14

Note :-
1. Hammer graphs for grain size distribution test result are drawn and attached herewith.
2. Fourteen graphs for direct shear test result are drawn and attached herewith.
3. Six graph for UU triaxial test result is drawn and attached here with.
4. Eight Tests - settlement, void ratio- pressure curve and the necessary data sheets for one - dimensional consolidation test result are attached herewith.

Tested by :- Emebet Workneh
Date :- 02/08/2015
Checked by :- Abate Legesse
Date :- 25/08/2015

Approved by :- Birek Abdi
Date :- 25/08/2015